Advanced Computational Methods

for electromagnetic modeling, simulation and design

Oscar P. Bruno
Caltech

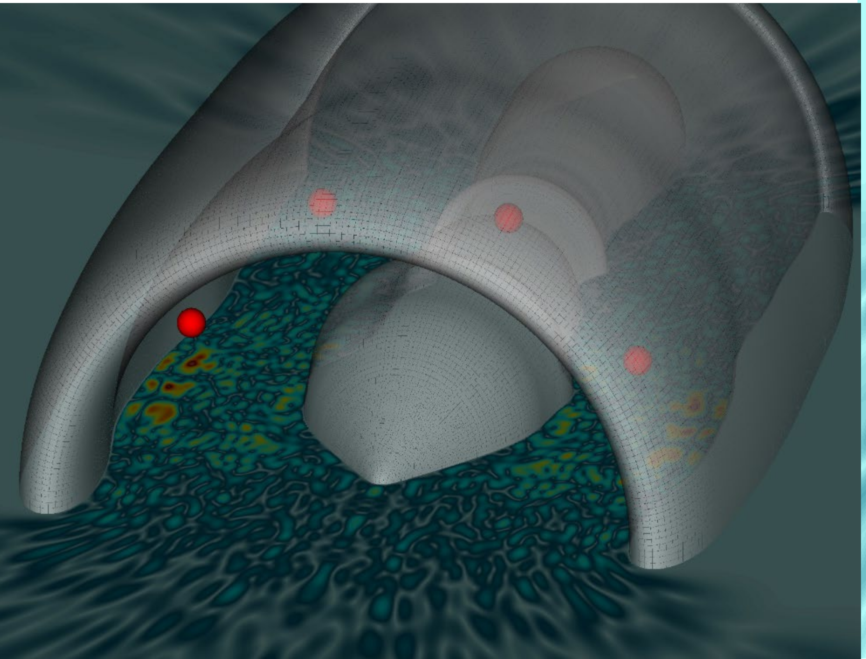

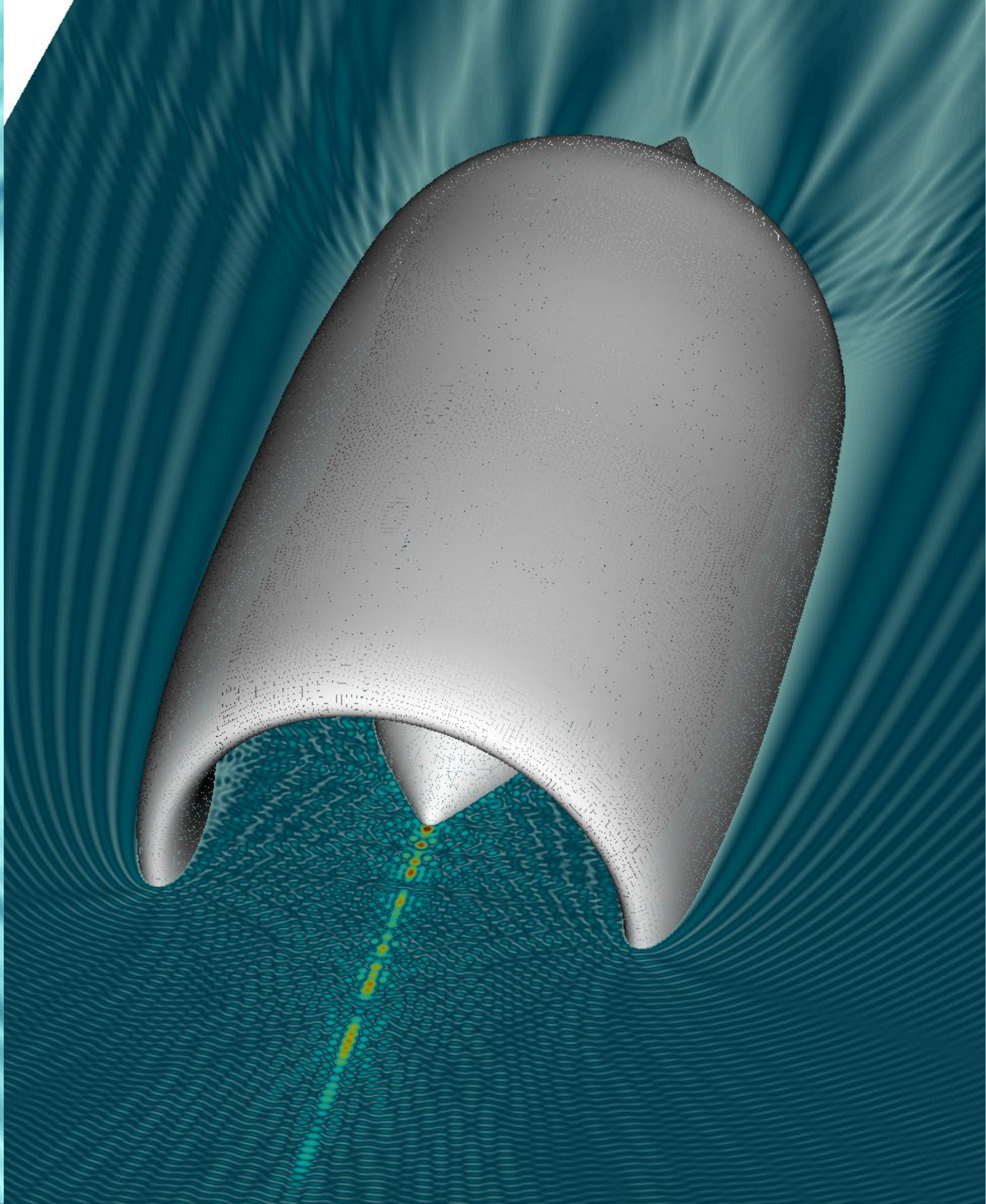

Pure Frequencies

(Time Harmonic Waves)

$$\nabla \times \mathbf{H} = \mathbf{J} + \frac{\partial \mathbf{D}}{\partial t}$$

$$\nabla \times \mathbf{E} + \frac{\partial \mathbf{B}}{\partial t} = 0$$

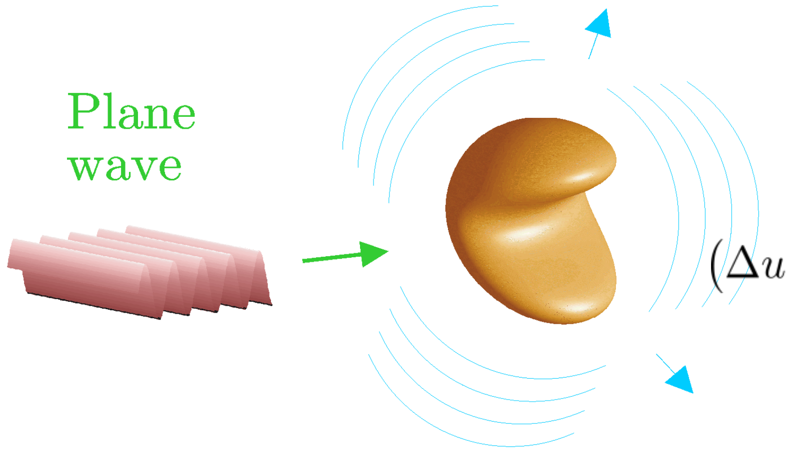

$$\frac{\partial^2 u}{\partial t^2} = c^2 \Delta u$$

$$(\Delta u = \nabla^2 u = u_{xx} + u_{yy} + u_{zz})$$

$$u(\mathbf{r}, t) = \psi(\mathbf{r}) e^{i\omega t}$$

Electromagnetic

$$\nabla \times E = i\omega\mu H$$

$$\nabla \times H = -i\omega\varepsilon E$$

Acoustic

$$\Delta\psi(\mathbf{r}) + k^2\psi(\mathbf{r}) = 0$$

Simple integral equation example

$$\Delta\psi^{\mathrm{scatt}}(\mathbf{r}) + k^2\psi^{\mathrm{scatt}}(\mathbf{r}) = 0$$

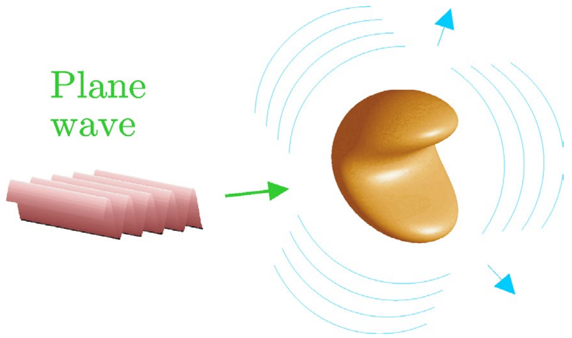

$$\psi^{\mathrm{scatt}}(\mathbf{r}) = \int_S G_k(\mathbf{r},\mathbf{r}')\mu(\mathbf{r}')dS'$$

$$\int_S G_k(\mathbf{r},\mathbf{r}')\mu(\mathbf{r}')dS' = -\psi^{\mathrm{inc}}(\mathbf{r}) \qquad \mathbf{r} \in S$$

$$G_k(\mathbf{r},\mathbf{r}') = \begin{cases} H_0^1(k|\mathbf{r}-\mathbf{r}'|) & \text{in two dimensions} \\ e^{ik|\mathbf{r}-\mathbf{r}'|}/|\mathbf{r}-\mathbf{r}'| & \text{in three dimensions} \end{cases}$$

Iterative linear algebra solution…

Well-posed Integral Equation Formulations

CFIE-R

$$\frac{\mathbf{J}}{2} + \mathcal{K}\mathbf{J} + \xi k\ (\mathbf{n} \times \mathcal{R}) \circ \mathcal{T}\mathbf{J} = \mathbf{n} \times \mathbf{H}^i - \xi k\ (\mathbf{n} \times \mathcal{R})(\mathbf{n} \times \mathbf{E}^i)$$

Theorem (General surface, arbitrary wavenumber k):
Using $\mathcal{R} = S_{iK},\ \ K = ik/2$ we have $\left(S\psi(\mathbf{x}) = \int_\Gamma G_k(\mathbf{x}-\mathbf{x}')\psi(\mathbf{x}')d\sigma(\mathbf{x}')\right)$

— CFIE-R are uniquely solvable;

— CFIE-R $\leftrightarrow$ Invertible diagonal operator + Compact operator

— Small iteration numbers

Bruno, Elling, Paffenroth and Turc, J. Comput. Phys. [2009]

Chebyshev rectangular-polar integration plus compressed FFT-acceleration

Polynomial refinement in rectangular region about singular or near-singular points

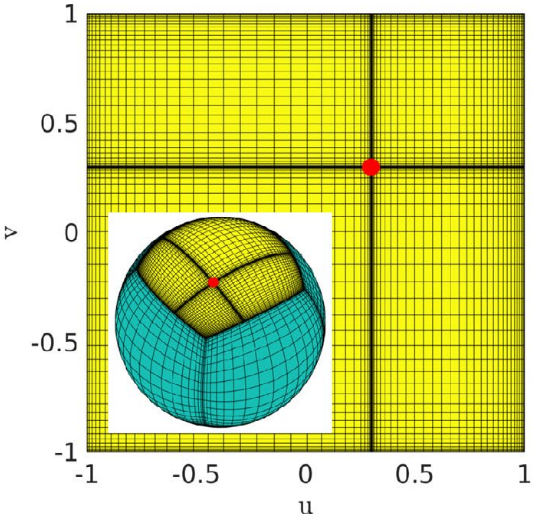

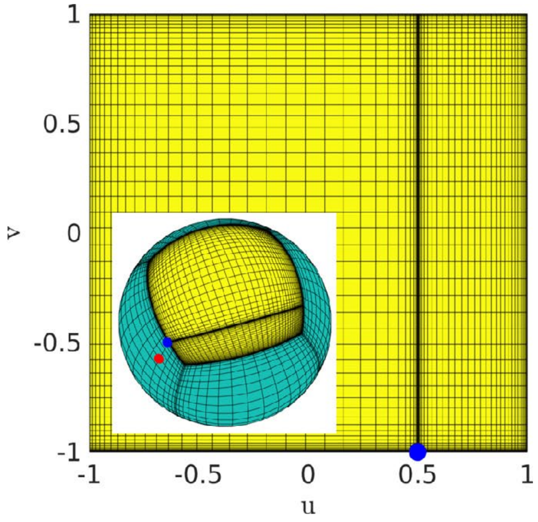

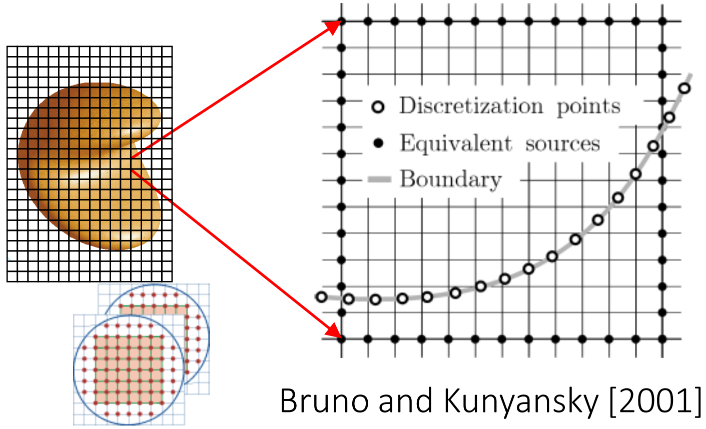

Bruno and Kunyansky [2001]

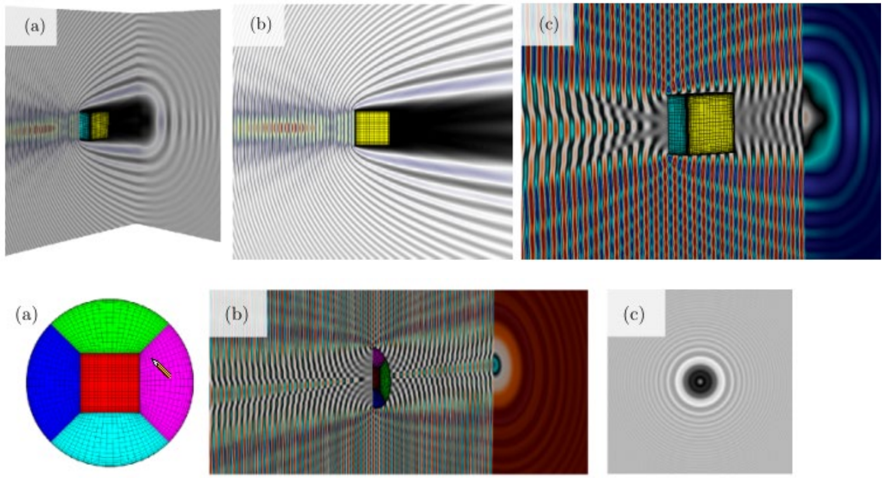

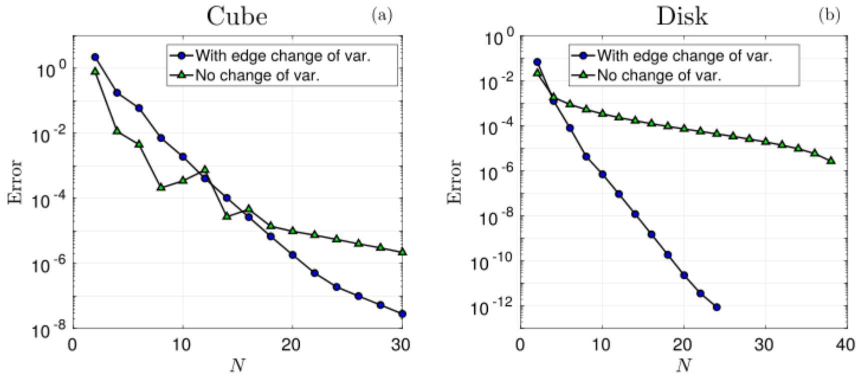

Bruno and Garza, JCP [2020]

Geometry Handling

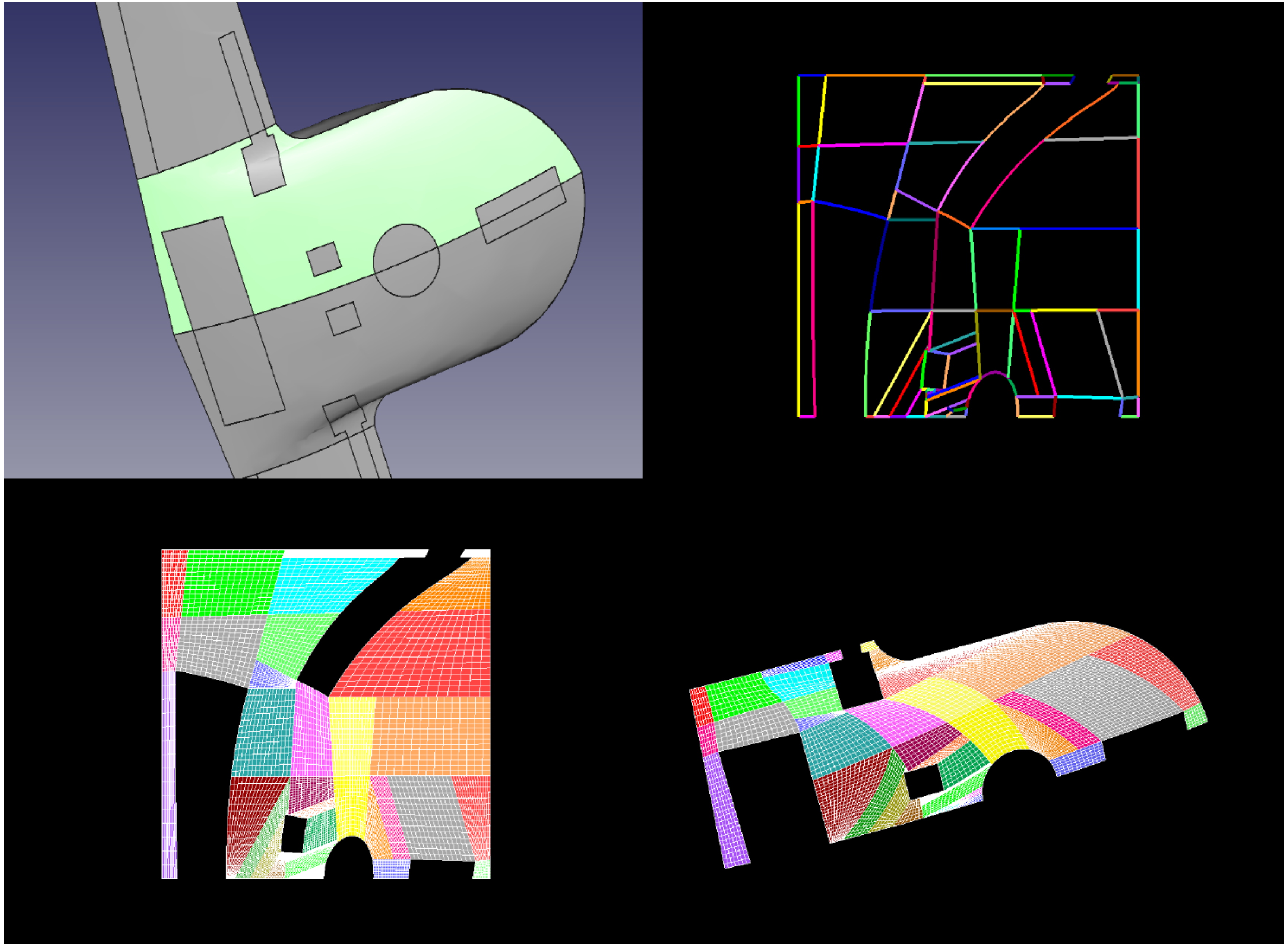

DarkStar

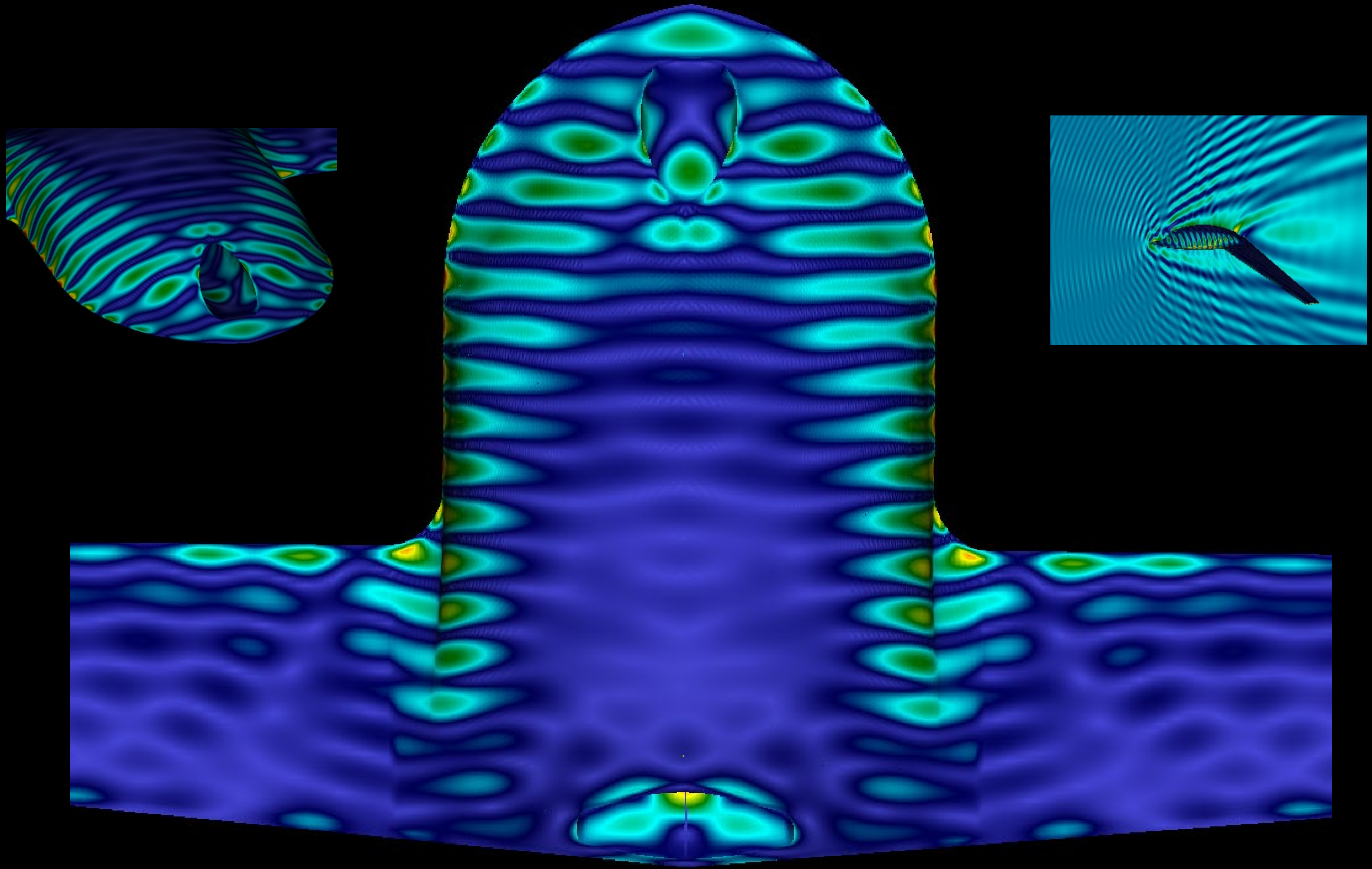

Osprey

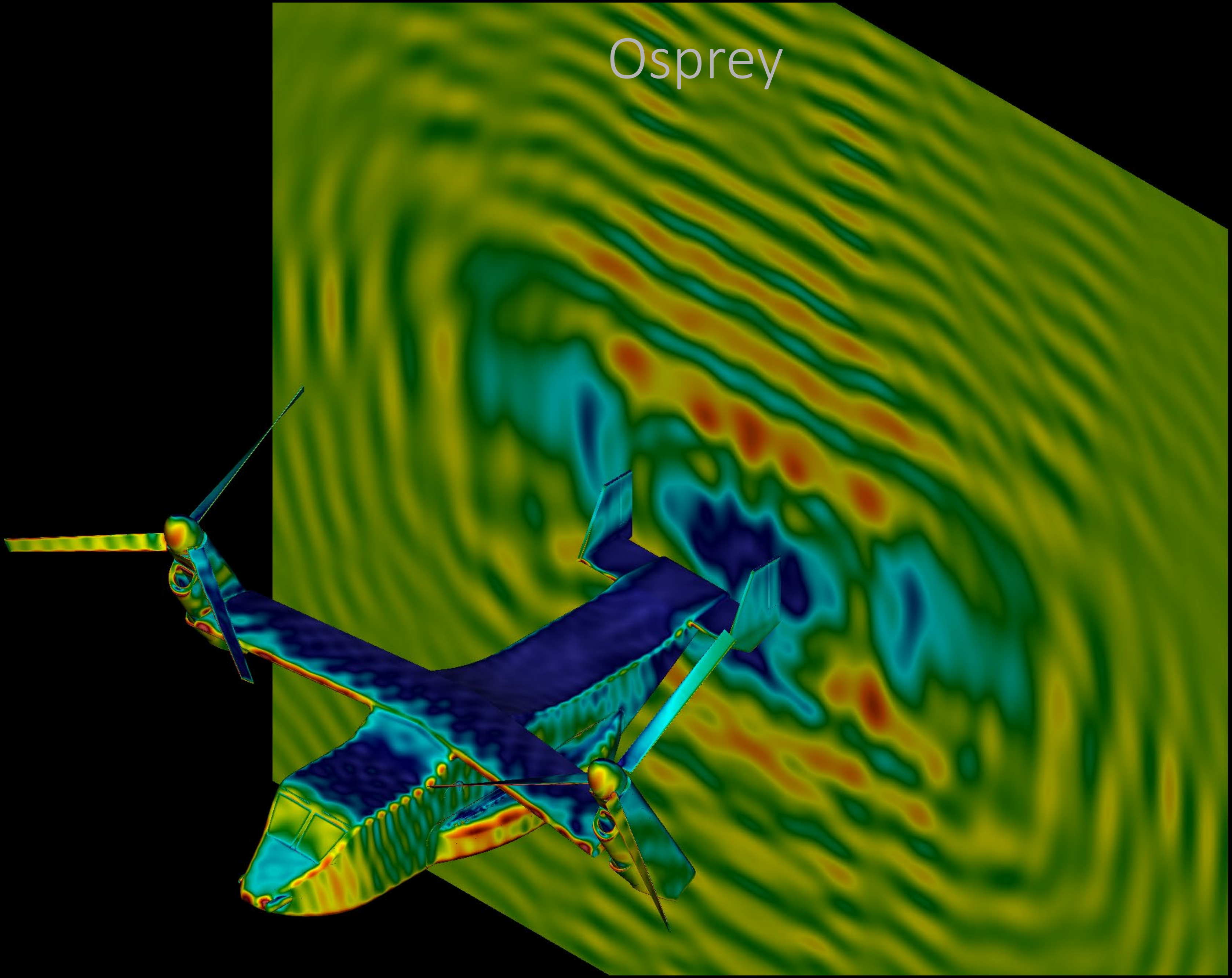

CAD-to-EM Solver

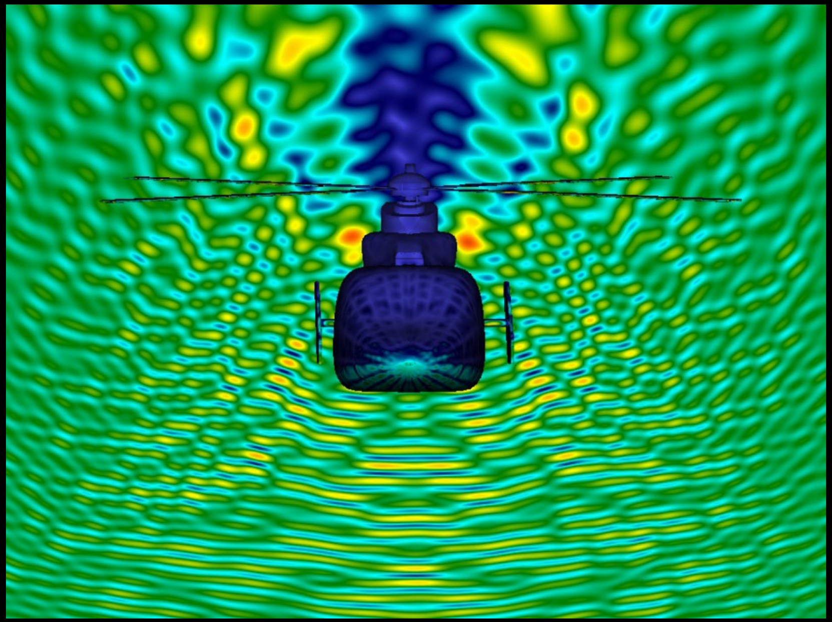

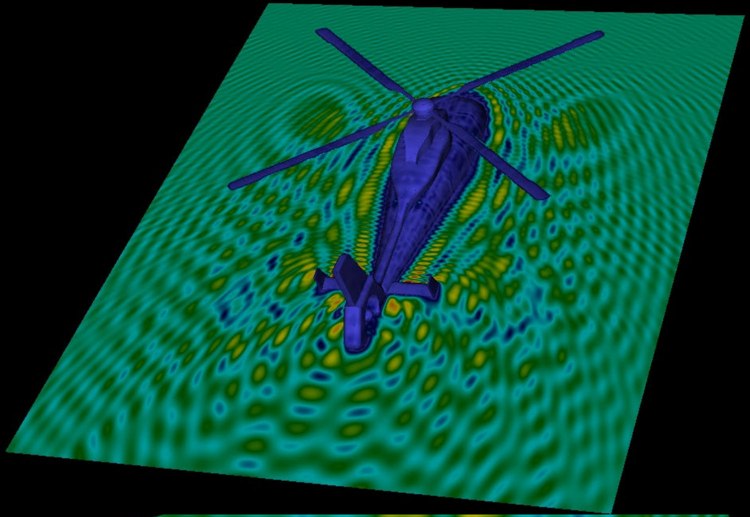

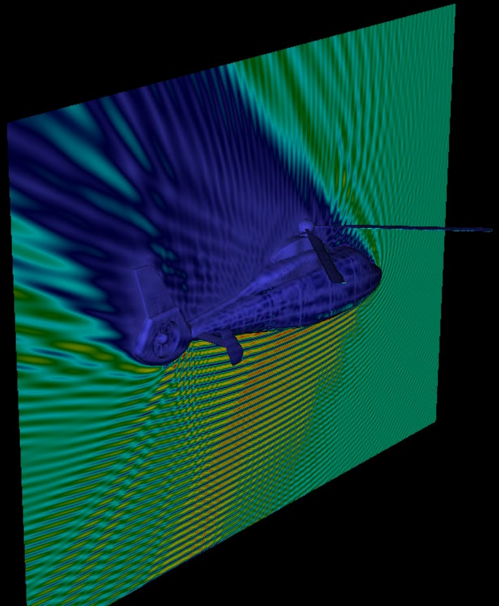

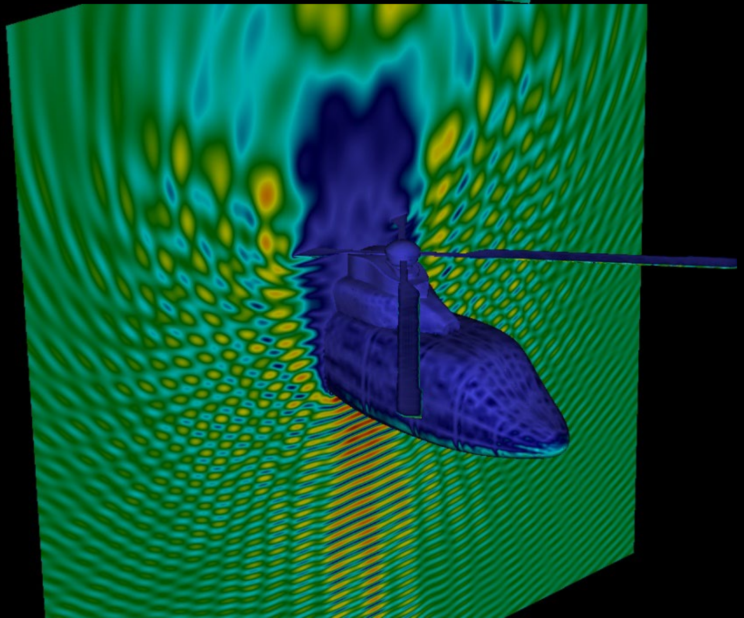

Submarine Acoustics

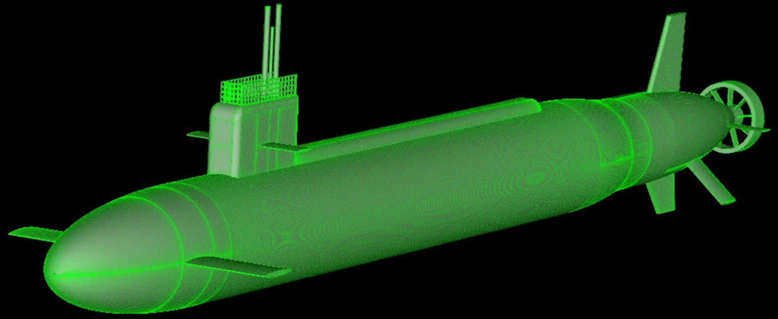

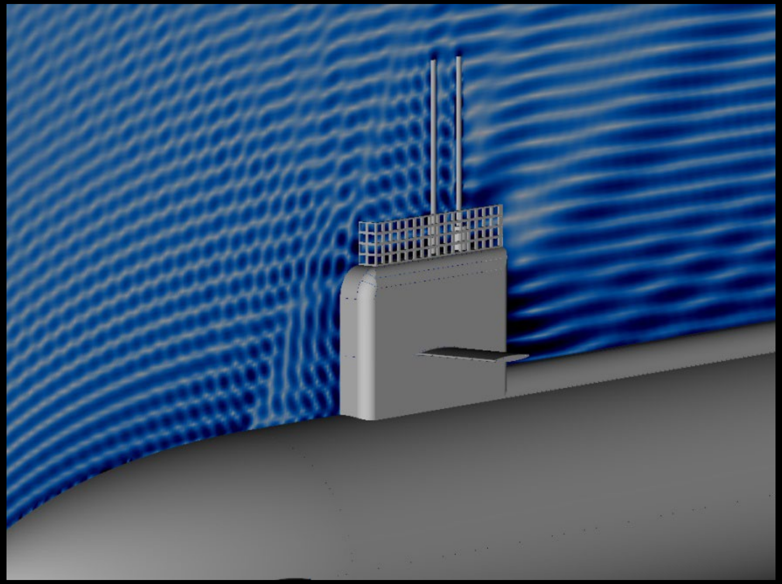

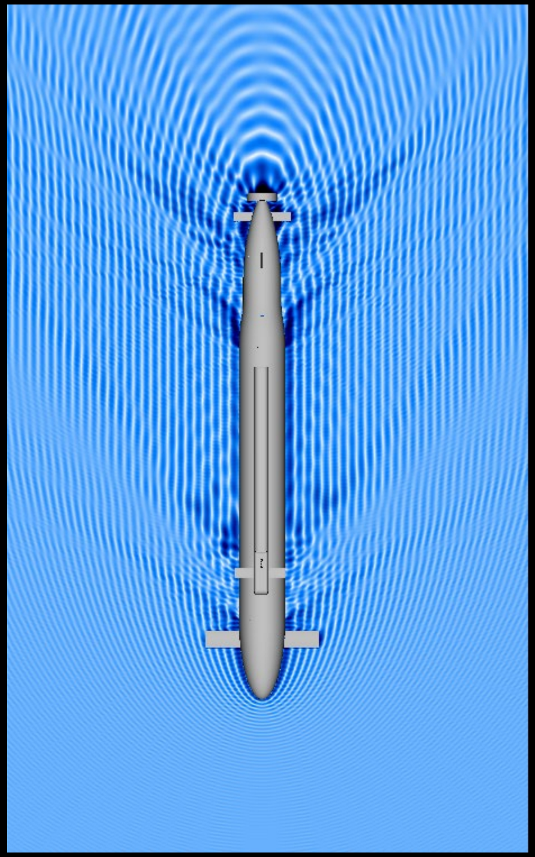

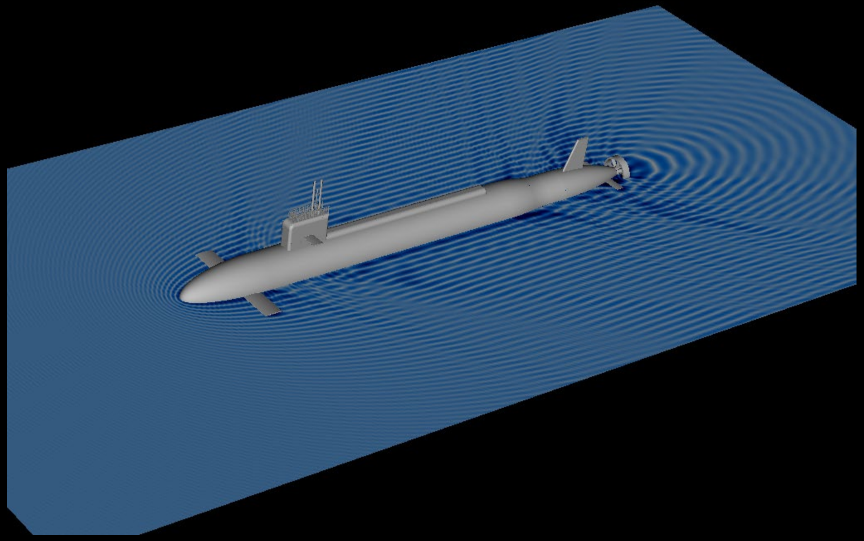

Topics

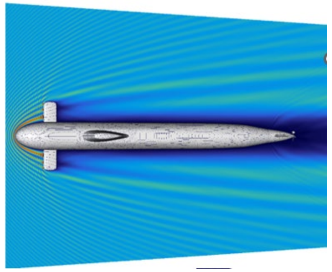

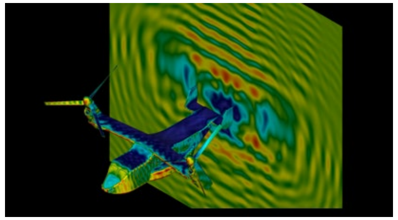

– Interpolated Factored Green Function (IFGF): FFT-free acceleration algorithm

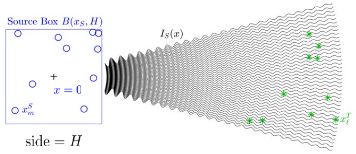

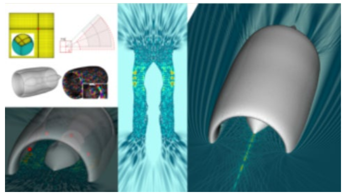

– OpenMP on 28-core server and MPI on 1680 cores

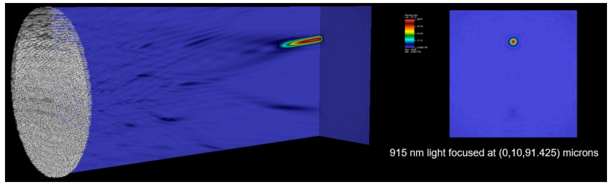

– Metamaterials: large computer cluster, photonics modeling

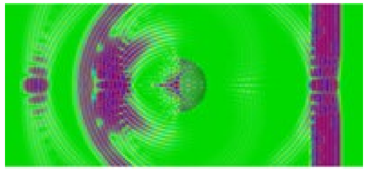

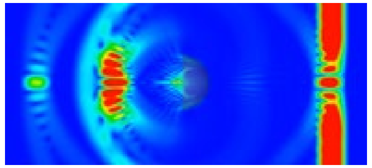

– Time-domain frequency-time hybrid solver

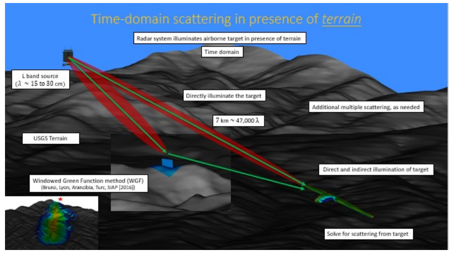

– Long-range time-domain propagation over terrain

– Long-range propagation: Screened WKB

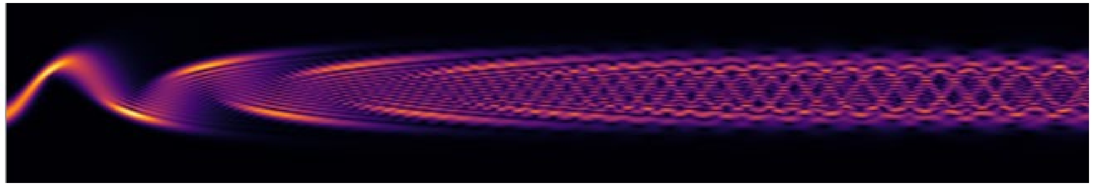

Topics

- ➢ Interpolated Factored Green Function (IFGF): FFT-free acceleration algorithm
- – OpenMP on 28-core server and MPI on 1680 cores
- – Metamaterials: large computer cluster, near cm-scale photonics modeling
- – Time-domain hybrid solver (time-domain from frequency-domain)
- – Long-range time-domain propagation over terrain
- – Long-range propagation: Screened WKB (S-WKB)

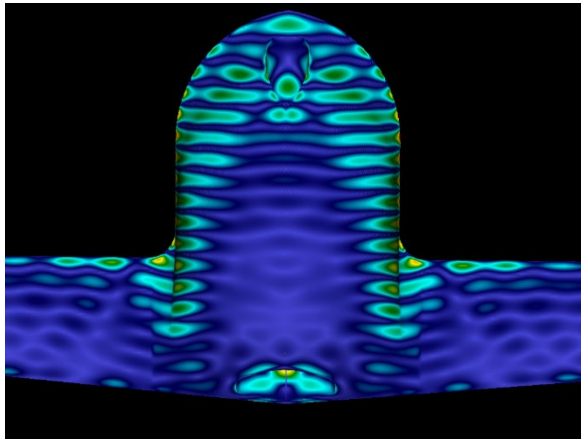

Simplest example. Discretizing the integral…

$$\int_S G_k(\mathbf{r},\mathbf{r}')\mu(\mathbf{r}')dS' = -\psi^{\mathrm{inc}}(\mathbf{r}) \quad \mathbf{r}\in S$$

…means to combine the result of many source points x_m^S onto target points x_ℓ^T.

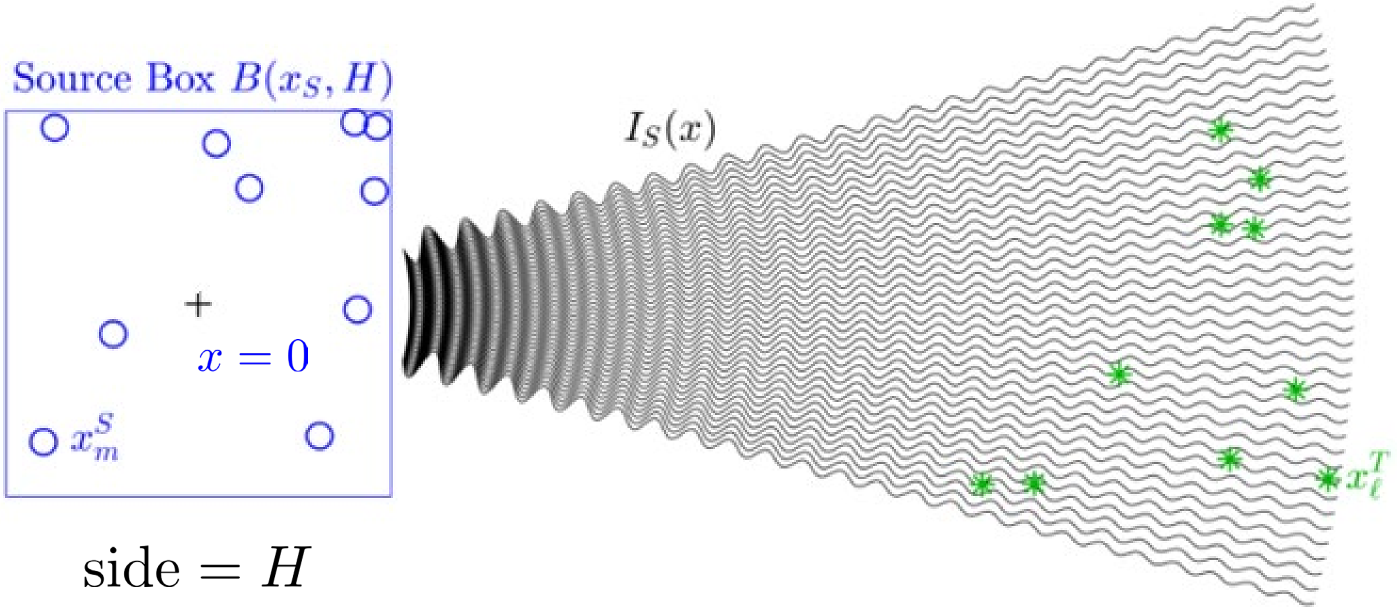

Accelerated Scattering evaluation:
Interpolated Factored Green Function (IFGF)

$$G(x,x') = \frac{e^{ik|x-x'|}}{|x-x'|}$$

$$G(x,x_m^S) = \frac{e^{ik|x-x_m^S|}}{|x-x_m^S|} = \overbrace{\left(\frac{e^{ik|x|}}{|x|}\right)}^{\text{Centered Factor } = G(x,0)} \underbrace{g_S(x,x_m^S)}_{\substack{\text{Analytic Factor} \\ \text{(slow radial variation)}}}$$

… to evaluate an N_S-source field $I_S(x)$ at N_T positions x_ℓ^T

(2D figures)

$$I_S(x_\ell^T) = \sum_{m=1}^{N_S} a_m^S G(x_\ell^T, x_m^S), \quad \ell = 1, \ldots, N_T.$$

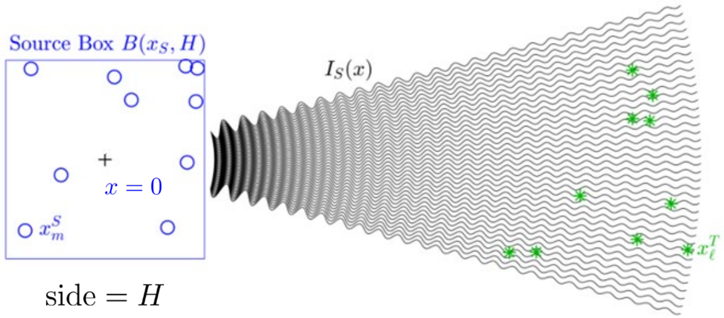

$$I_S(x) = \underbrace{G(x,0)}_{\text{Common Factor}} \overbrace{\sum_{m=1}^{N_S} a_m^S \underbrace{g(x,x_m^S)}_{\text{Slow radial variation}}}^{\substack{\text{Slow radial variation} \\ \text{Interpolate!}}}, \quad \ell = 1, \ldots, N_T.$$

Slow variation! Instead of evaluating every single source at every target, we can just evaluate at a few points and then interpolate!

IFGF Factorization in detail

- Green Function Factorization: $$\frac{e^{\imath\kappa|x-x'|}}{|x-x'|} = \left(\frac{e^{\imath\kappa|x|}}{|x|}\right)\left(\frac{|x|}{|x-x'|}e^{\imath\kappa\left(|x-x'|-|x|\right)}\right)$$
- First factor is a common factor (independent of the source position x')
- Second factor is slowly oscillatory (and more and more so for large $|x|$: analytic at ∞!)
- Second factor is nonsingular (finite) even as $x, x' \to 0$, as long as $x' \leq \eta x, (0 < \eta < 1)$

Example

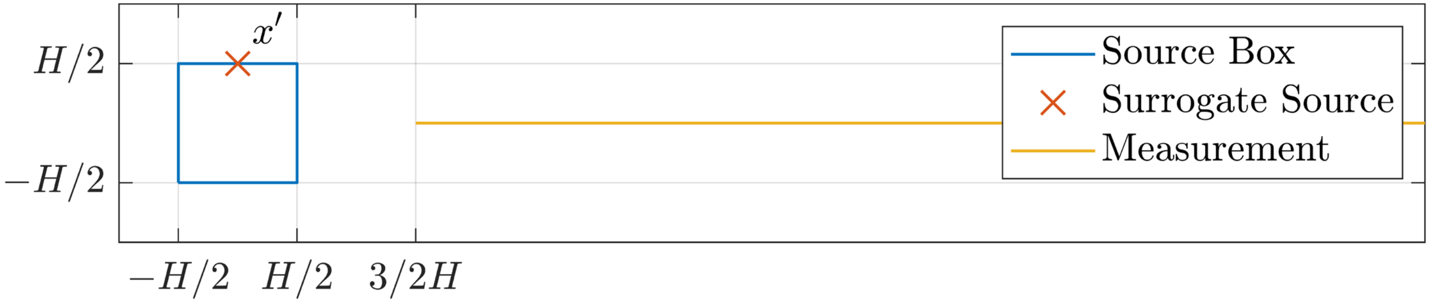

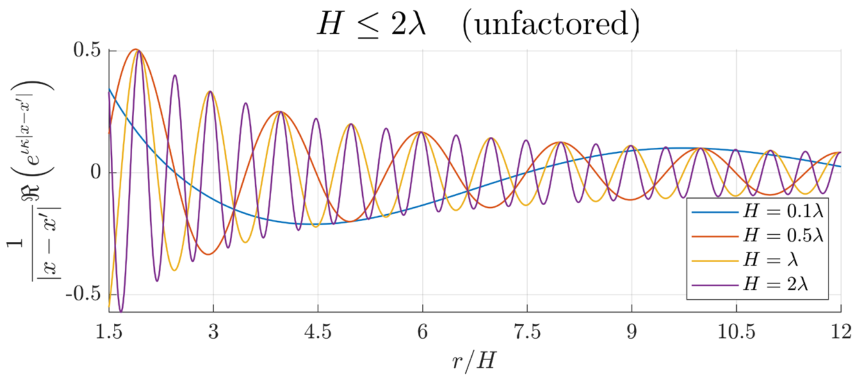

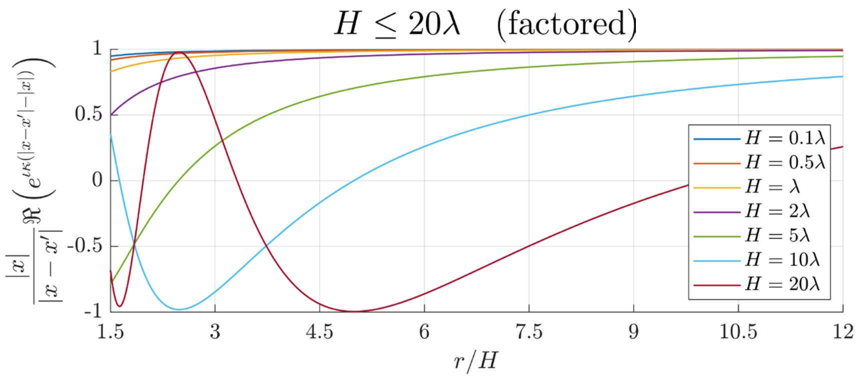

C. Bauinger and O. Bruno, JCP [2021]

Error remains constant across levels as the cost is optimized

(First installment: derivatives of the analytic factor g_S)

Theorem. For $0 \le s \le \eta < 1$ and for $\xi = s$, $\xi = \theta$ and $\xi = \varphi$, we have

$$\left|\frac{\partial^n g_S}{\partial \xi^n}\right| \le M(\eta, n) \max\{(\kappa H)^n, 1\}.$$

Proof lines:

$$r = |x|, \quad s = \frac{h}{r} \quad (0 \le s \le \eta < 1)$$

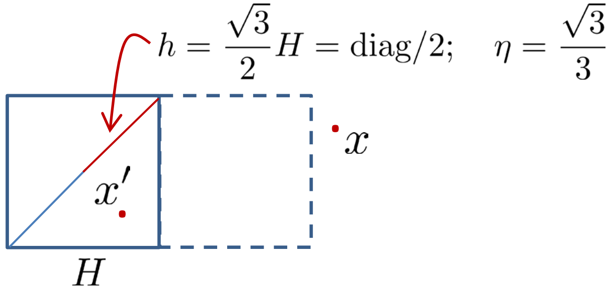

$$\frac{e^{ik|x-x'|}}{|x-x'|} = \left(\frac{e^{ik|x|}}{|x|}\right)\left(\frac{|x|}{|x-x'|} e^{ik(|x-x'|-|x|)}\right) = \left(\frac{e^{ikr}}{r}\right) g_S(x, x')$$

$$g_S(x, x') = \frac{1}{4\pi \left|\boxed{\frac{x}{r}} - \boxed{\frac{x'}{h}} s\right|} \exp\left(ik\frac{h}{s}\left(\left|\boxed{\frac{x}{r}} - \boxed{\frac{x'}{h}} s\right| - 1\right)\right) = \text{“Analytic Factor”}$$

Length = 1 Length $\le$ 1

Error remains constant across levels as the cost is optimized

(Second installment: Interpolation bounds)

Theorem. For $0 \le s \le \eta < 1$ and for $\xi = s$, $\xi = \theta$ and $\xi = \varphi$, we have

$$\left| \frac{\partial^n g_S}{\partial \xi^n} \right| \le M(\eta, n) \max\{(\kappa H)^n, 1\}.$$

Chebyshev interpolation in φ, θ and s

Theorem.

$$|g_S(\mathbf{x}(s,\theta,\varphi),x') - I^{\varphi}_{P_{\rm ang}} I^{\theta}_{P_{\rm ang}} I^{s}_{P_s} g_S(\mathbf{x}(s,\theta,\varphi),x')| \le$$
$$C\left[(\Delta_s)^{P_s} \left\| \frac{\partial^{P_s} g_S}{\partial s^{P_s}} \right\|_\infty + (\Delta_\theta)^{P_{\rm ang}} \left\| \frac{\partial^{P_{\rm ang}} g_S}{\partial \theta^{P_{\rm ang}}} \right\|_\infty + (\Delta_\varphi)^{P_{\rm ang}} \left\| \frac{\partial^{P_{\rm ang}} g_S}{\partial \varphi^{P_{\rm ang}}} \right\|_\infty \right].$$

$kH \ge 1$

$$\le C' \left[(kH\Delta_s)^{P_s} + (kH\Delta_\theta)^{P_{\rm ang}} + (kH\Delta_\varphi)^{P_{\rm ang}}\right]$$

Conclusion: for $kH \ge 1$ keep error constant by letting

$$\Delta_s \to \Delta_s/2, \quad \Delta_\theta \to \Delta_\theta/2 \quad \text{and} \quad \Delta_\varphi \to \Delta_\varphi/2 \quad \text{as} \quad H \to 2H!$$

For $kH < 1$ keep Δ_s, Δ_θ and Δ_φ unchanged.

Cost reduction: interpolate only to *cousin surface points* and *parent interpolation points*!

- Only interpolate to **cousin** surface points (non-neighboring children of the parent's neighbors)

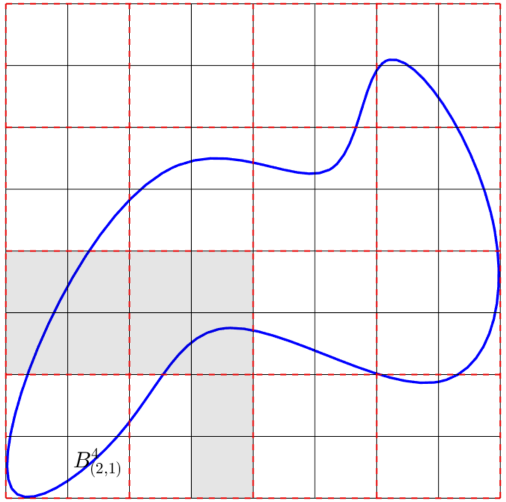

Cousin boxes to the box $B^4_{(2,1)}$ in gray

- Points close are either covered directly or by levels with smaller boxes

- Points farther away are covered by levels with larger boxes: the information is carried over via the parent interpolation points!

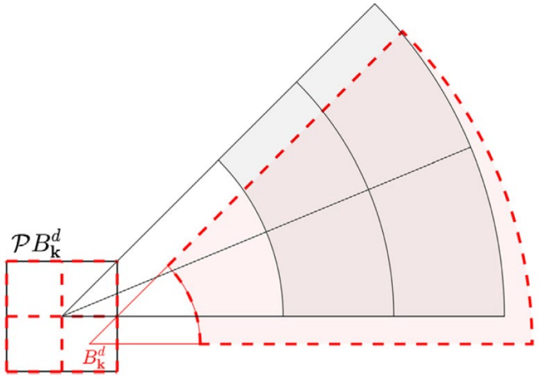

Error remains constant across levels precisely as the cost is optimized!

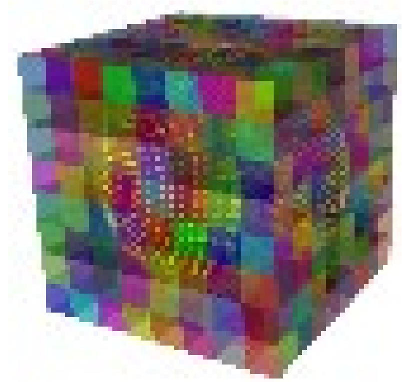

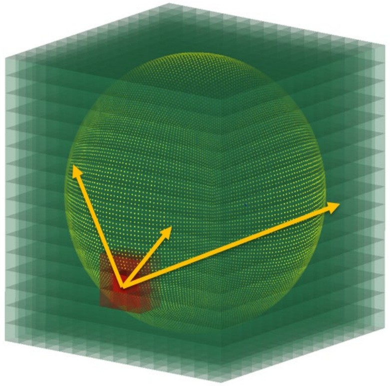

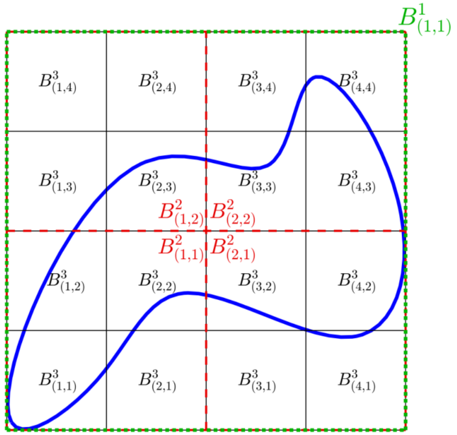

As we move from one level to the next larger level...

... cost per level remains constant!

- E.g. for $kH \geq 1$ (case $kH < 1$ is analogous but less expensive):
- $H \to 2H$
- $\Delta_s \to \Delta_s/2$, $\Delta_\theta \to \Delta_\theta/2$ and $\Delta_\varphi \to \Delta_\varphi/2$
- Relevant boxes: $|\mathcal{R}_B| \to |\mathcal{R}_B|/4$
- Relevant cone segments per box: $|\mathcal{R}_C| \to 4|\mathcal{R}_C|$
- Cousin points (interpolation): $|\mathcal{V}| \to 4|\mathcal{V}|$
- Parent cone interpolation points (interpolation): $|\mathcal{P}| \to 4|\mathcal{P}|$

- $\log N$ levels
- N operations per level
- $\mathcal{O}(N \log N)$ overall operations

Simple!

Algorithm 1 IFGF Method

\\\\Initialization.
for $d = 1, \dots, D$ **do**
    Determine relevant boxes $\mathcal{R}_B^d$ and cone segments $\mathcal{R}_C^d$.
end for

\\\\Direct evaluations on the lowest level.
for $B_{\mathbf{k}}^D \in \mathcal{R}_B^D$ **do**
    for $x \in \mathcal{U}B_{\mathbf{k}}^D \cap \Gamma_N$ **do** ▷ Direct evaluations onto neighboring surface points
        Evaluate $I_{\mathbf{k}}^D(x)$
    end for
    for $C_{\mathbf{k};\gamma}^D \in \mathcal{R}_C B_{\mathbf{k}}^D$ **do** ▷ Evaluate F at all relevant interpolation points
        for $x \in \mathcal{X}C_{\mathbf{k};\gamma}^D$ **do**
            Evaluate and store $F_{\mathbf{k}}^D(x)$.
        end for
    end for
end for

\\\\Interpolation onto surface discretization points and parent interpolation points.
for $d = D, \dots, 3$ **do**
    for $B_{\mathbf{k}}^d \in \mathcal{R}_B^d$ **do**
        for $x \in \mathcal{V}B_{\mathbf{k}}^d \cap \Gamma_N$ **do** ▷ Interpolate at cousin surface points
            Evaluate $I_{\mathbf{k}}^d(x)$ by interpolation
        end for
        if $d > 3$ **then** ▷ Evaluate F at parent interpolation points
            Determine parent $B_{\mathbf{j}}^{d-1} = \mathcal{P}B_{\mathbf{k}}^d$
            for $C_{\mathbf{j};\gamma}^{d-1} \in \mathcal{R}_C B_{\mathbf{j}}^{d-1}$ **do**
                for $x \in \mathcal{X}C_{\mathbf{j};\gamma}^{d-1}$ **do**
                    Evaluate and add $F_{\mathbf{k}}^d(x)G(x, x_{\mathbf{k}}^d)/G(x, x_{\mathbf{j}}^{d-1})$
                end for
            end for
        end if
    end for
end for

Ubiquitous use of FFTs in previous integral acceleration methods

- FFTs make parallelization challenging: well-known problem for massive parallelization.
- Obvious impact of FFT in equivalent-source methods. FMM methods also rely on FFT.
- References [1], [2] indicate that

  "the top part of the [FMM] octree is a bottleneck".

- Reference [3] calls parallelization "bottleneck" the part of the FMM relying on FFTs, as it suffers from "lowest arithmetic intensity" and "likely suffering from bandwidth contention".
- Reference [4] mentions two alternatives to use of FFT in the FMM which, however, it discards as less efficient than an FFT-based procedure.

[1] B. Engquist and L. Ying. Fast directional multilevel algorithms for oscillatory kernels. Journal of Scientific Computing, 29(4):1710–1737, 2007.

[2] L. Ying, G. Biros, D. Zorin, and M. H. Langston. A new parallel kernel-independent fast multipole method. Proceedings of the ACM/IEEE SC2003 Conference on Supercomputing (SC'03), 2003.

[3] A. Chandramowlishwaran, S. Williams, L. Oliker, I. Lashuk, G. Biros, and R. Vuduc. Optimizing and tuning the fast multipole method for state-of-the-art multicore architectures. In 2010 IEEE International Symposium on Parallel Distributed Processing (IPDPS), pages 1–12, 2010.

[4] N. A. Gumerov and R. Duraiswami. Fast Multipole Methods for the Helmholtz Equation in Three Dimensions. Elsevier Science, 2004.

Topics

- – Interpolated Factored Green Function (IFGF): FFT-free acceleration algorithm
- ➢ OpenMP on 28-core server and MPI on 1680 cores
- – Metamaterials: large computer cluster, near cm-scale photonics modeling
- – Time-domain hybrid solver (time-domain from frequency-domain)
- – Long-range time-domain propagation over terrain
- – Long-range propagation: Screened WKB (S-WKB)

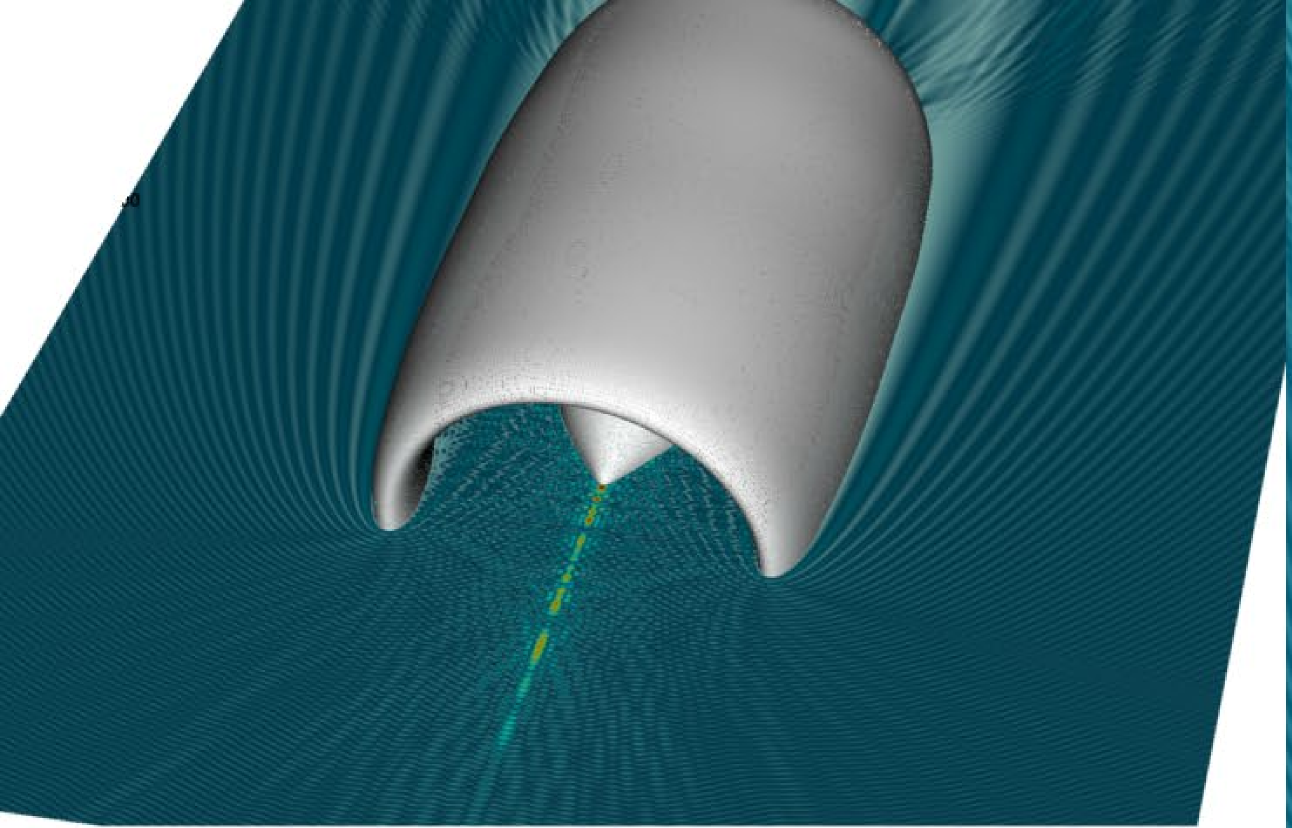

IFGF-based full solvers

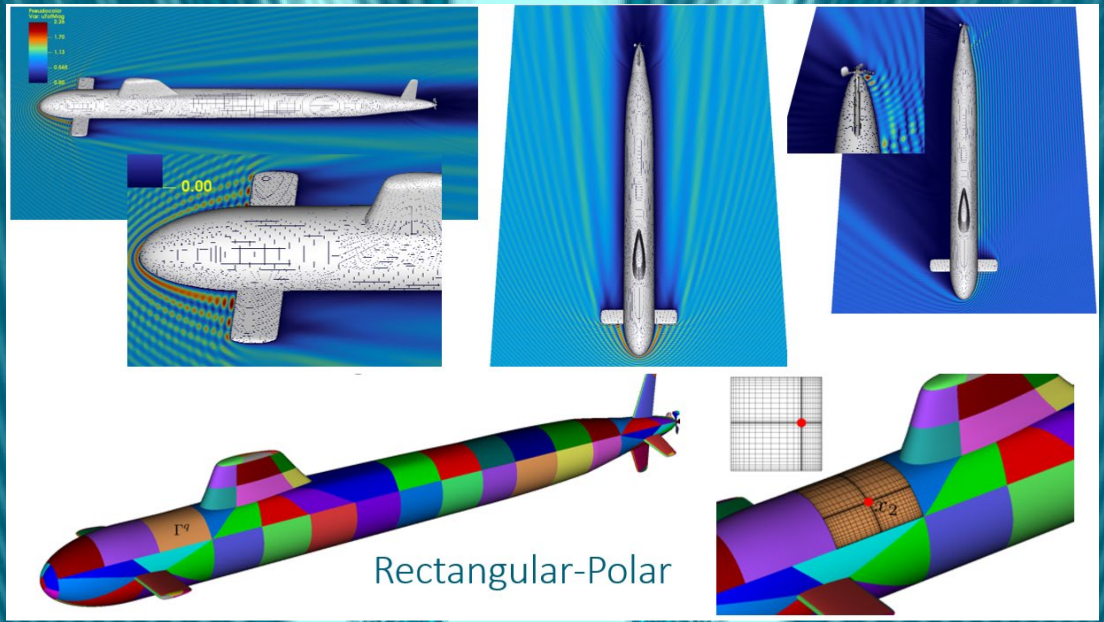

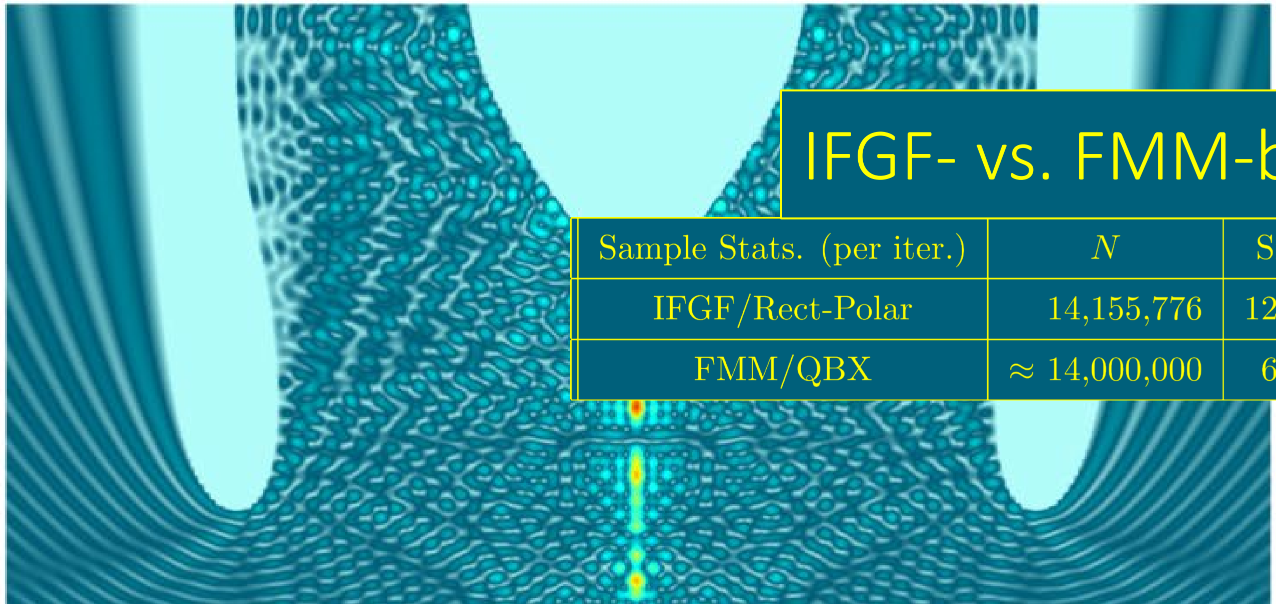

IFGF- vs. FMM-based full solvers

Sample Stats. (per iter.)	N	Size	ε	T (s)	# Comput. Cores
IFGF/Rect-Polar	14,155,776	128 λ	3.8×10^{-4}	443	28
FMM/QBX	$\approx$ 14,000,000	64 λ	2.5×10^{-3}	2,500	20

Rect-Polar, Bruno and Garza, JCP [2020]
FMM accelerated QBX, Wala and Klöckner, JCP [2019]
IFGF/Rect-Polar Jimenez, Bauinger and Bruno, arXiv:2112.06316 [2022]

Comparison of BEMFMM and IFGF: acceleration of matrix-vector multiply

$$I(x_\ell) = \sum_{m=1}^{N} a_m G(x_\ell, x_m), \quad \ell = 1, \ldots, N.$$

Comparison vs. BEMFMM authors' code download, in our computer cluster. (Only small test provided → low speedup.)

IFGF: $O(N \log N)$ complexity

(1,680 cores, frequency proportionally increased)

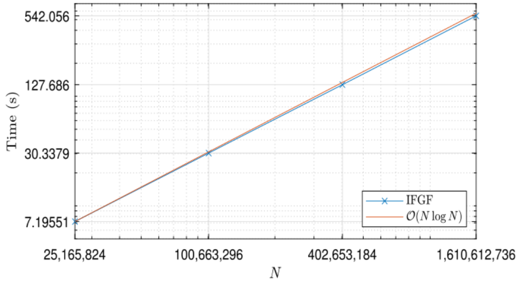

	BEMFMM	IFGF	BEMFMM/IFGF
N	361,224	393,216	
1 Node (s)	14.95	1.60	9.3
30 Nodes (s)	4.99	0.12	41.6
Speedup	3.00	13.33	

IFGF: Strong Scaling

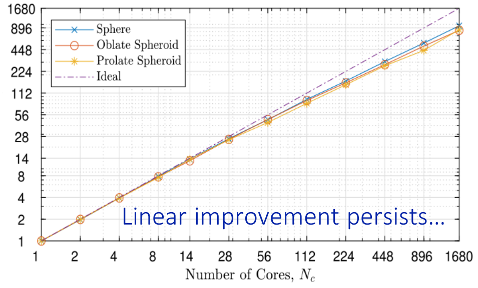

Comparison with the BEMFMM published results

Ratio: 1.07 Inv Ratio: 16.87 Ratio: 84

	N	A	ε	T (s)	# Comput. Cores	Memory
IFGF	2,147,483,648	1,389 λ	6×10^{-3}	877	1,680	10.4 TB
BEMFMM	2,300,067,840	1,389 λ	Unspecified	52	131,072	Unspecified

(Largest problem considered) (Configured for 1×10^{-3}) (> 500 TB available)

Parallel IFGF: C. Bauinger and O. Bruno, JCP [2023]

BEMFMM: "Extreme scale solver…" Abduljabbar, Keyes et. al. SISC [2019]

Comparison of BEMFMM and IFGF: acceleration of matrix-vector multiply

IFGF: Strong Scaling test

Exponential computing-time decay under iterated hardware doubling

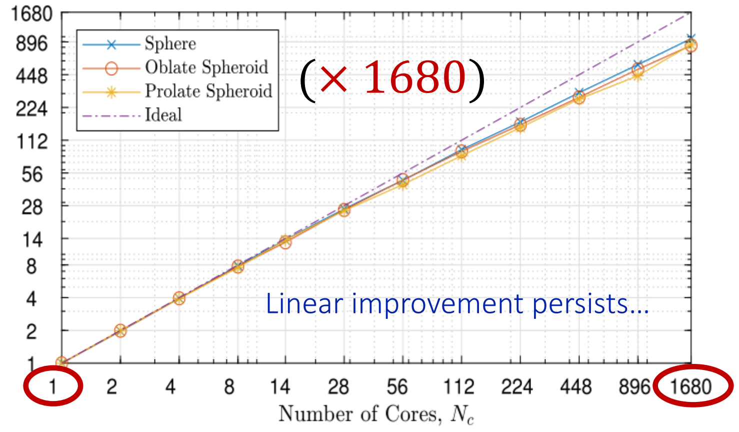

1,572,864 DoF

128λ sphere and oblate spheroid

256λ prolate spheroid

Computing time divided by 1.84 for every hardware doubling (Asymptotically)

BEMFMM, SISC [2019]. Sphere problem. (Acoustic size not specified.)

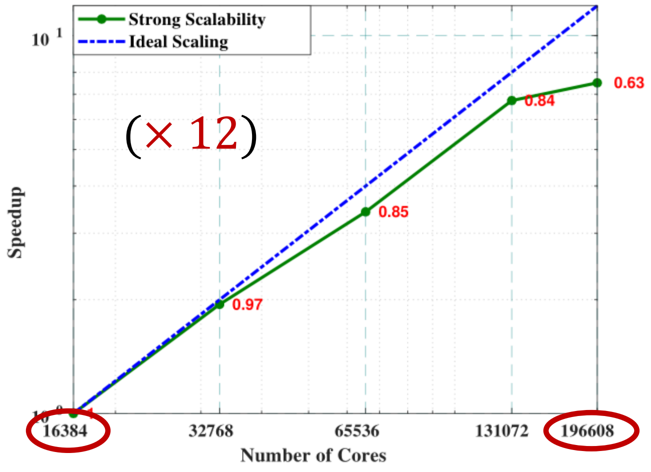

(b) 2,300,067,840 DoF

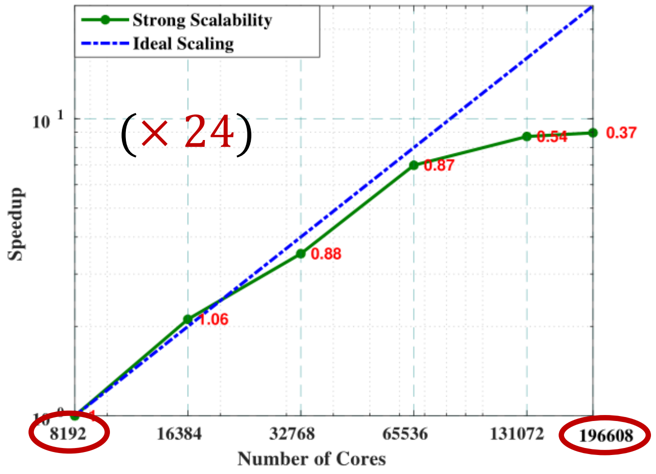

(c) 575,016,960 DoF

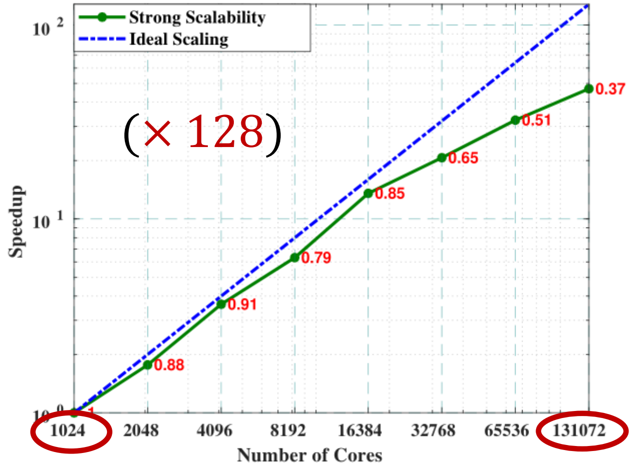

(d) 143,754,240 DoF

Topics

- IFGF Parallelization approach: space-filling Z-curves and cone-segment parallelization
- OpenMP on 28-core server and MPI on 1680 cores
- ➢ Metamaterials: near cm-scale photonics modeling, optimization and design
- Time-domain hybrid solver (time-domain from frequency-domain)
- Long-range time-domain propagation over terrain
- Long-range propagation: Screened WKB (S-WKB)

Adjoint Optimization
(gradient descent; one solve per full gradient)

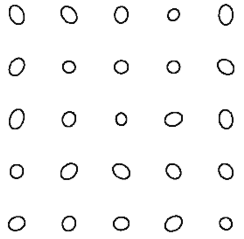

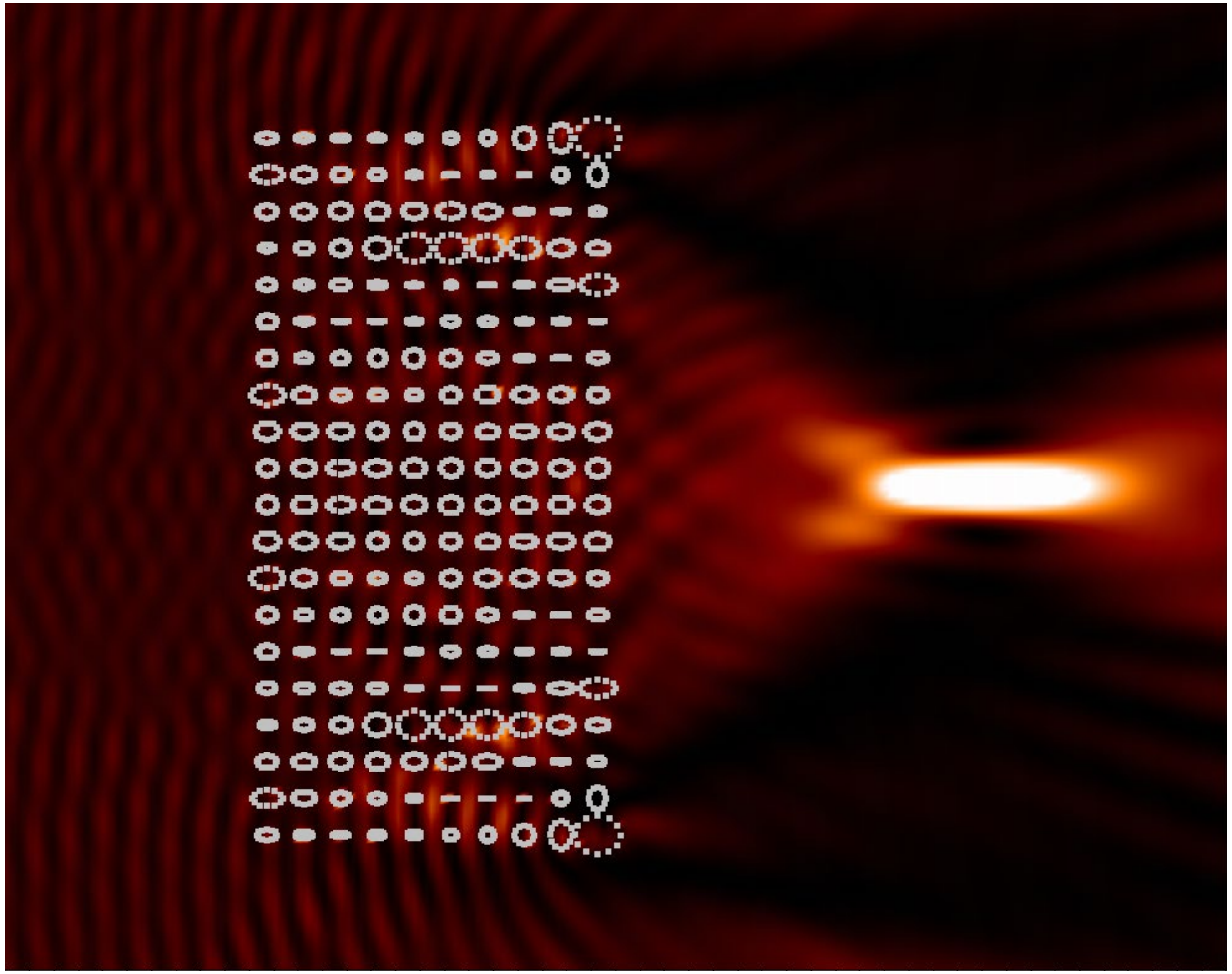

O. Bruno and E. Garza [2018]

Wavelength Splitting Grating Coupler

GOAL: Maximize/minimize (resp. minimize/maximize) the amount of 1.3μ light (resp. 1.55μ light) going to the right/left (resp. left/right)

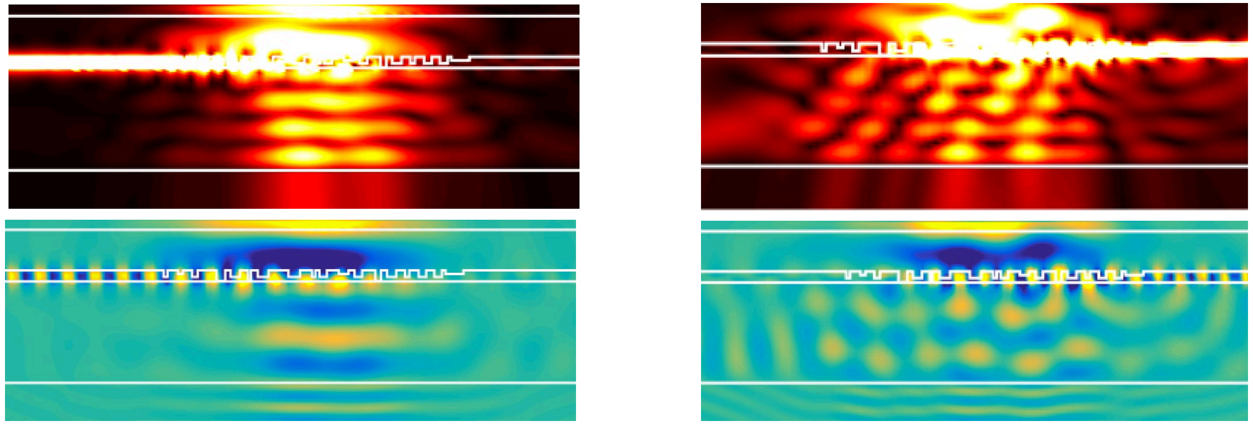

$\lambda = 1.55\mu$		$\lambda = 1.3\mu$	
← **42.7%**	→ **0.3%**	← **0.04%**	→ **42.2%**

Single solve requires
6.4 min in Lumerical
(commercial FDTD solver)
Vs.
10 sec in our solver
(at comparable accuracy).
Optimization is not available in Lumerical.

Left-right symmetric performance, as desired!

Optimized Wavelength Splitting Grating
(multiple heights)

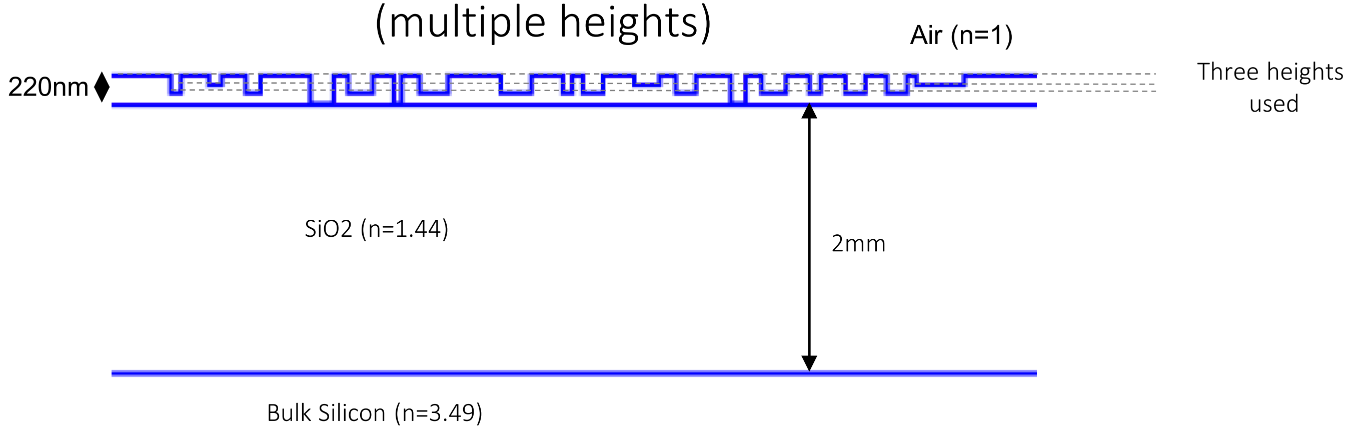

O. Bruno, E. Garza, C. Sideris, [2018]

Negligible termination errors

Windowed Green Function (WGF)

$\lambda = 1.55\mu$ $\lambda = 1.3\mu$

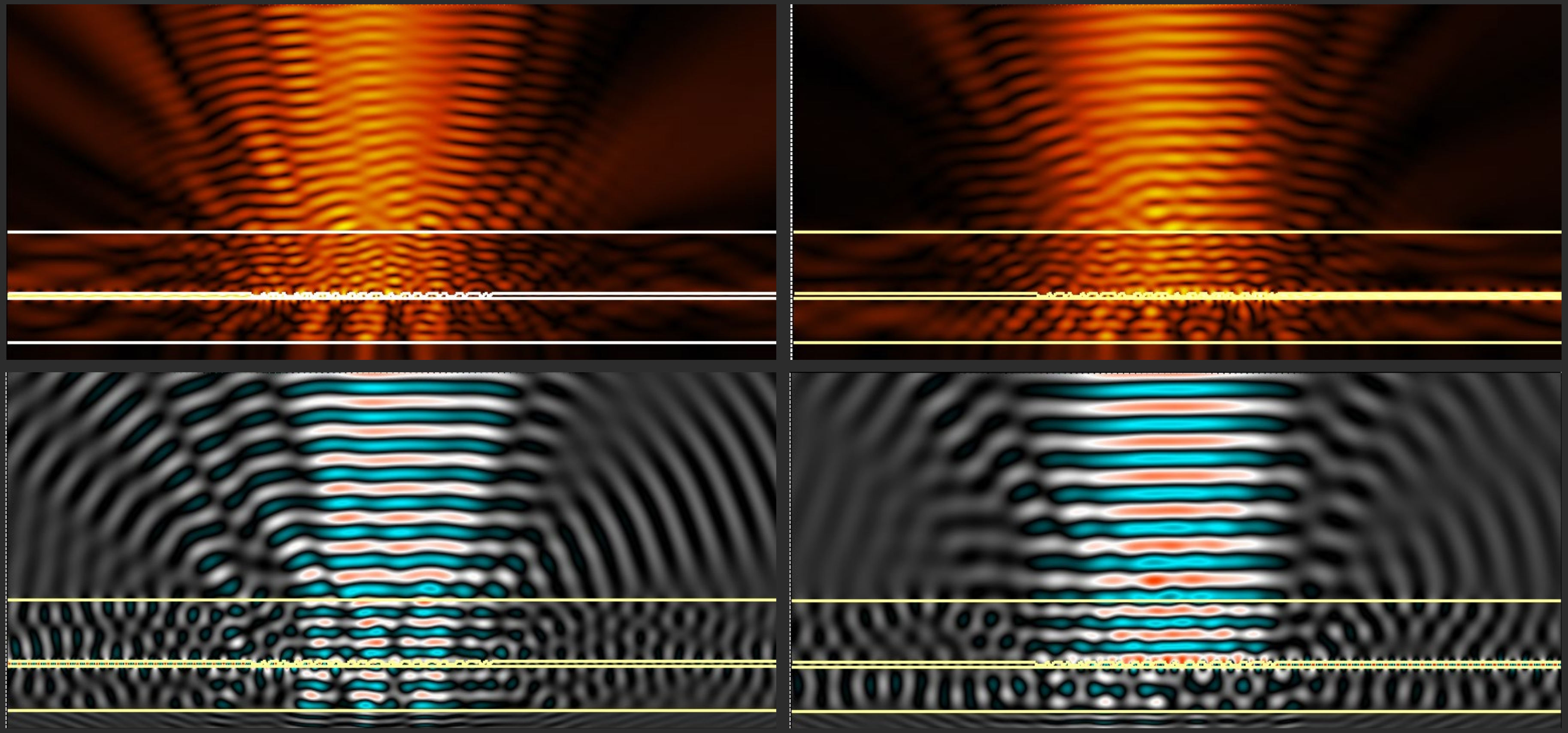

Design method: Sideris, Garza, Bruno [2019]

Scattering in presence of layered media

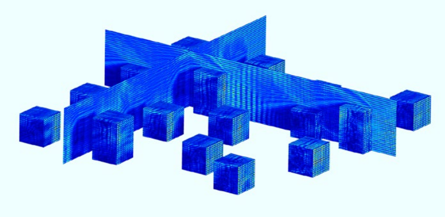

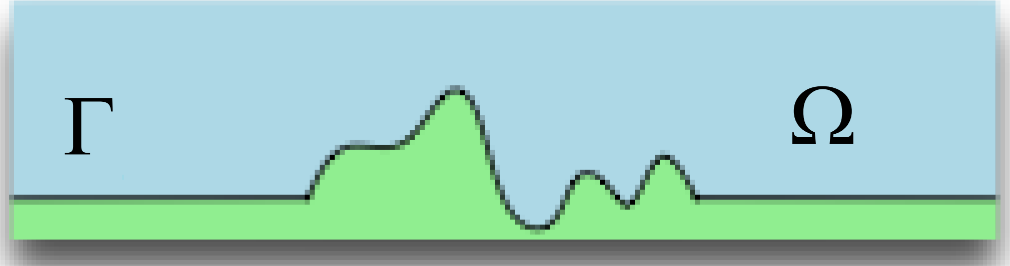

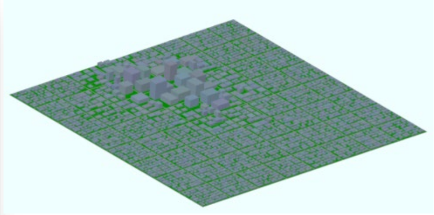

$$(I + T)\,J = f^{inc}$$

Windowed Green Function (WGF) method

Preliminary idea: solve $\left(\tilde{I} + Tw\right) J = f^{inc}$ instead

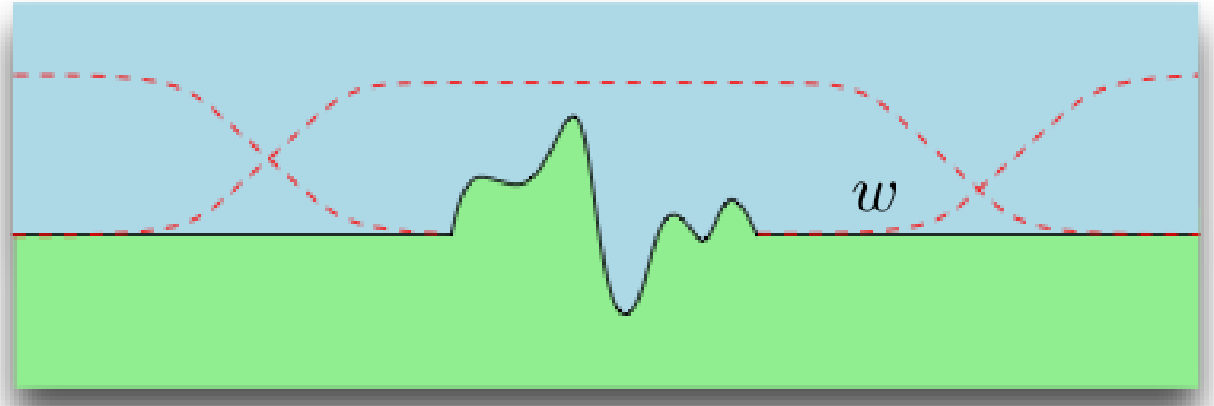

Exact equation: $\left(\tilde{I} + Tw\right) J = f^{inc} - T(1-w)J$

But…

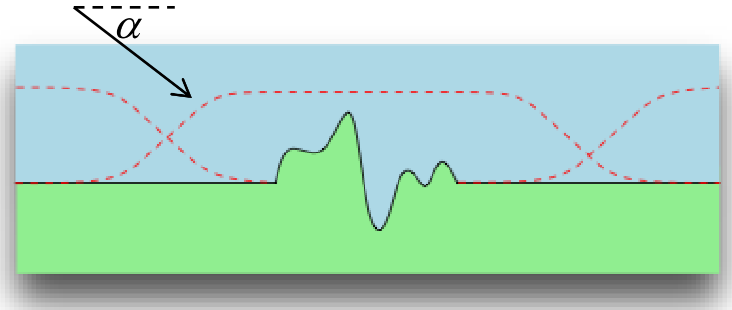

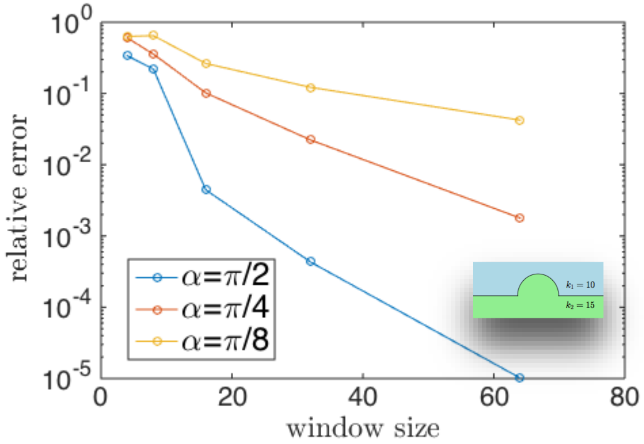

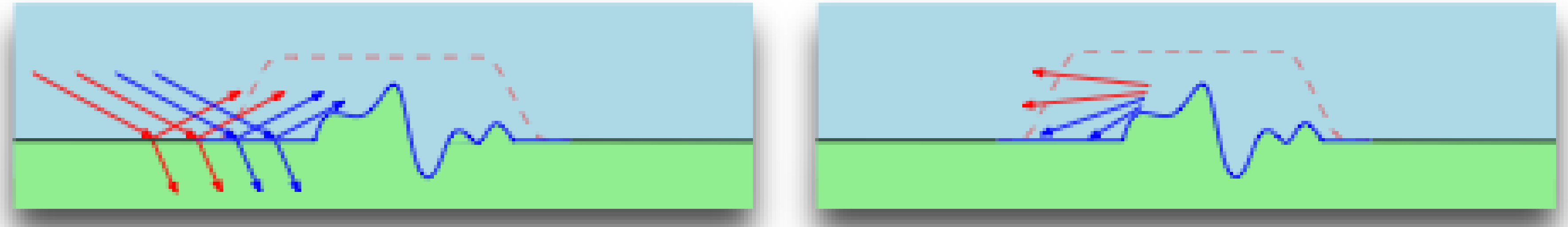

…red beams are not accounted for!

Idea: approximate the exact equation $\left(\tilde{I} + Tw\right) J = f^{inc} - T(1-w)J$

$$\left(\tilde{I} + Tw\right) J = f^{inc} - T(1-w)J^{plane}$$

Closed form + bounded integral!

Bruno, Lyon, Perez-Arancibia, Turc [2016]

WGF method: two-layer problem

Solution times compared to Sommerfeld-integral layer-Green function approach

Solution times — incidence angle $\alpha = \pi/32$

k_+	Sommerfeld Int.	WGF	Max error
1.0	0.883962 secs.	**0.285474 secs.**	9.44E-05
3.0	2.850011 secs.	**0.239336 secs.**	9.58E-05
10.0	84.728028 secs.	**0.769704 secs.**	9.48E-05
20.0	146.709174 secs.	**1.348077 secs.**	8.47E-05

Error dependence on the angle of incidence

Errors for fixed window size and fixed integration parameters

α	Relative error
$\pi/4$	**8.492047E-06**
$\pi/16$	**9.632631E-06**
$\pi/64$	**7.274729E-06**
$\pi/256$	**7.176513E-06**
$\pi/1024$	**7.170516E-06**

Error dependence on the window size

Errors for fixed incidence angle and fixed integration parameters

W	Relative error
4λ	**1.582366E-02**
8λ	**9.460171E-05**
16λ	**2.121492E-07**
32λ	**1.077599E-09**

<u>super algebraic convergence</u>

Efficient Solver Strategy Based on Windowed Subproblem Decomposition

Optimization requires **multiple efficient direct solutions**

Windowed solvers

- **Partition large or even infinite domains leading to efficient concurrent solves**
- **Minimize edge effects through smooth windowing**

Objective gradient calculation:

- **Adjoint integral method**

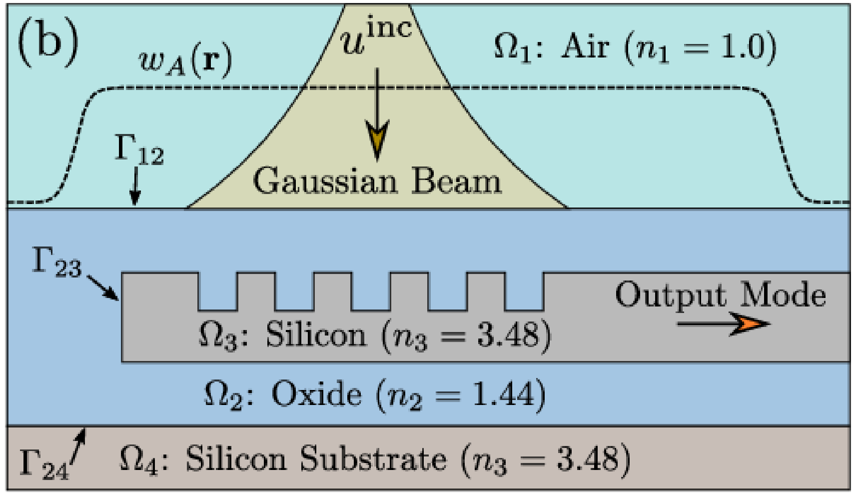

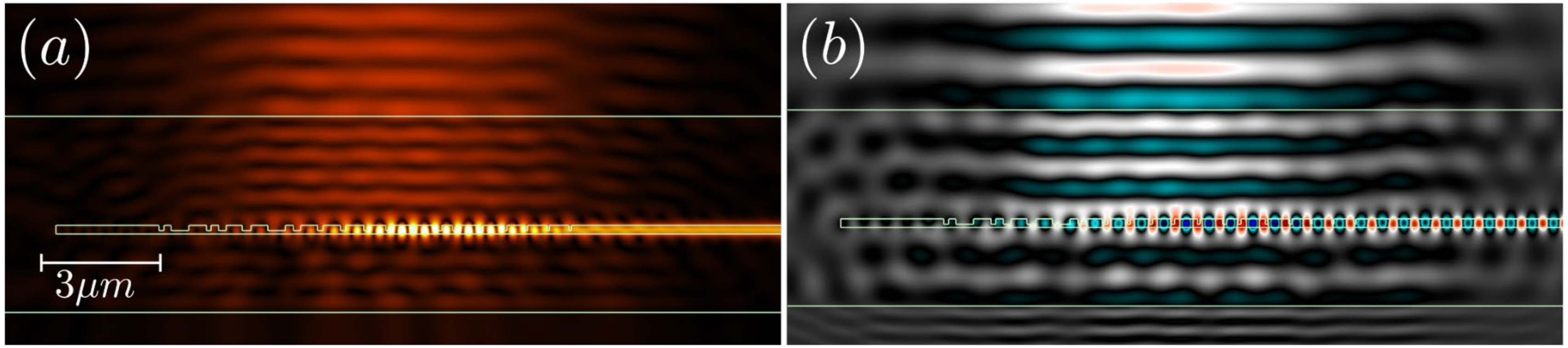

Sideris, Garza, Bruno [2019]

Grating Coupler Wavelength Demultiplexer

Design method: Sideris, Garza, Bruno

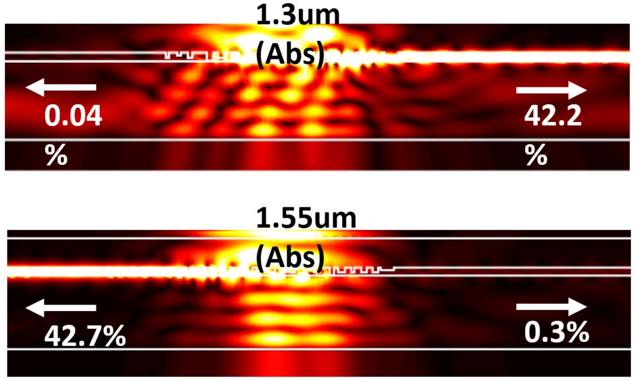

Fabrication and Measurement:
Hajimiri's lab (Caltech)
(Sideris, Bruno et al.)

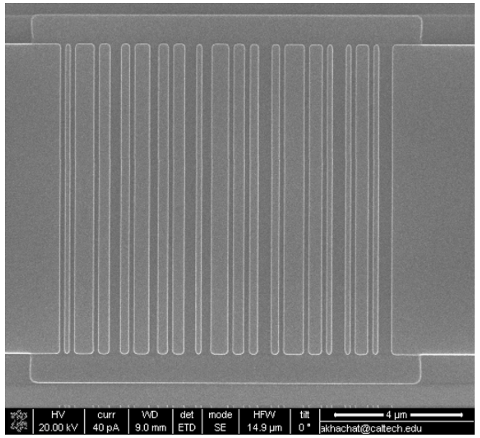

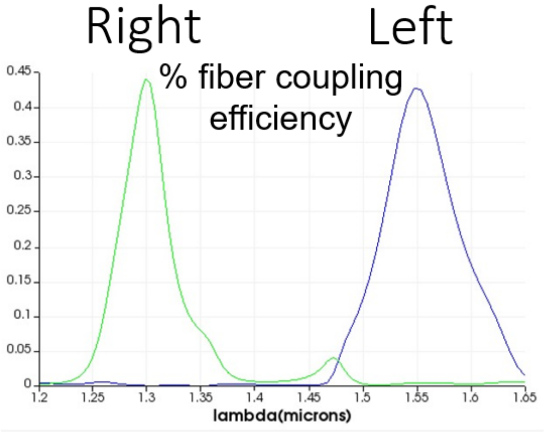

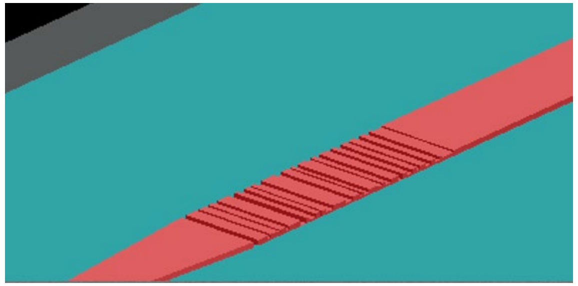

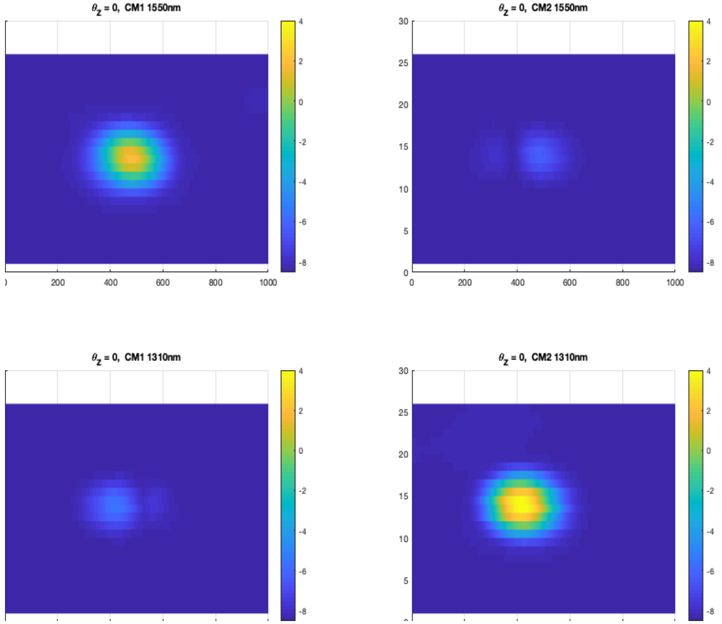

Minimum feature size: 160 nm (suitable for scalable standard foundry process. e beam lithography not required.)

Absolute insertion losses: 3.77dB for 1310nm port and 4.7dB for the 1510nm port. Isolation: ~10dB at each frequency (measured power at the correct port divided by measured power at the wrong port).

Sideris, Bruno et al.,
Nature Commun. Phys. [2022]

Waveguide Taper / Mode Converter

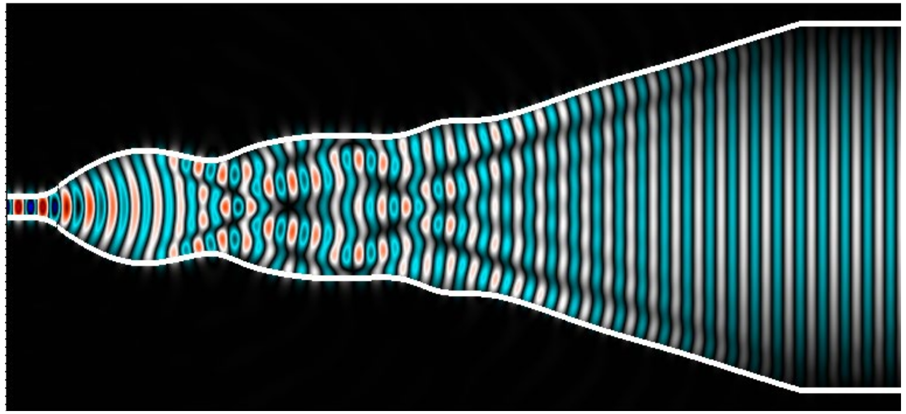

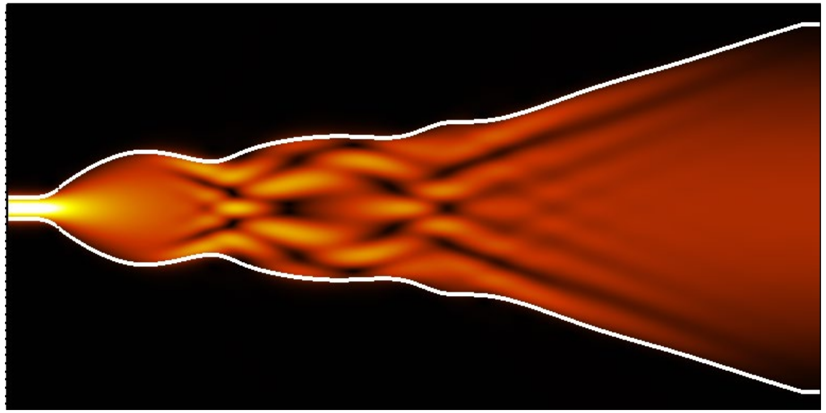

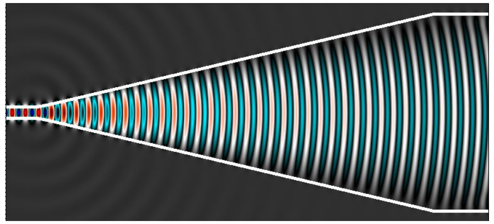

— 15 min single core run
— 99% efficiency

Bruno, Garza and Sideris [2019]

Reference: Yablonovitch et. al [2018]

— FDTD-based
— 35.7 hr single core equivalent
— 99% efficiency
— (2hr 33min on 14-core)

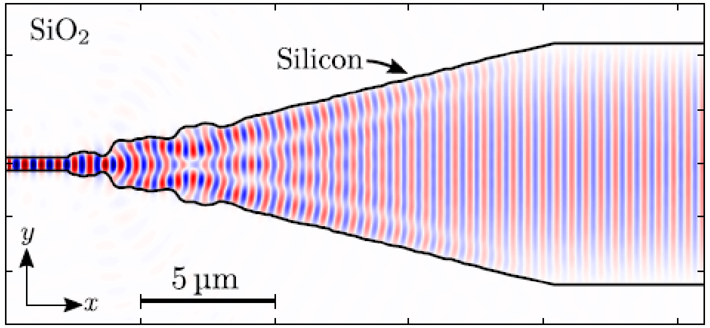

Adjoint Optimization

(gradient descent; one solve per full gradient)

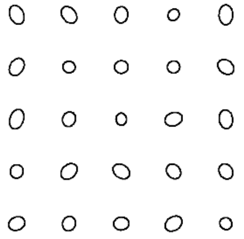

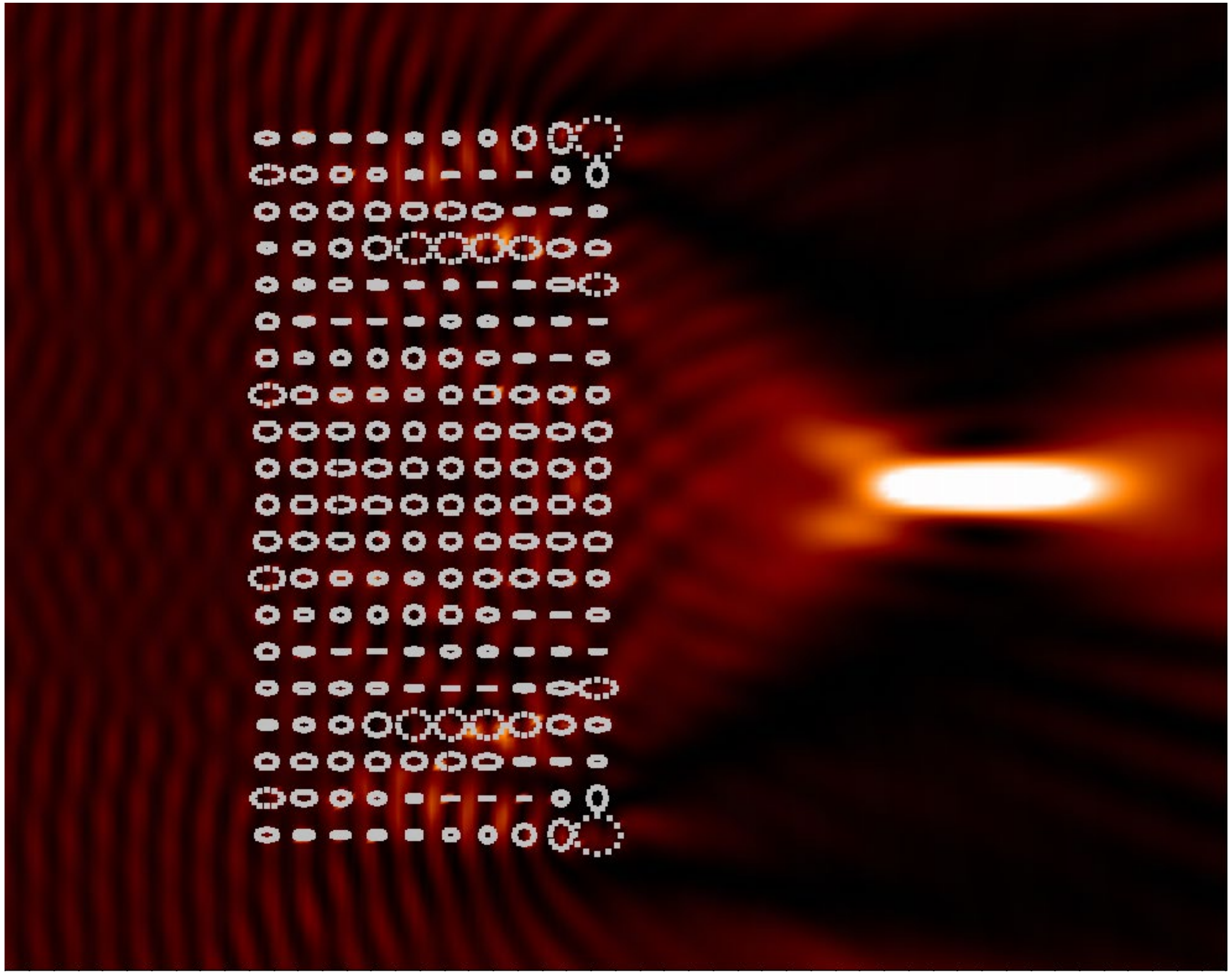

O. Bruno and E. Garza [2018]

Adjoint Optimization
Array of Elliptical Cylinders
(gradient descent; two solves per full gradient)

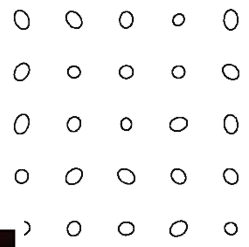

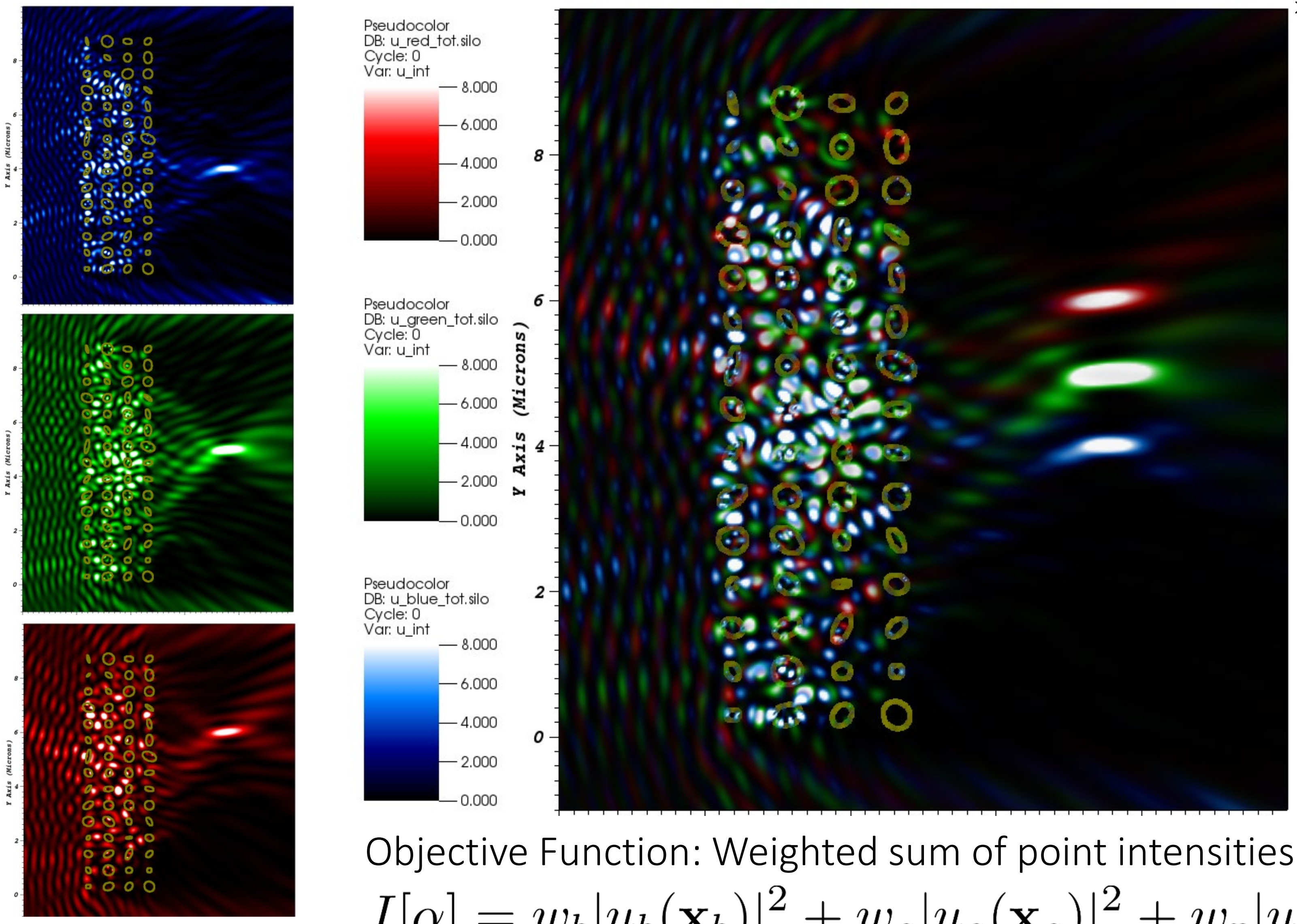

Objective Function: Weighted sum of point intensities:

$$I[\alpha] = w_b|u_b(\mathbf{x}_b)|^2 + w_g|u_g(\mathbf{x}_g)|^2 + w_r|u_r(\mathbf{x}_r)|^2$$

Single-Objective Optimization

SiO$_2$ nanoposts in transparent matrix

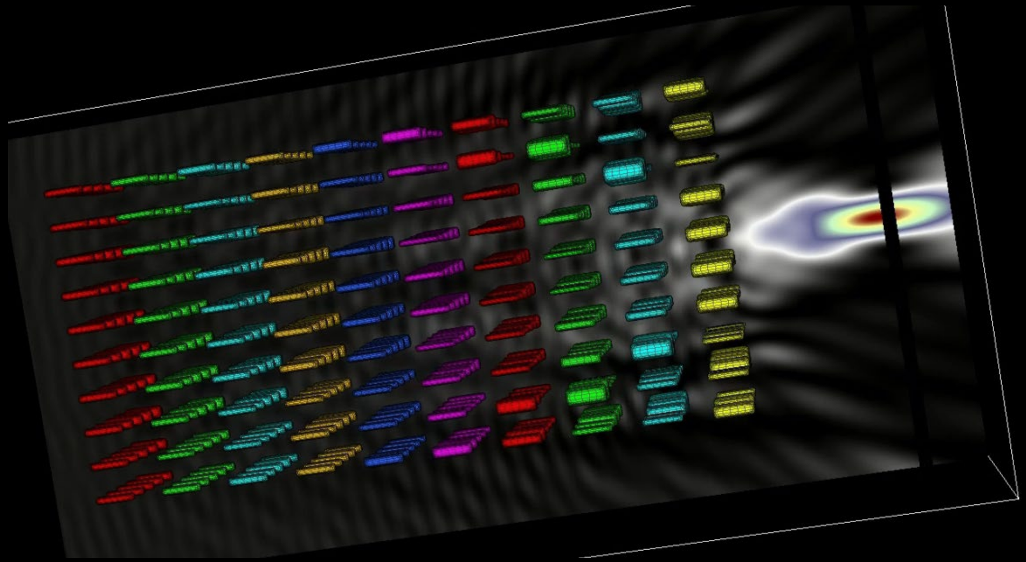

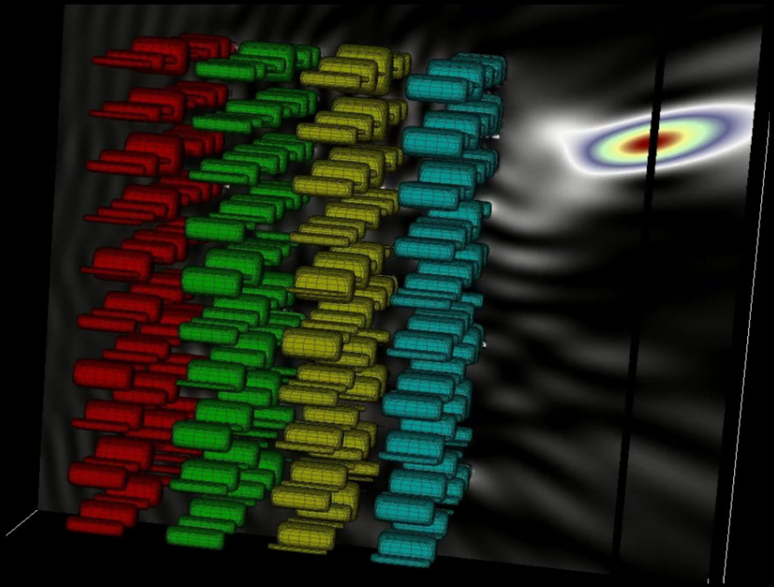

Bruno, Fernandez-Lado, Garza, [2018]

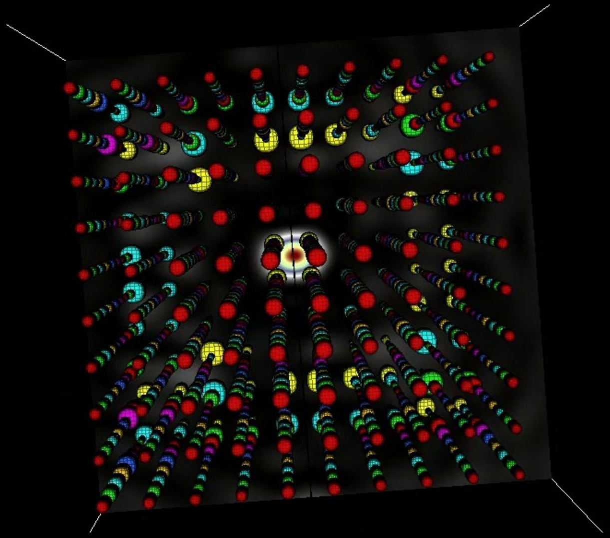

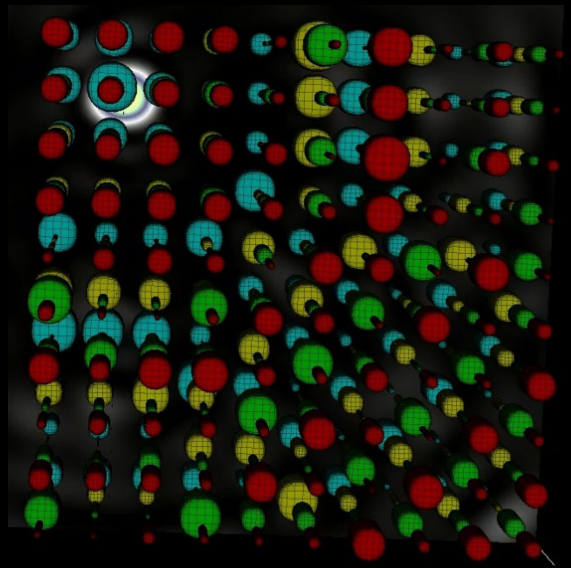

4,178 $(\lambda_{int})^3$= 1,315.3 $(\lambda_{ext})^3$

1,671 $(\lambda_{int})^3$= 540.5 $(\lambda_{ext})^3$

Multi-objective Wavelength and Polarization Splitter

TiO_2 nanoposts in SiO_2 matrix. Array size: 2,439 $(\lambda_{int})^3$

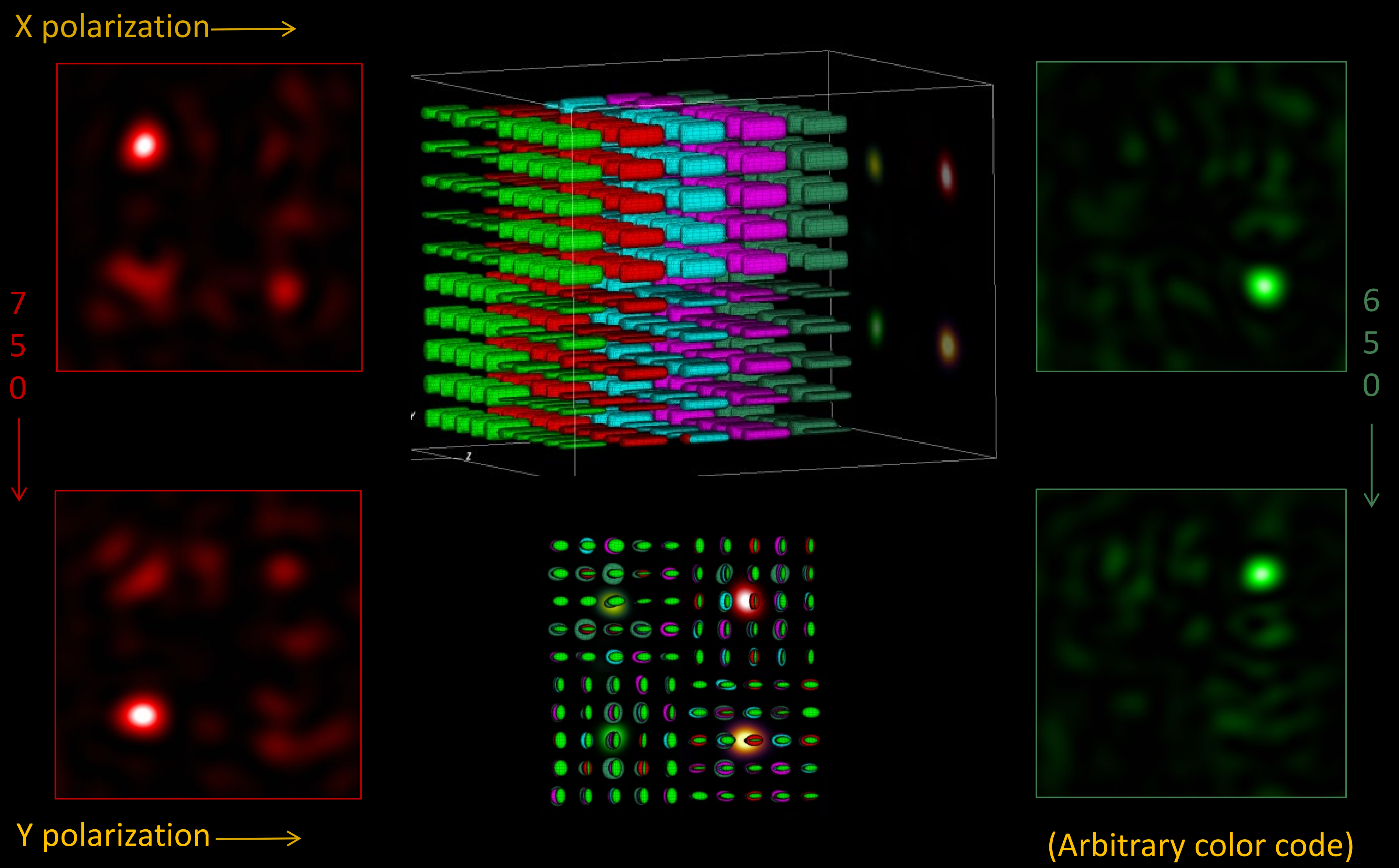

Multiobjective Optimization:
Single array achieves both words

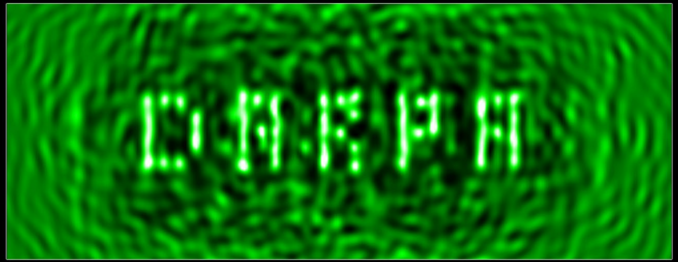

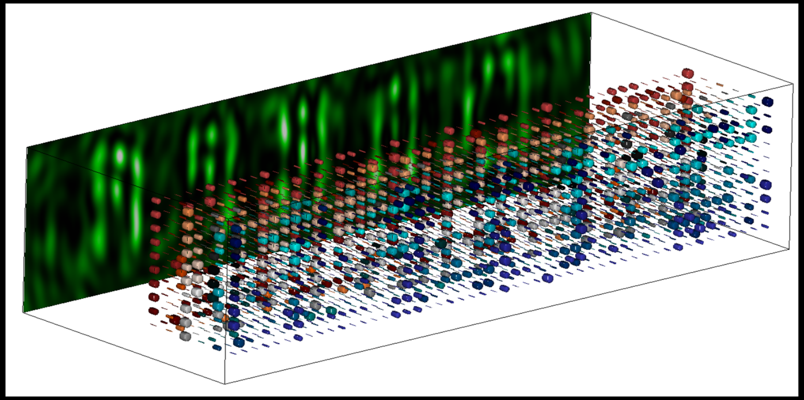

pt_472nm.silo

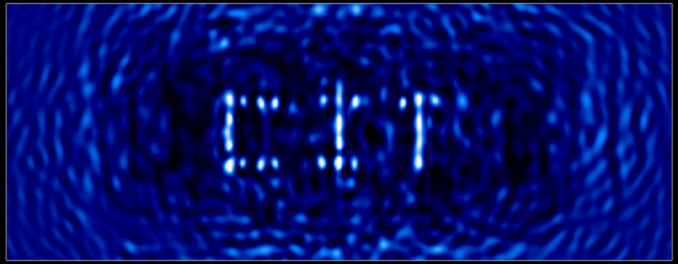

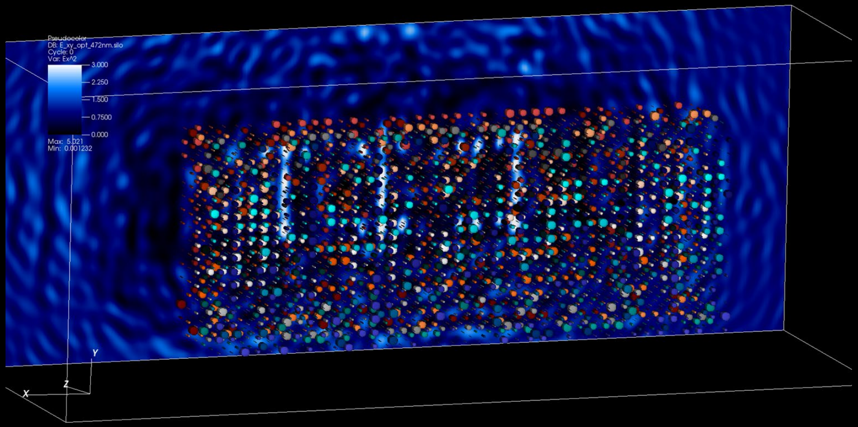

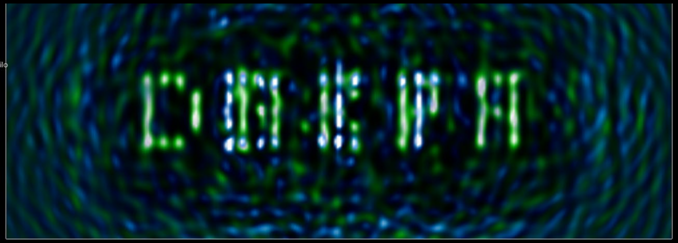

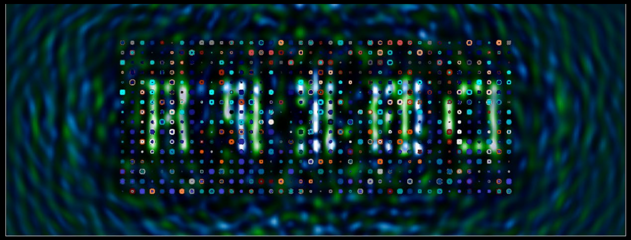

Double Wavelength Lens

λ_0= 780 nm
a-Si posts, ref. index = 3.66
Fused silica substrate, ref. index = 1.453

λ_0= 915 nm
a-Si posts, ref. index = 3.554
Fused silica substrate, ref. index = 1.453

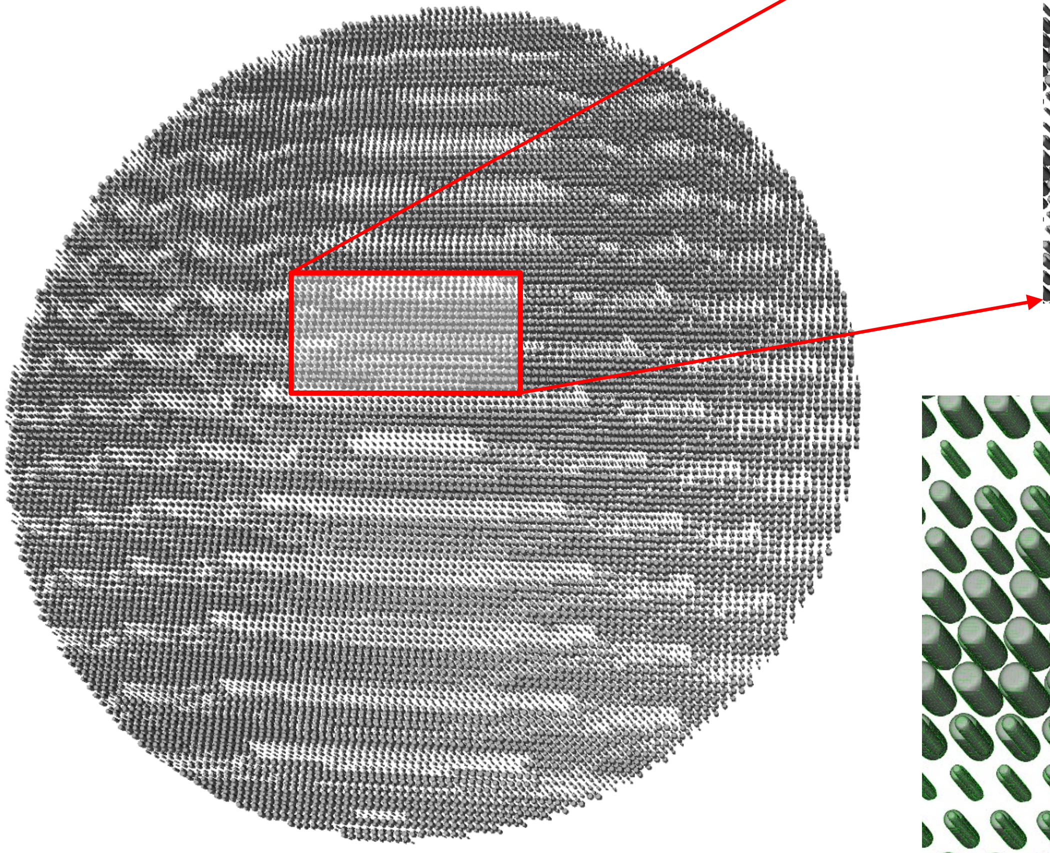

40x40x1.7 microns

2 layers x 10,261 posts = 20,522 posts

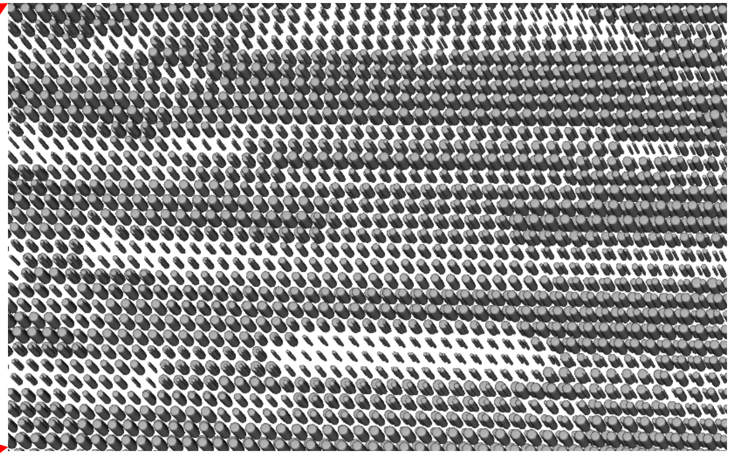

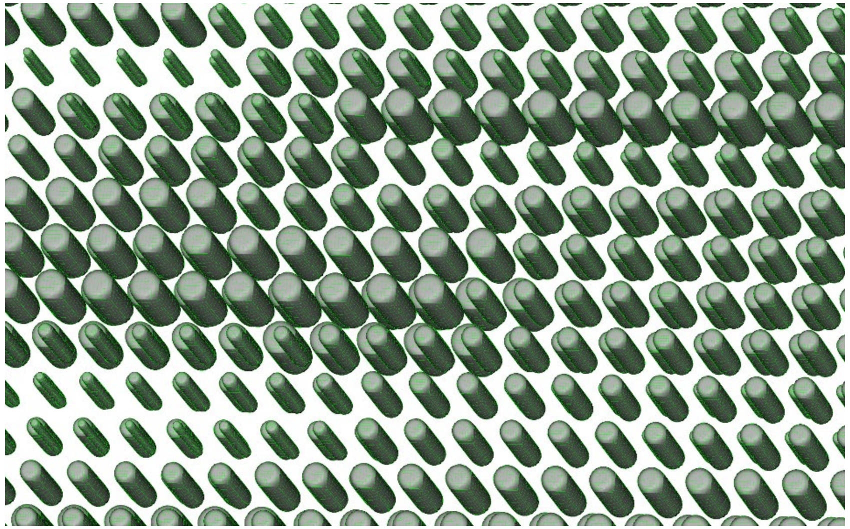

(Device design courtesy of Prof. Amir Arbabi.)

OpenMP IFGF-Accelerated Dielectric Simulation: single node (28 cores)

(Previously run in a 30-node 56 core/node computer cluster. Preliminary results; work in progress)

λ = 915 nm

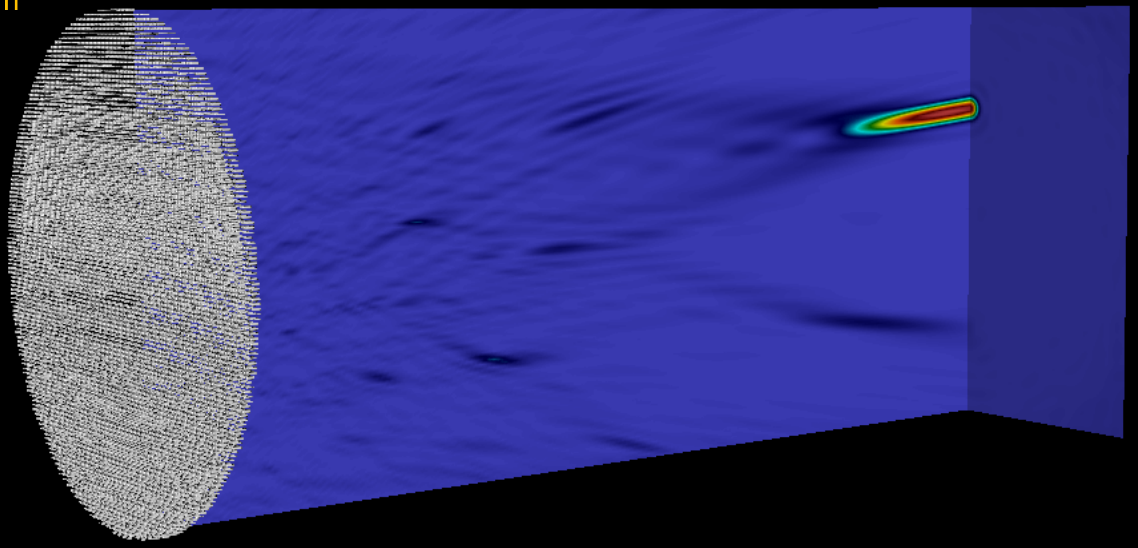

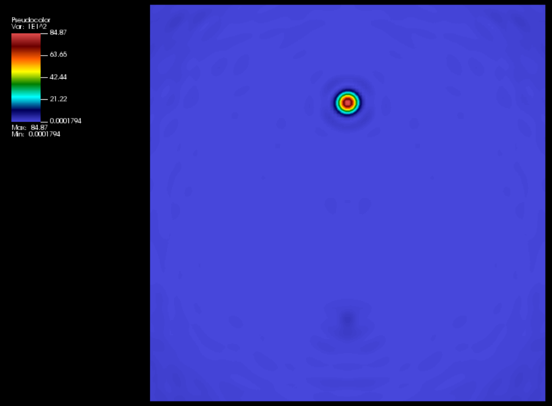

915 nm light focused at (0,10,91.425) microns

λ = 780 nm

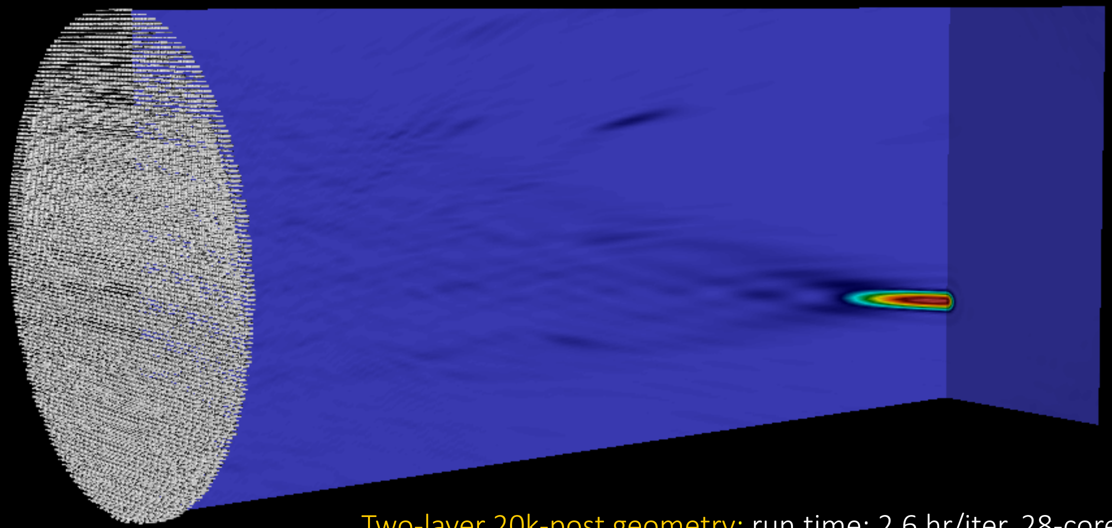

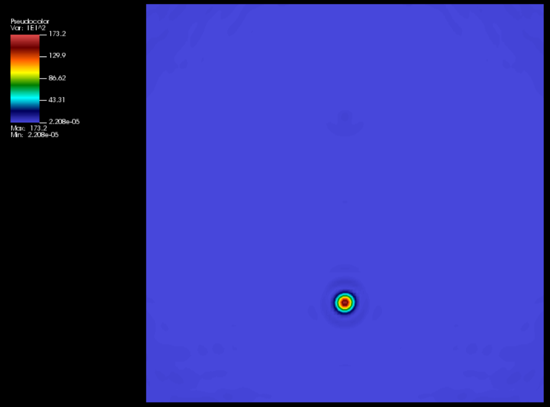

780 nm light focused at (0,-10,91.425) microns

Two-layer 20k-post geometry: run time: 2.6 hr/iter, 28-cores, ***78.8 million*** unknowns,
20 GMRES iter, total memory: 146 GB

C. Bauinger, O. Bruno and E. Jimenez, [2021]

Complete Hybrid OpenMP/MPI Solvers: 41k-post geometry

(Preliminary results; work in progress)

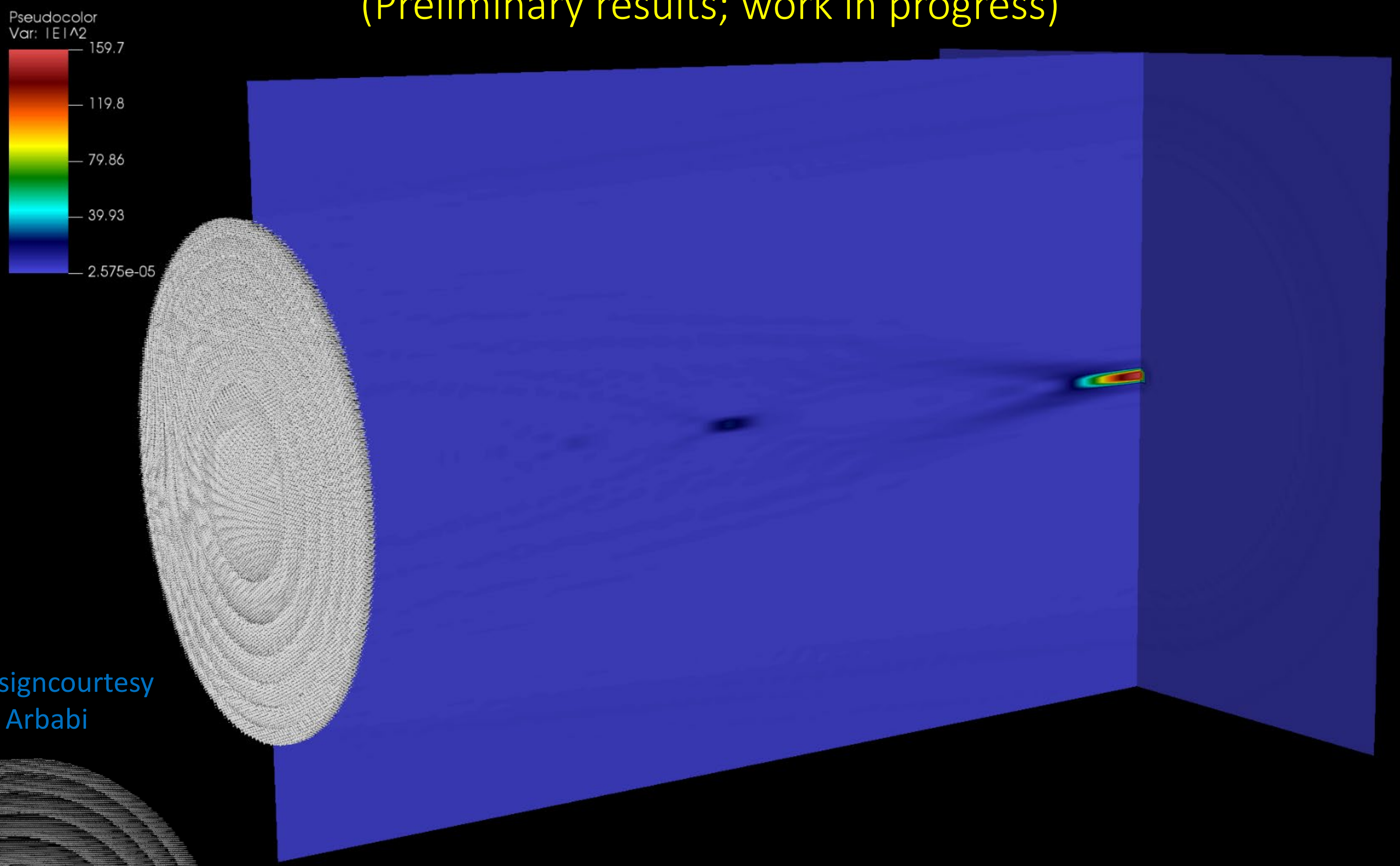

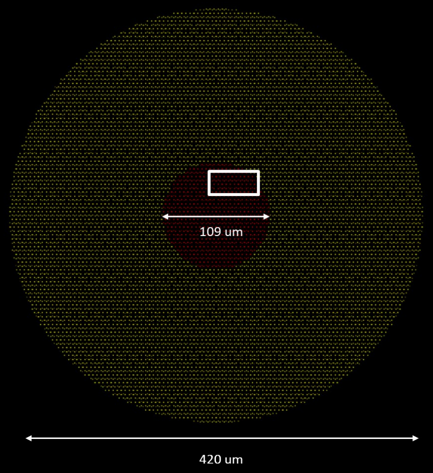

Device designcourtesy
Prof. Arbabi

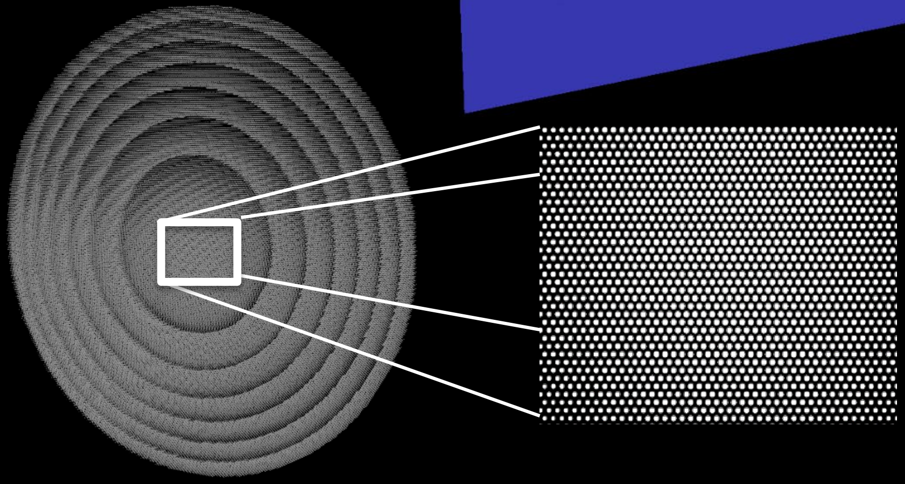

$66\mu m \times 66\mu m \times 1.1\mu m$

λ_0= 780 nm, posts ref. index = 2.5, substrate ref. index = 1.47

One-layer 41k-post geometry:
run time: 15.7min/iter, 16 nodes (28-cores/threads) per node, 448 total cores) ,
157.6 million unknowns

Complete Hybrid OpenMP/MPI Solvers: 82k-post geometry

IFGF-based acceleration

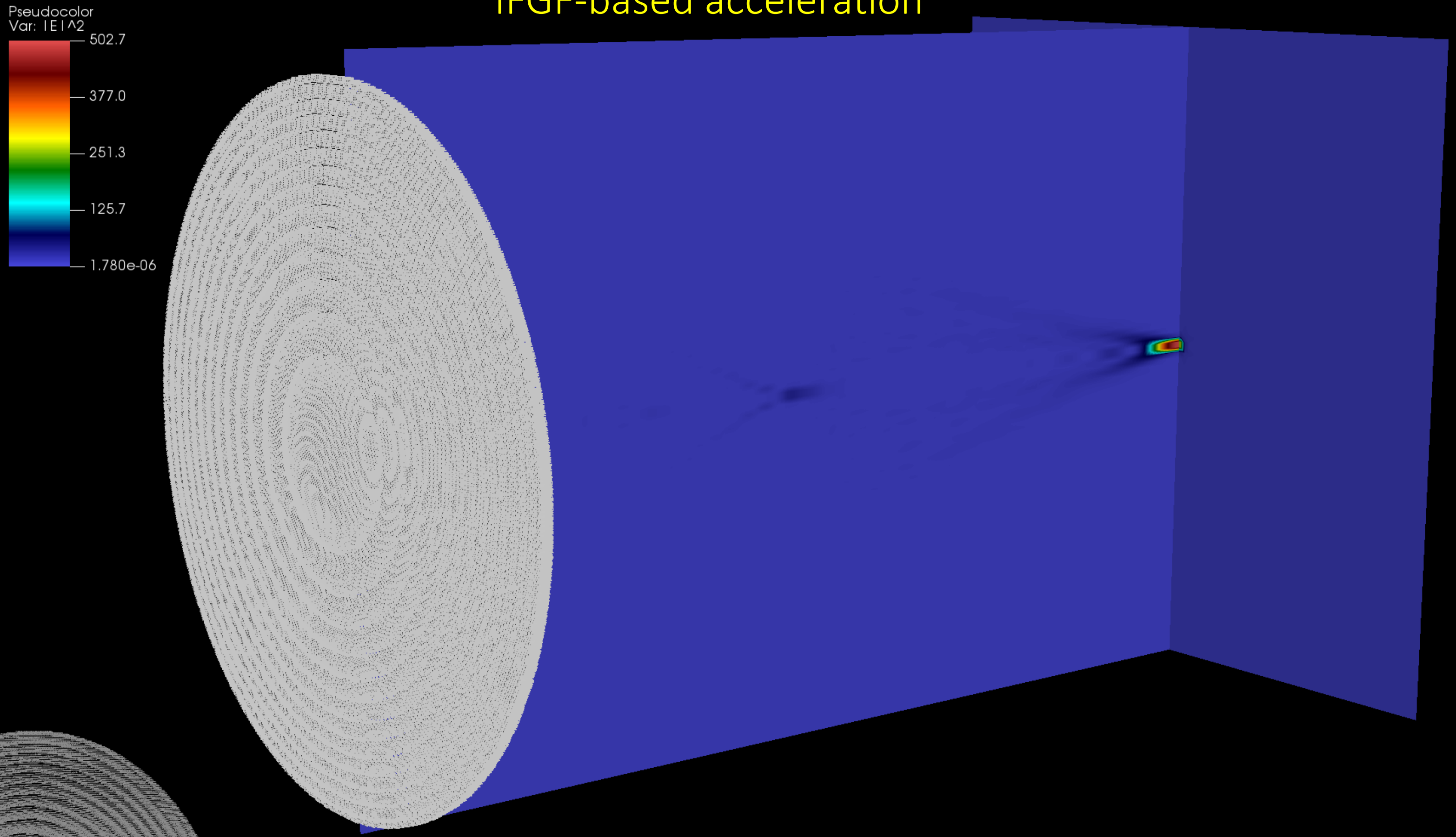

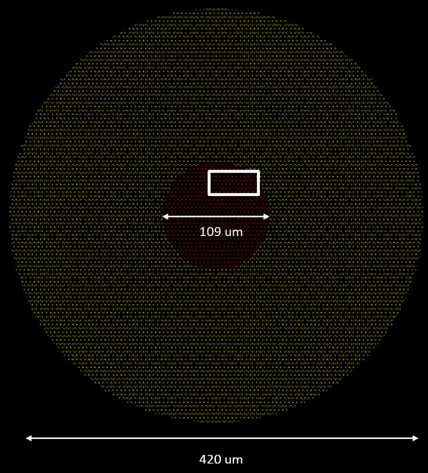

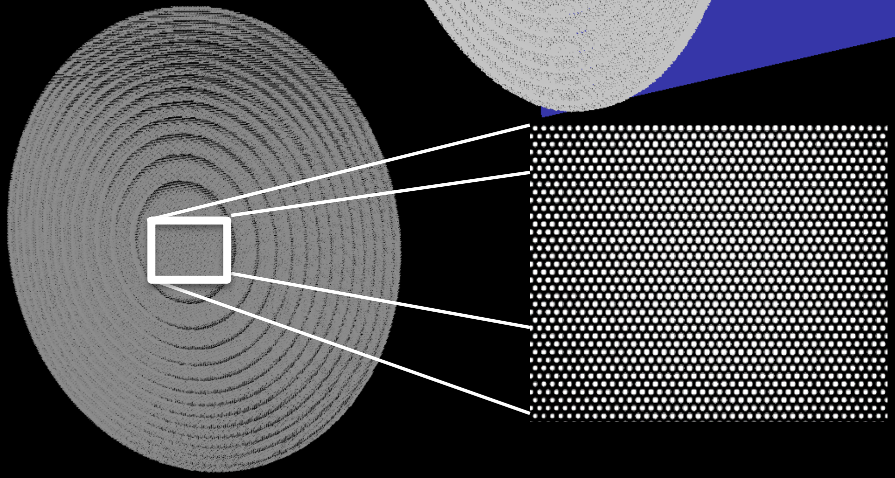

94x94x1.1 microns

λ_0= 780 nm, posts ref. index = 2.5, substrate ref. index = 1.47

One-layer 82k-post geometry:
(28-cores/threads per node, 448 total cores) ,
315.3 million unknowns

Topics

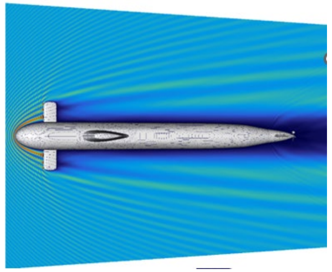
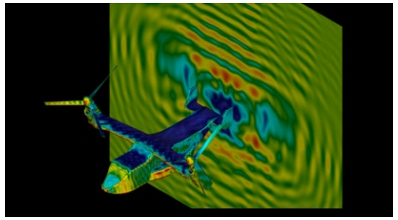

– Interpolated Factored Green Function (IFGF): FFT-free acceleration algorithm

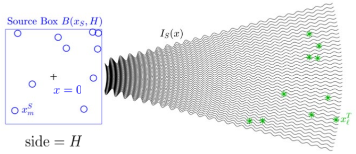

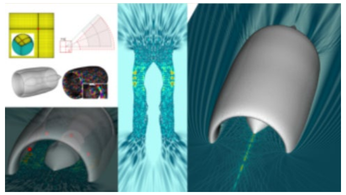

– OpenMP on 28-core server and MPI on 1680 cores

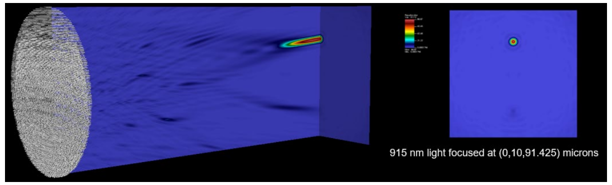

– Metamaterials: large computer cluster, photonics modeling

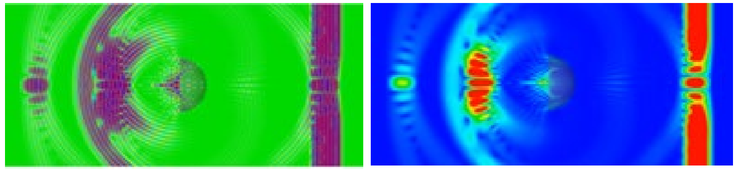

– Time-domain frequency-time hybrid solver

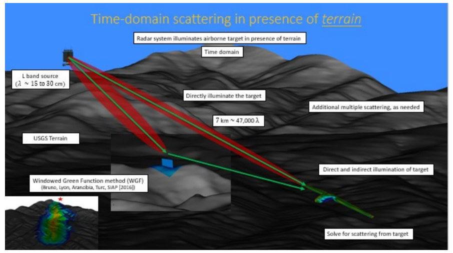

– Long-range time-domain propagation over terrain

– Long-range propagation: Screened WKB

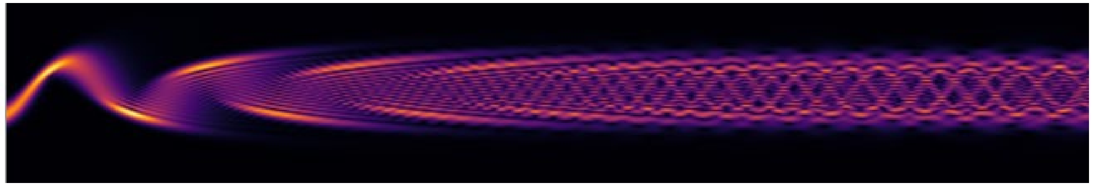

Advanced Computational Methods

for electromagnetic modeling, simulation and design

Oscar P. Bruno
Caltech

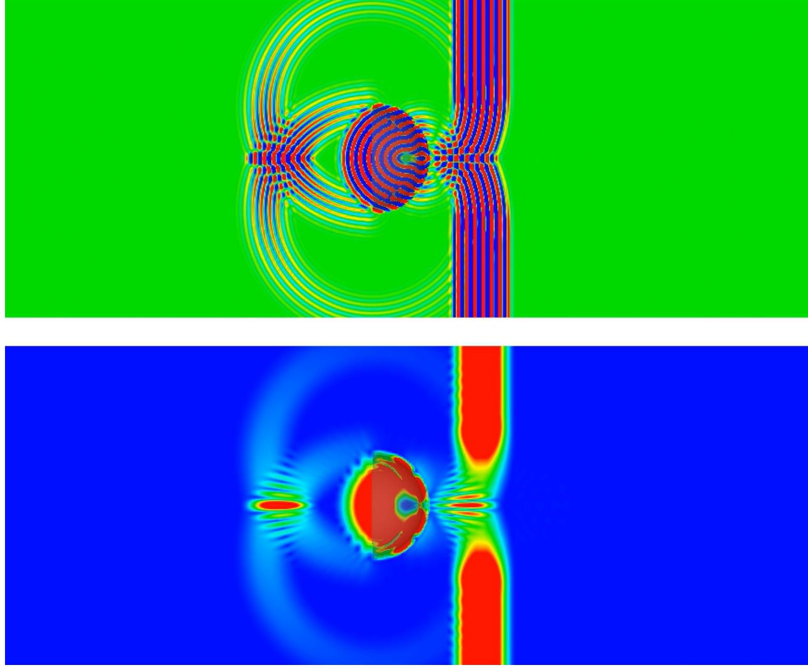

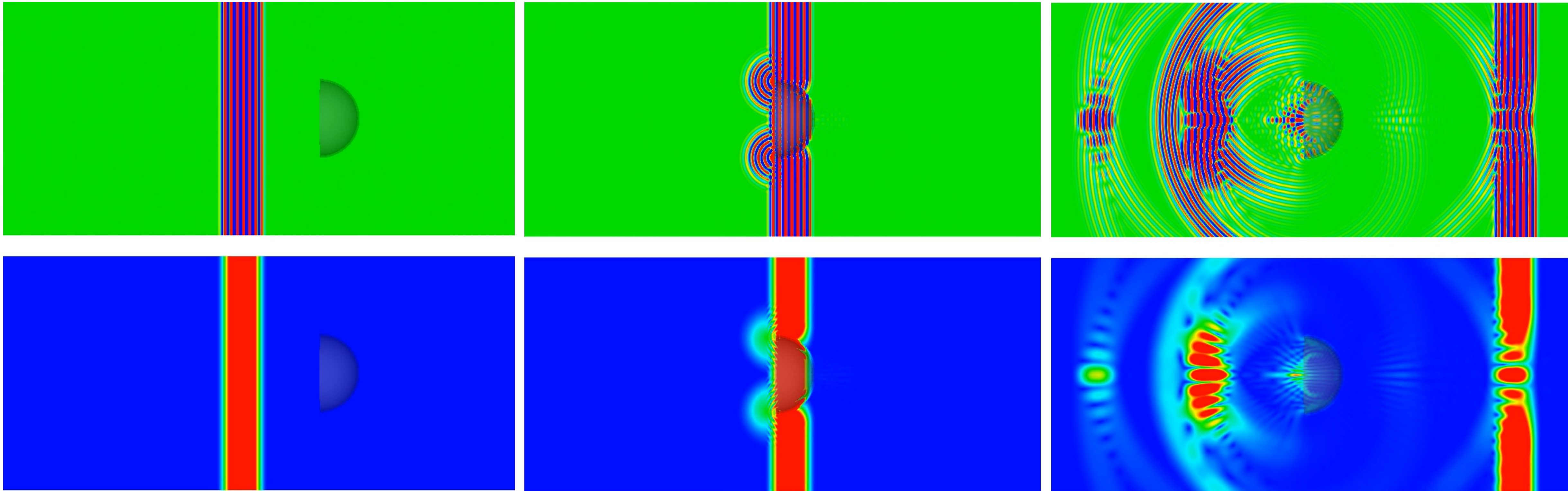

Topics

– Interpolated Factored Green Function (IFGF): FFT-free acceleration algorithm

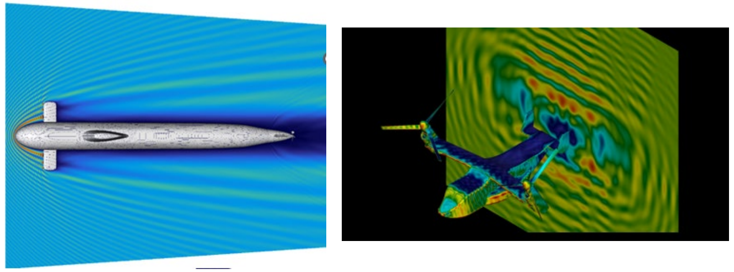

– OpenMP on 28-core server and MPI on 1680 cores

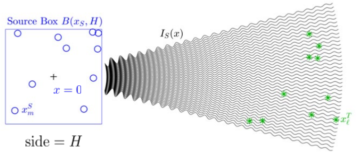

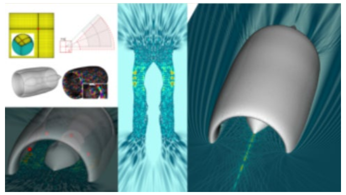

– Metamaterials: large computer cluster, photonics modeling

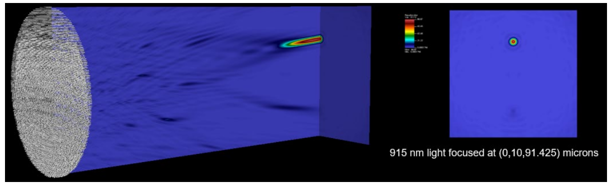

– Time-domain frequency-time hybrid solver

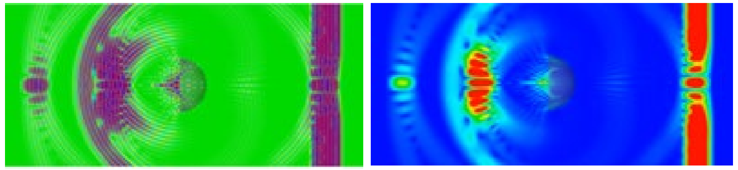

– Long-range time-domain propagation over terrain

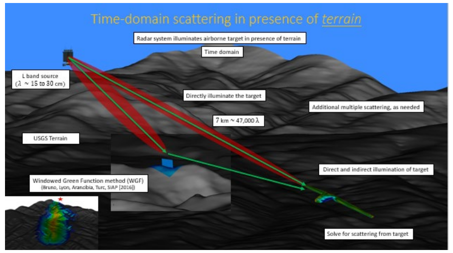

– Long-range propagation: Screened WKB

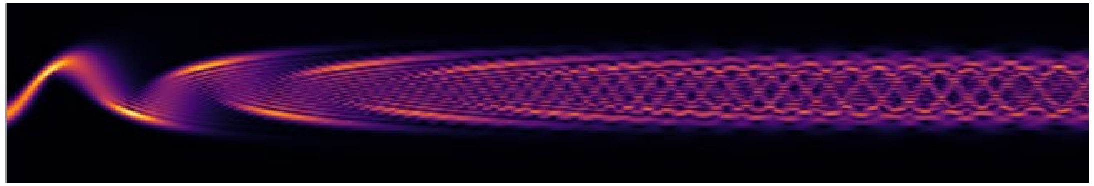

Topics

- IFGF Parallelization approach: space-filling Z-curves and cone-segment parallelization
- OpenMP on 28-core server and MPI on 1680 cores
- Metamaterials: near cm-scale photonics modeling, optimization and design
- ➢ Time-domain frequency-time hybrid solver
- Long-range time-domain propagation over terrain
- Long-range propagation: Screened WKB (S-WKB)

“Hybrid” Time-domain from frequency domain

Time-parallel, time-leaping, wave equation/Maxwell solver

<u>Freq. Domain vs. Time Transients:</u>

$$\frac{\partial^2 u}{\partial t^2} = c^2 \Delta u \quad \Longleftrightarrow \quad \Delta \psi_\omega + k^2 \psi_\omega = 0$$

(Fourier Transform)

$$u(\mathbf{r}, t) = \psi_\omega(\mathbf{r}) e^{i\omega t}$$

No need to discretize space
Spectrally accurate in time

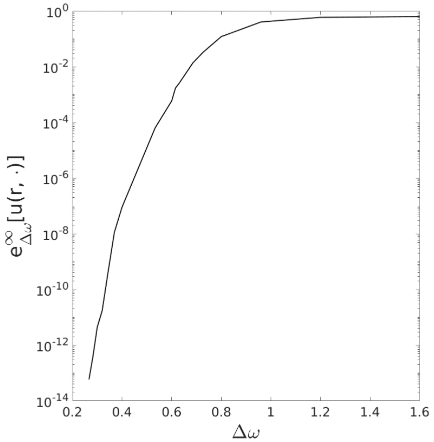

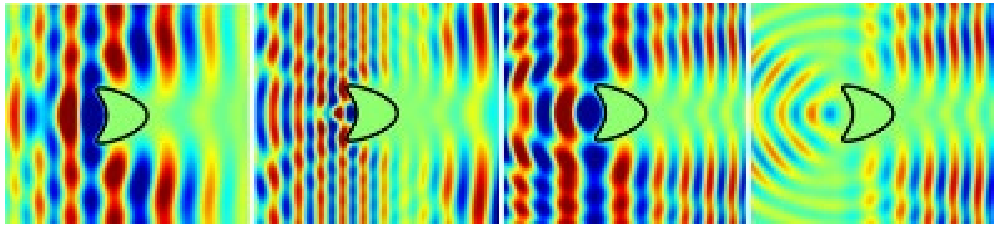

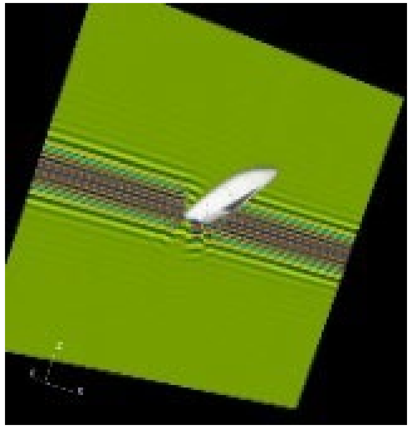

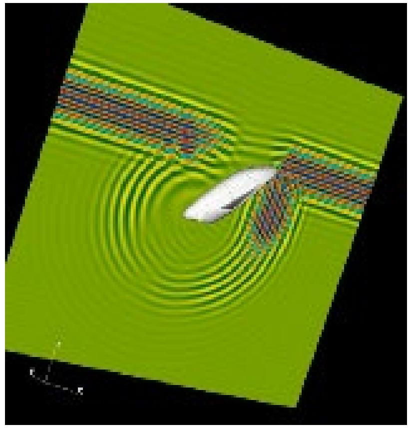

Windowing and recentering
High-frequency time integration

Anderson, Bruno and Lyon, SISC [2020]

Smooth Incident-Field Time Partitioning

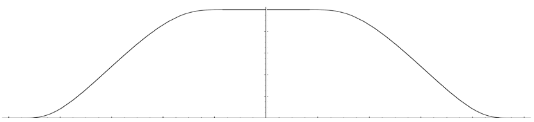
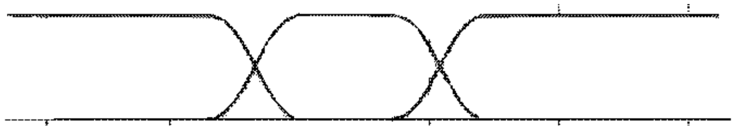

— Use a partition of unity to decompose the long duration signal $u^{inc}(x,t)$ into multiple relatively short duration signals which require only a fixed discretization in frequency space.

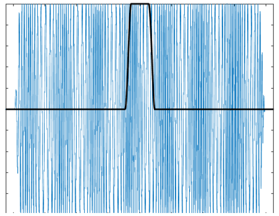

$$F_k(\omega) = \int_{-T}^{T} w_k(t) u^{inc}(x,t) e^{i\omega t} dt = \int_{t_k-h}^{t_k+h} w_k(t) u^{inc}(x,t) e^{i\omega t} dt$$

$$= \boxed{e^{i\omega t_k}} \int_{-h}^{h} w_k(t+t_k) u^{inc}(x, t+t_k) e^{i\omega t} dt$$

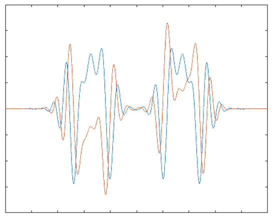

— Using the same discretization in frequency space for each time-windowed problem, the Helmholtz solutions at each frequency may be reused.

$$\int_{-h}^{h} w_k(t+t_k) u^{inc}(x, t+t_k) e^{i\omega t} dt \longrightarrow \hat{G}_k(x,\omega)$$

Time evolution via FFT-based “scaled convolution”

After time windowing and recentering, $u^{inc}(x,\omega)$, and thus, the solution $u(x,\omega)$, become a slowly varying, approximately band-limited functions of ω:

$$u(x,t) = \int_{-\infty}^{\infty} u(x,\omega)e^{-i\omega t}d\omega \approx \int_{-W}^{W} u(x,\omega)e^{-i\omega t}d\omega$$

Higher frequency integration for larger t! Substitute $u(x,\omega)$ by its truncated Fourier Series approximation in ω:

$$u(x,t) \approx \sum_{m=-N/2}^{N/2-1} c_m(x) \int_{-W}^{W} e^{i\frac{\pi}{W}(m-\frac{W}{\pi}t)\omega} d\omega = \sum_{m=-N/2}^{N/2-1} c_m(x)(2W\mathrm{sinc}(\alpha t - m))$$

Then, discretizing in t we obtain a “scaled convolution”:

$$u(x,t_\ell) \approx \sum_{-N/2}^{N/2-1} c_m b_{\beta\ell-m}, \quad \text{where} \quad b_q = 2W\mathrm{sinc}(q)$$

Use FFT-accelerated *Fractional Fourier Transform*-based scaled discrete convolutions

Benefits

- Overall cost: linear in time and proportional to the cost of the frequency domain solver. Less expensive asymptotics than FDTD.
- No time-domain numerical dispersion error (!!).
- Natural Parallelism for frequency-domain solutions.
- Natural Parallelism in time! (cf. P. L. Lions "para-real" algorithm).
- Time- and Space-Leaping (!!).
- $O(1)$ cost for solution sampling at arbitrarily large times (!!)
- Use of absorbing boundaries, PML, etc., not necessary.
- High-order accuracy (periodic time integration).

Example: High-altitude glider

NASA's X-24A Lifting Body

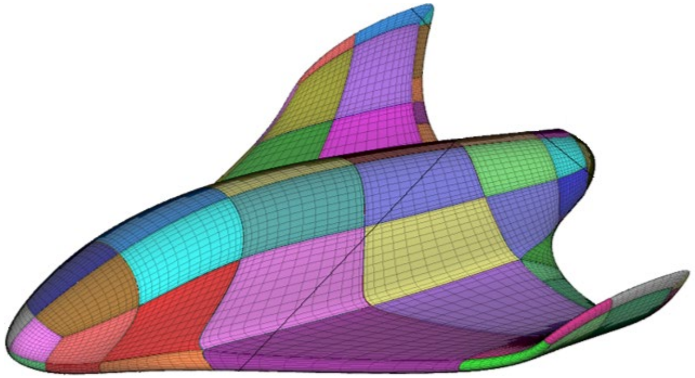

Utilizing frequency-domain solutions…

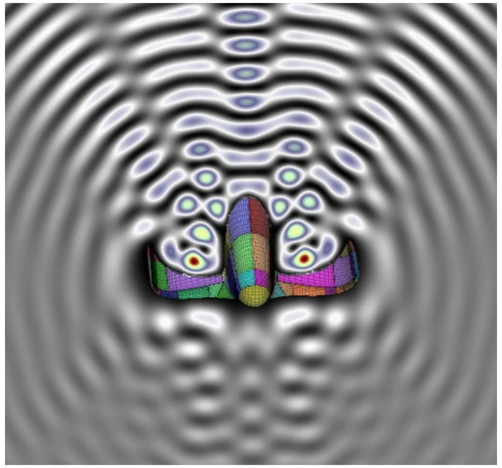

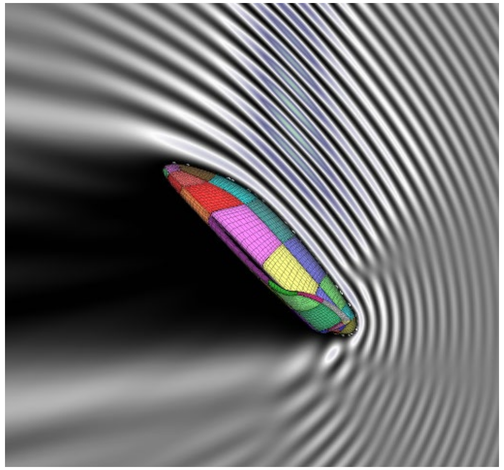

(Bruno and Garza, “Rectangular-polar integral solver”, arXiv [2018])

…the Fast-Hybrid method produces solutions in the time domain

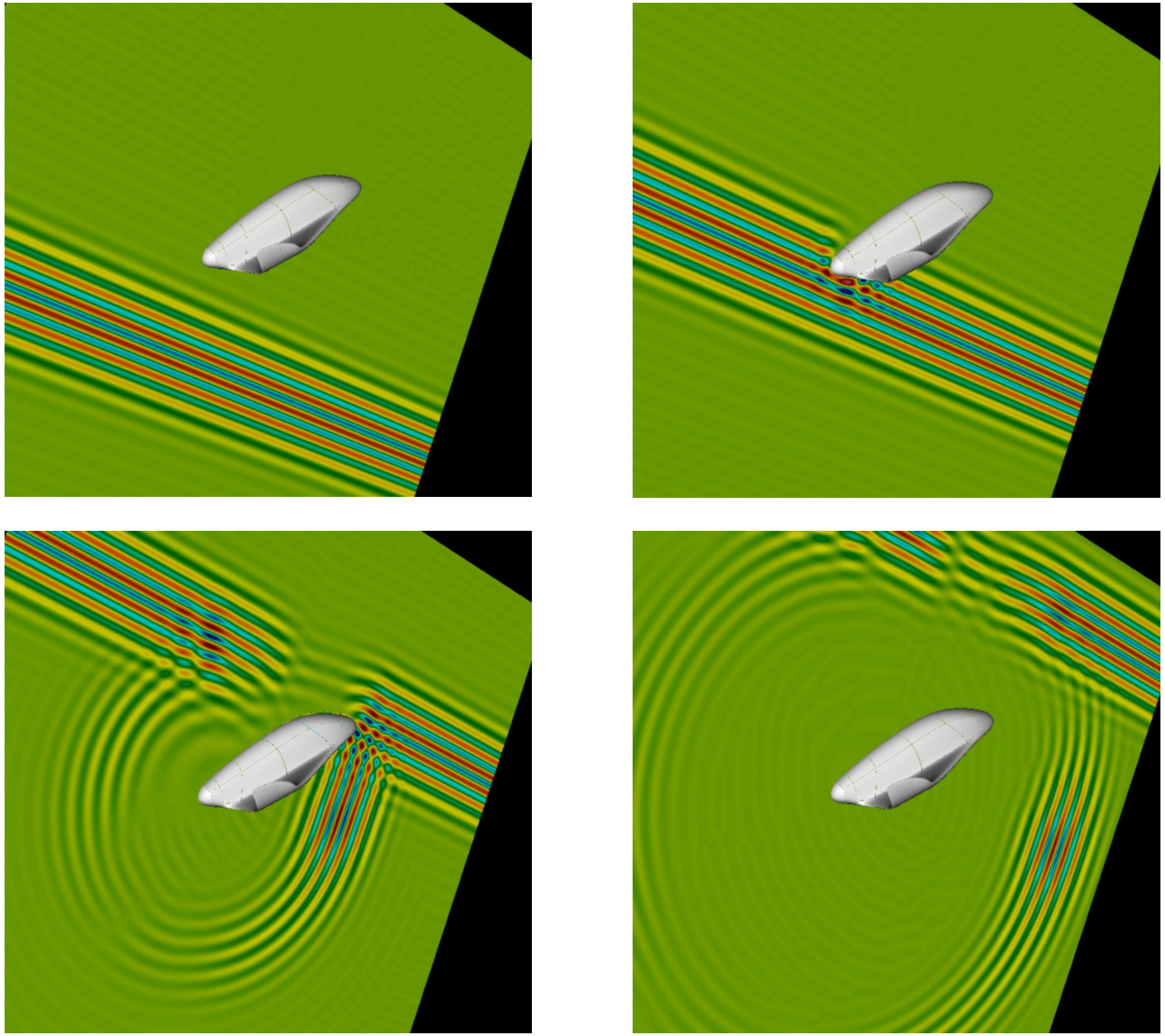

Anderson, Bruno and Lyon [2018]

Cost comparisons** with…

…time-domain integral equations *and* convolution quadrature

Significant advantages even for short (Gaussian) incident pulses

(worst case for hybrid method)

—	$\|\|e\|\|_\infty$	CPU Time (hrs)	Mem (GB)
Hybrid method (unaccel.)	$2.2 \cdot 10^{-4}$	4.3	1.6
[BK14] (accel.)	$2.1 \cdot 10^{-3}$	40.1	56.8

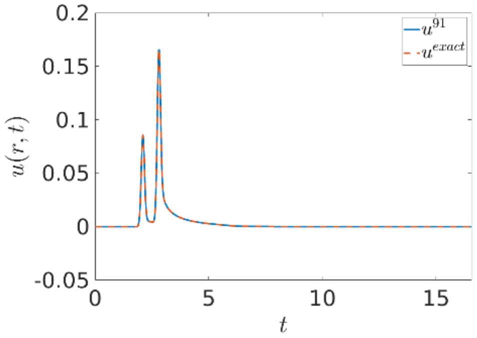

—	$\|\|e\|\|_\infty$	Wall Time (mins)	Mem (GB)
Hybrid method (unaccel.)	$1.6 \cdot 10^{-7}$	4.1	1.2
[BGH19] (unaccel.)	$\approx 10^{-7}$	101.75	290

[BK14]: L. Banjai and M. Kachanovska, *Fast convolution quadrature for the wave equation in three dimensions*, JCP, (2014)

[BGH19]: A. H. Barnett, L. Greengard, and T. Hagstrom, *High-order discretization of a stable time-domain integral equation for 3d acoustic scattering*, JCP, (2020)

**For full details concerning these comparisons see the arXiv publication

[ABL20] T. G. Anderson, O. P. Bruno and M. Lyon, *High-order, Dispersionless ``Fast-Hybrid'' Wave Equation Solver. Part I: O(1) Sampling Cost via Incident-Field Windowing and Recentering*, SISC, (2020)

Challenges Re. near-resonant cavities: Part 1

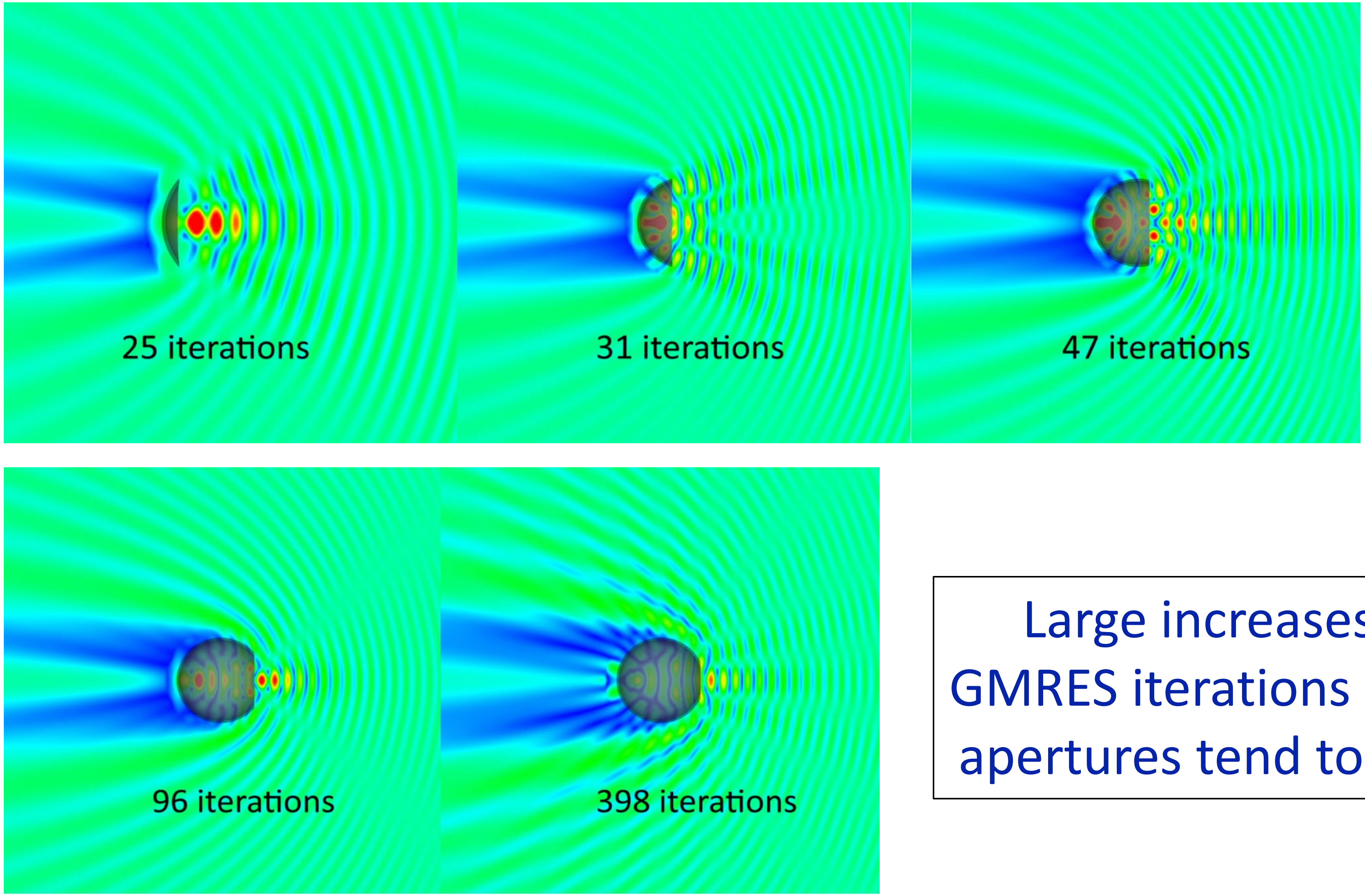

Large increases in GMRES iterations as the apertures tend to close

Frequency-domain resonant scattering problems

(Obtained by experimentation)

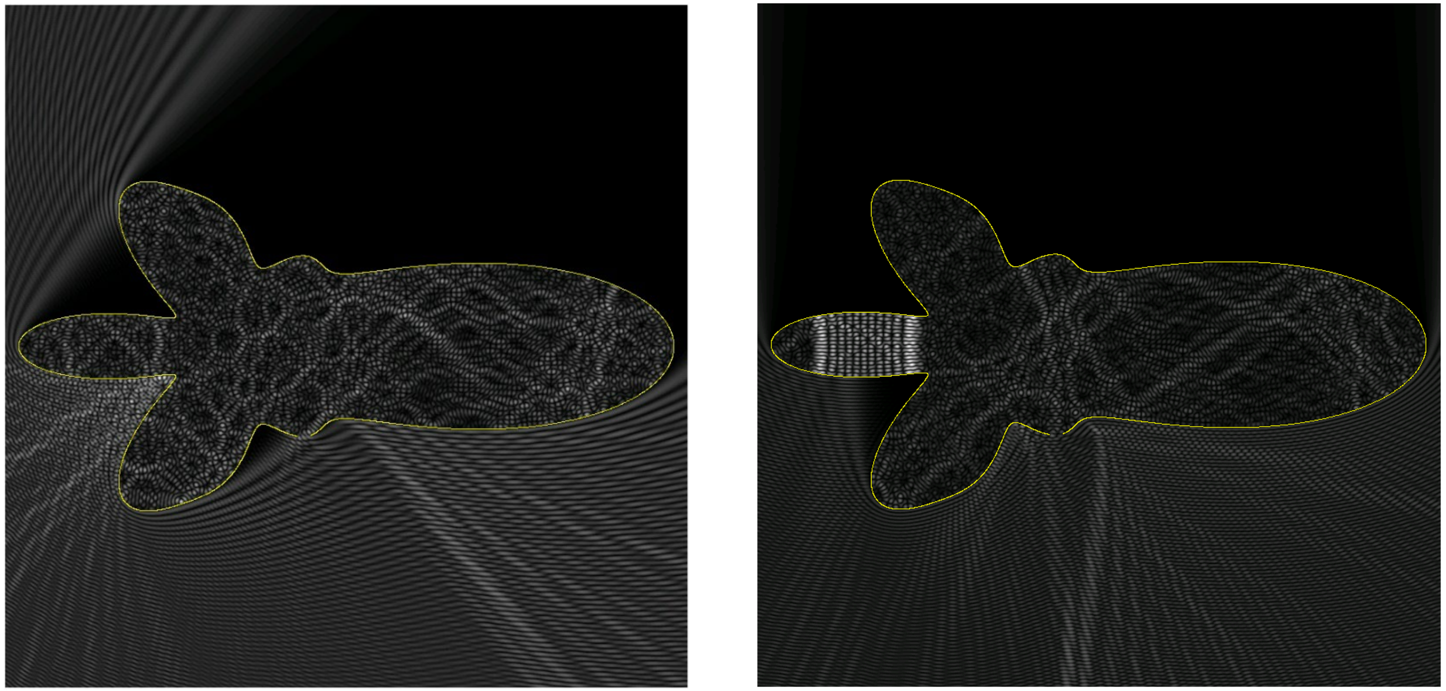

Bruno and Lintner, Radio Science [2012]

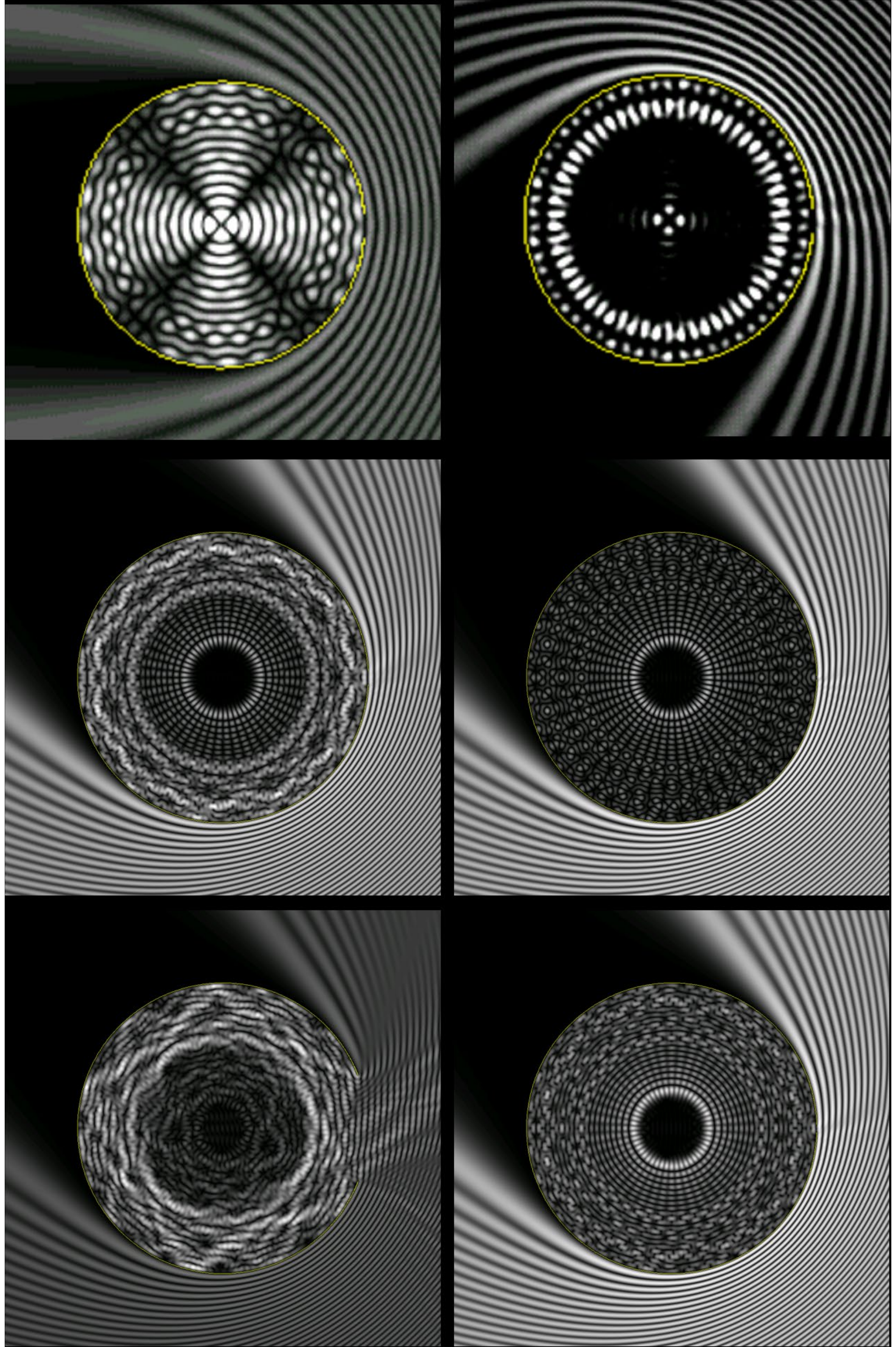

A menagerie of eigenfunctions

(Interior problems)

Dirichlet case

$$\Delta u = -k^2 u, \qquad x \in \Omega$$
$$u = 0, \qquad x \in \Gamma$$

$$\int_\Gamma G_k(x,y)\phi(y)ds_y = 0 \quad \text{for } x \in \Gamma$$

Real singular k (integral): eigenvalues

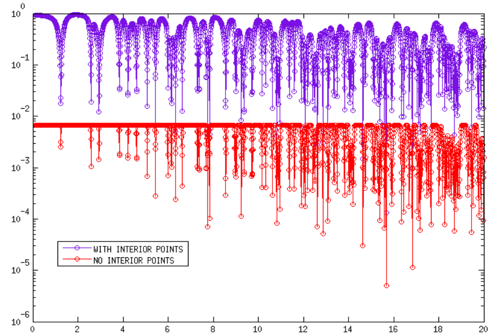

Complex singular k (integral): scattering poles

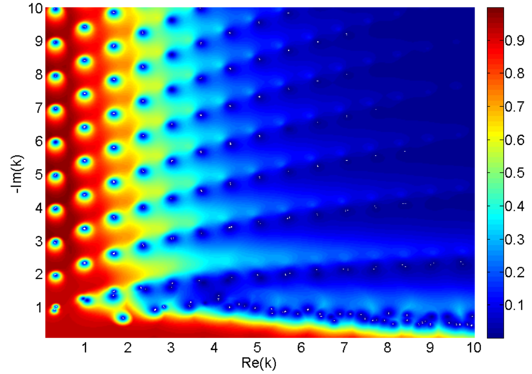

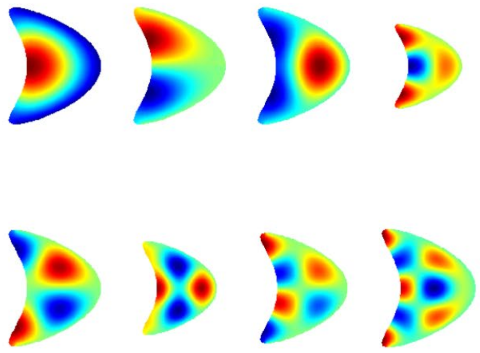

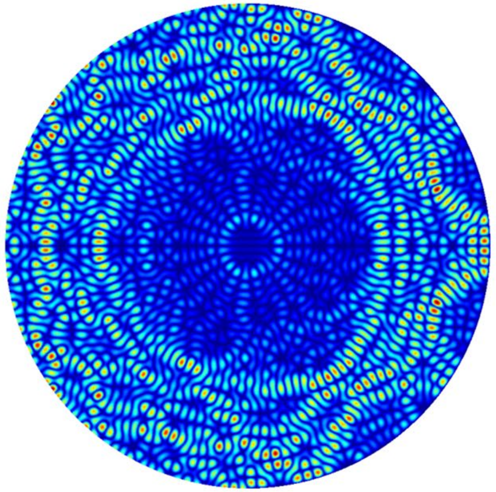

$$\Delta u = -\lambda u$$

Neumann on Left; Dirichlet on Right

$\lambda = 10.005, 97295$

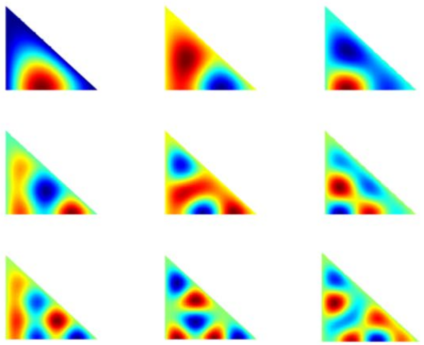

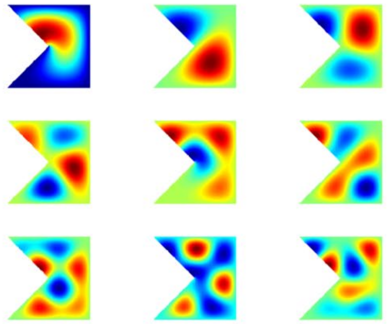

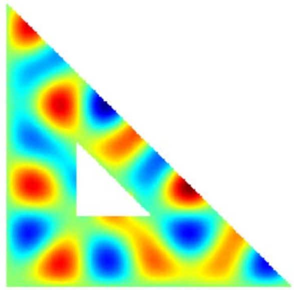

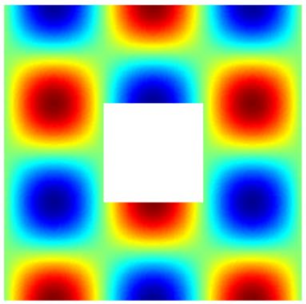

Akhmetgaliev, Bruno and Nigam JCP [2015]

New approach

(Interior and exterior problems, including cavities with apertures)

$$F_k[\psi](x) = \int_\Gamma G_k(x,y)\psi(y)ds_y, \quad x \in \Gamma$$

$S(k) = u^T F_k^{-1} v, \quad$ where $\quad u, v \in \mathbb{C}^n \quad$ are fixed random vectors.

Eigenvalues/scattering poles are poles of $S(k)$

Obtain AAA rational interpolants.

Their poles closely approximate eigenvalues/scattering poles!

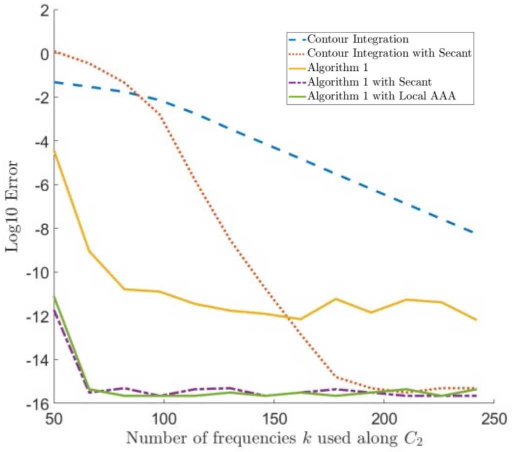

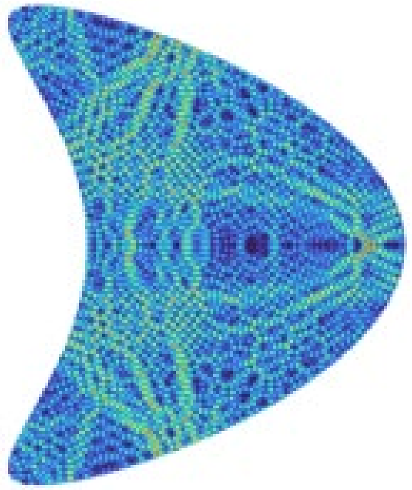

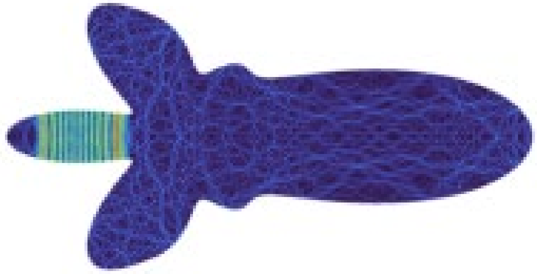

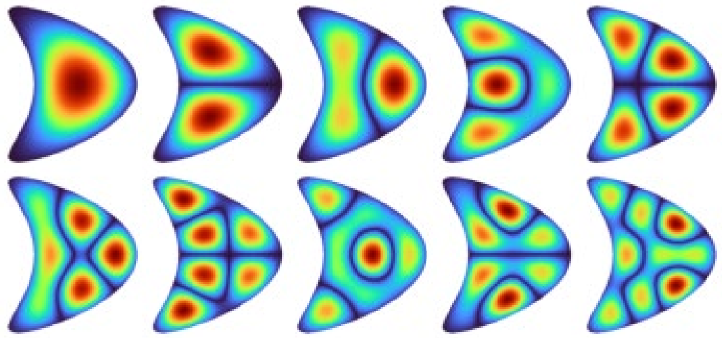

Bruno, Santana and Trefethen, in preparation [2024]

(Available in arXiv soon)

Cavities with apertures

(Exterior problems!)

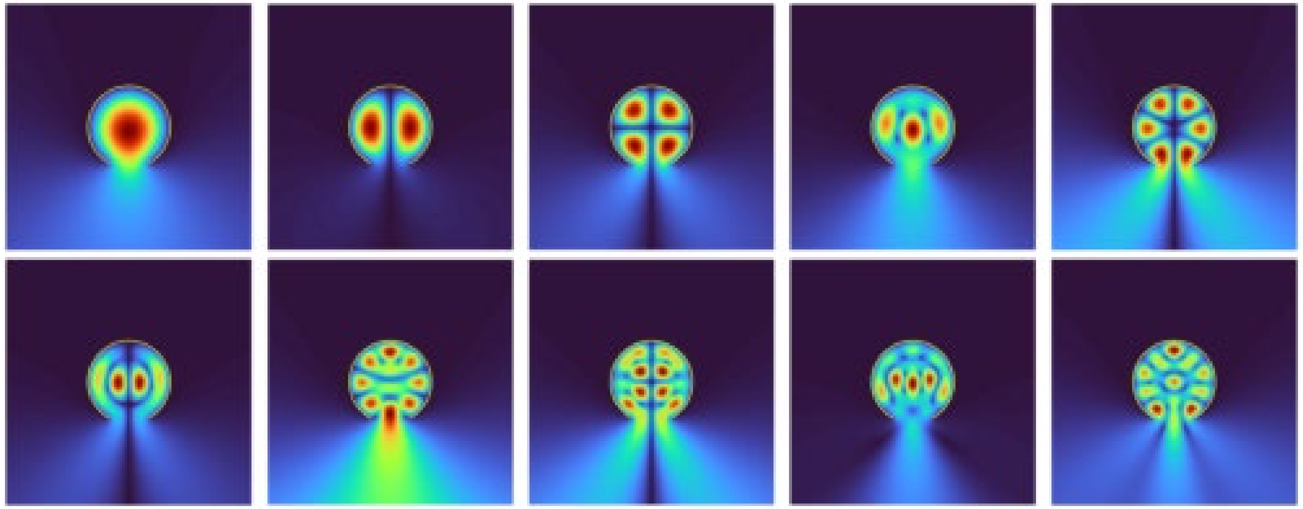

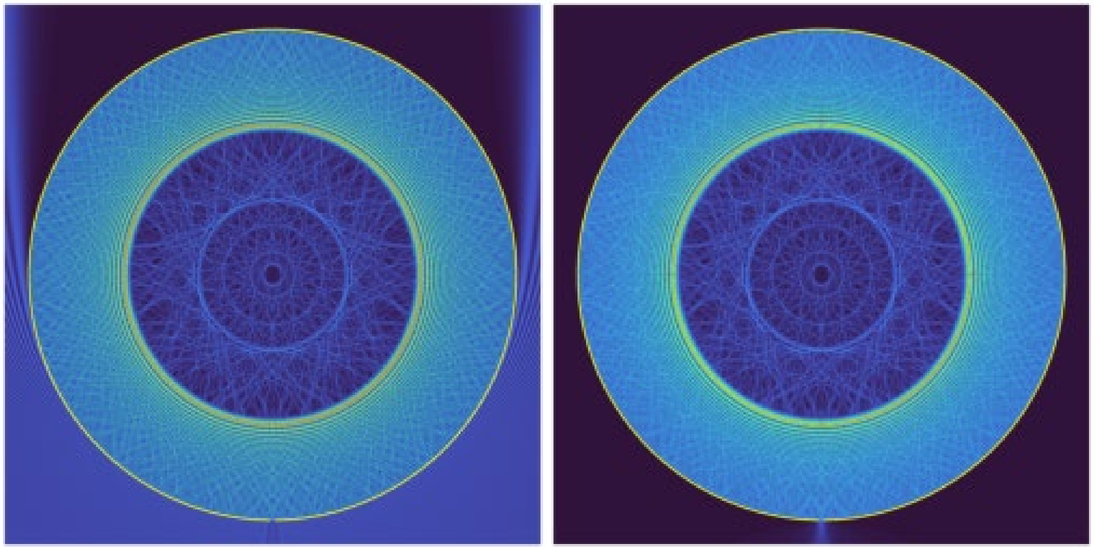

Trial and error scattering frequency
(Bruno and Lintner, [2012])
$k = 400$

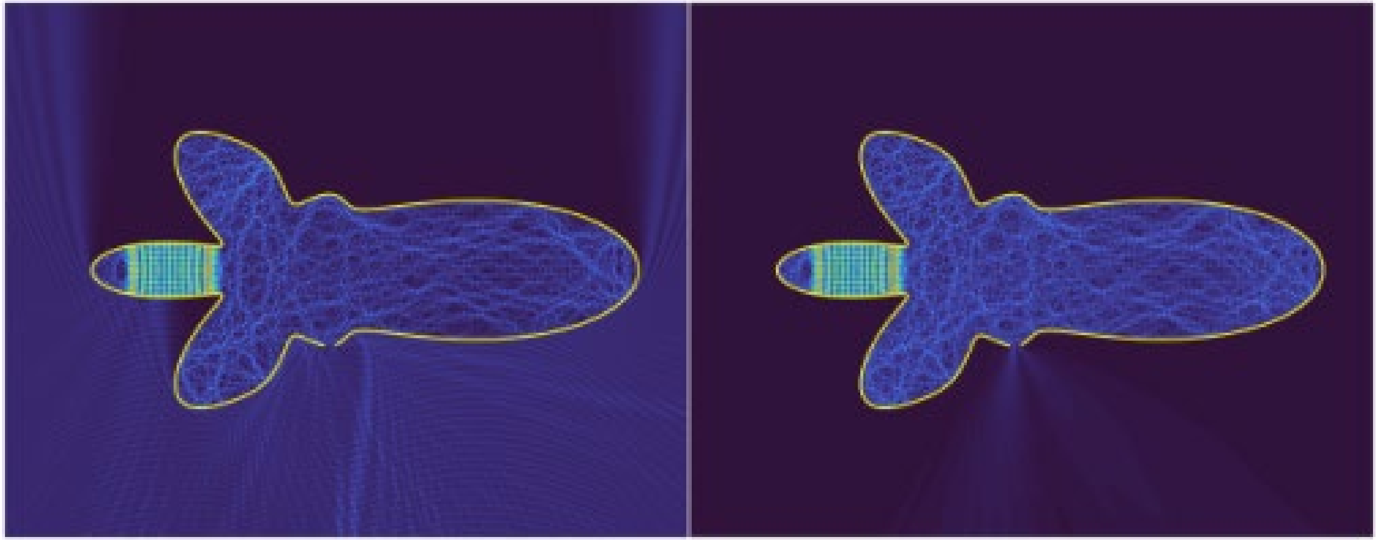

Actual scattering pole
(Bruno, Santana and Trefethen [2024])
$k = 399.969480881$

Multiple-scattering time-domain methods

Near-resonant cavities can take many GMRES iterations to converge, which impacts the computational cost of the frequency-domain solutions.

Partitioning the cavity boundary into multiple non-resonant parts can speed up frequency-domain solutions.

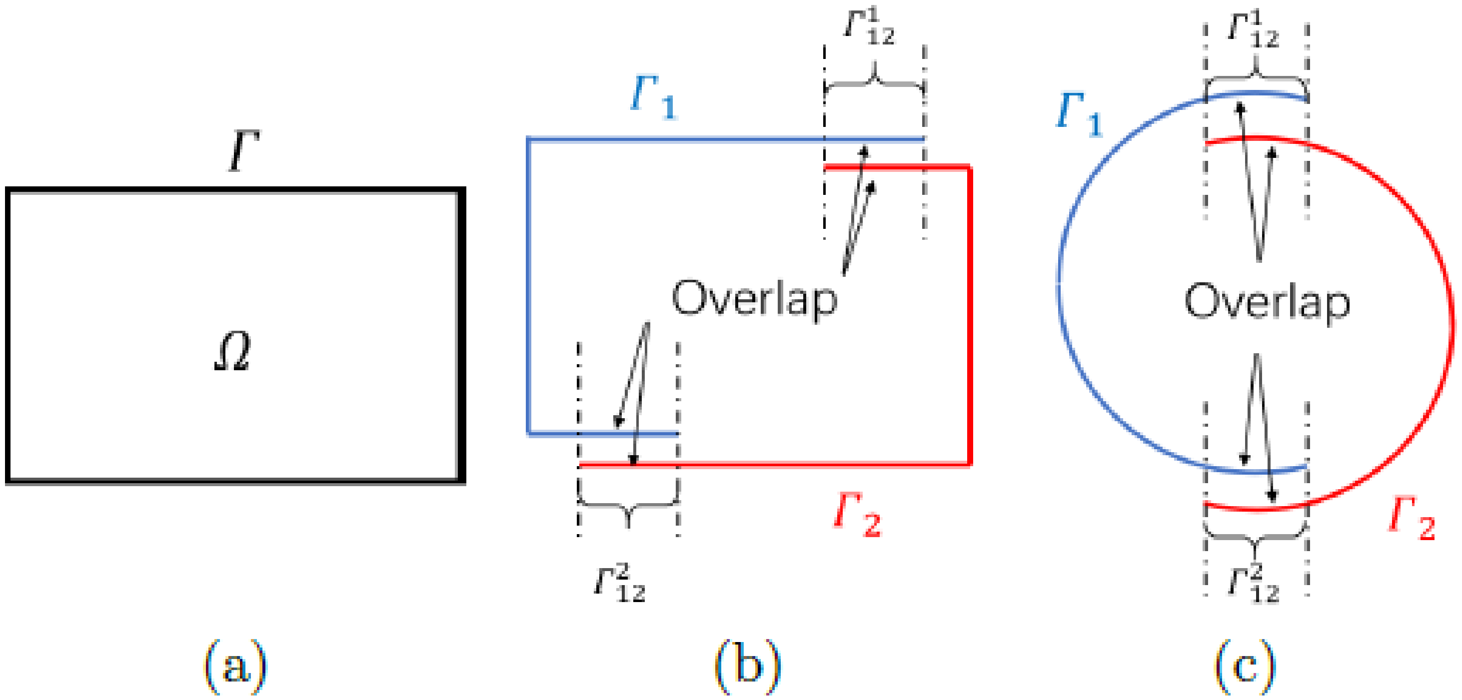

A "multiple-scattering" methodology can be used to recover the correct time-domain behavior from the partitioned boundary segments (see numerical examples next slide)

Bruno and Yin [2022]

Multiple-scattering techniques for interior-like problems

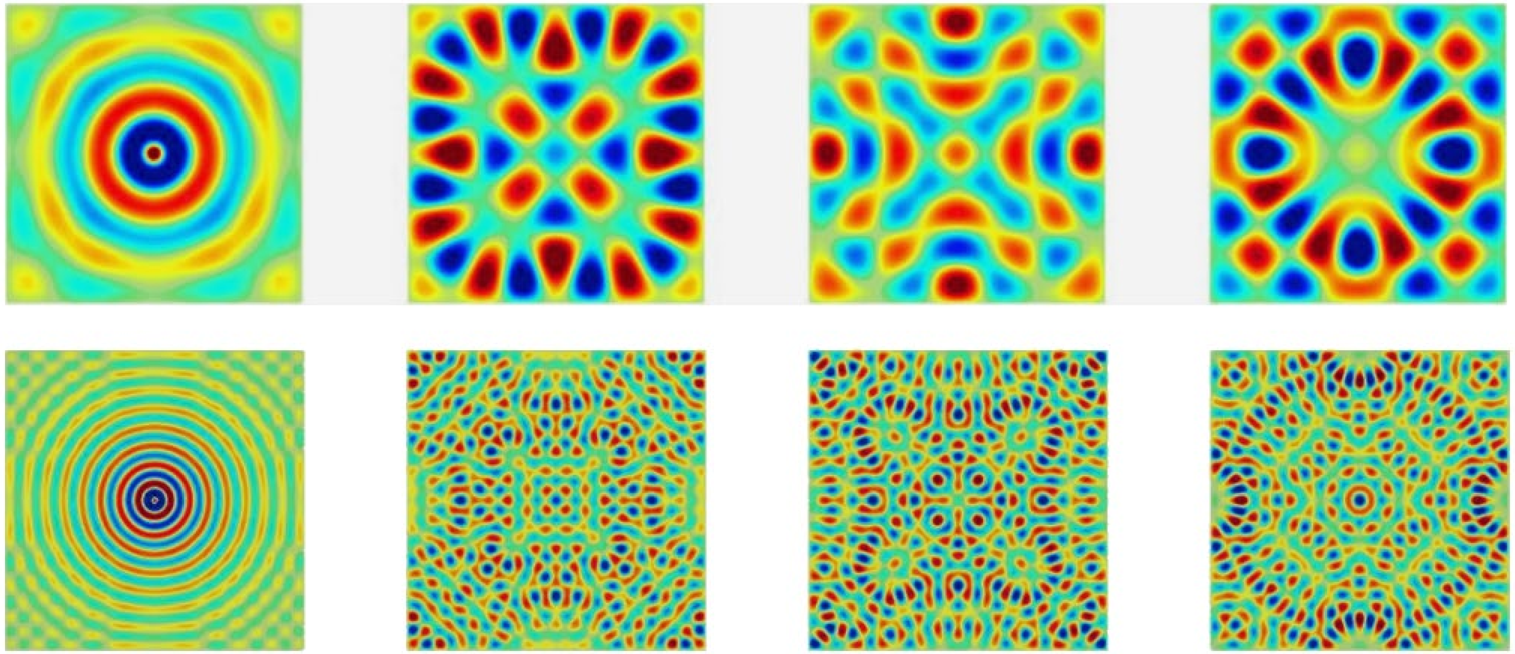

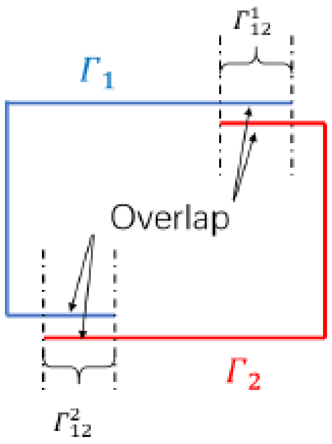

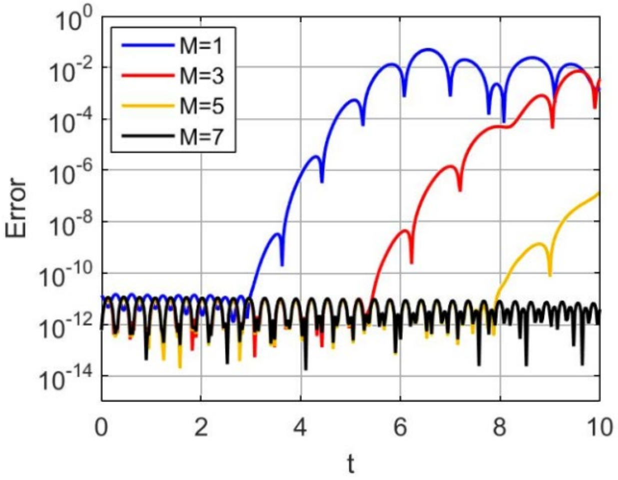

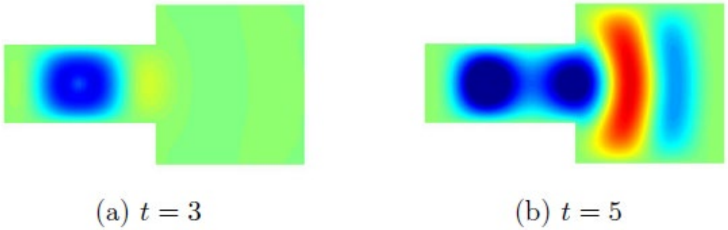

(a) $t = 3$ (b) $t = 5$

(c) $t = 7$ (d) $t = 9$

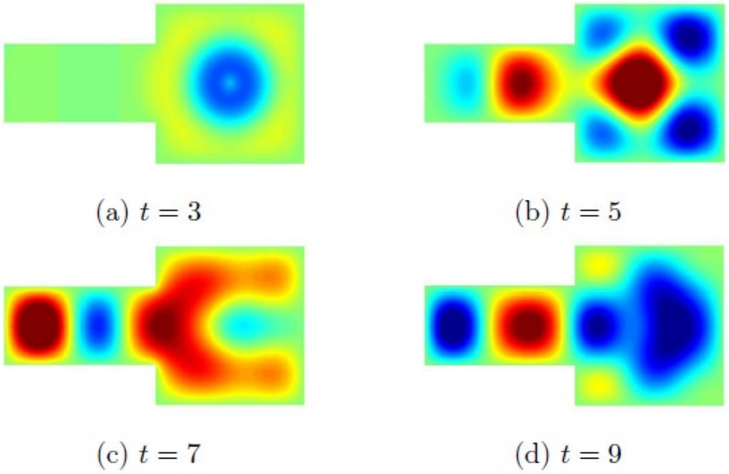

(a) $t = 3$ (b) $t = 5$

(c) $t = 7$ (d) $t = 9$

Bruno and Yin, Math. Comp. [2023]

Topics

- – IFGF Parallelization approach: space-filling Z-curves and cone-segment parallelization
- – OpenMP on 28-core server and MPI on 1680 cores
- – Metamaterials: near cm-scale photonics modeling, optimization and design
- – Time-domain frequency-time hybrid solver
- ➢ Long-range time-domain propagation over terrain
- – Long-range propagation: Screened WKB (S-WKB)

Time-domain scattering in presence of *terrain*

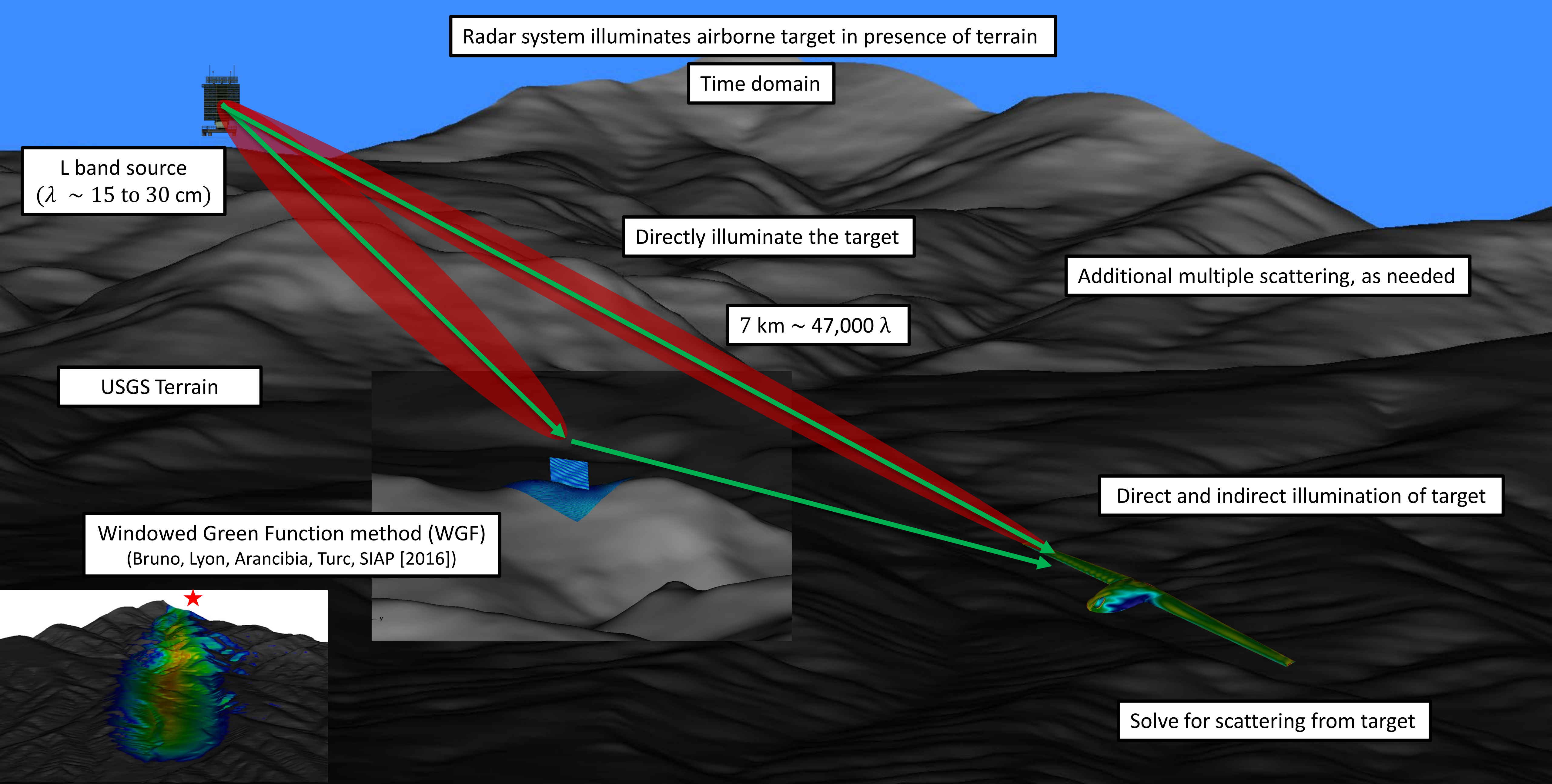

View of terrain toward radar source from aircraft

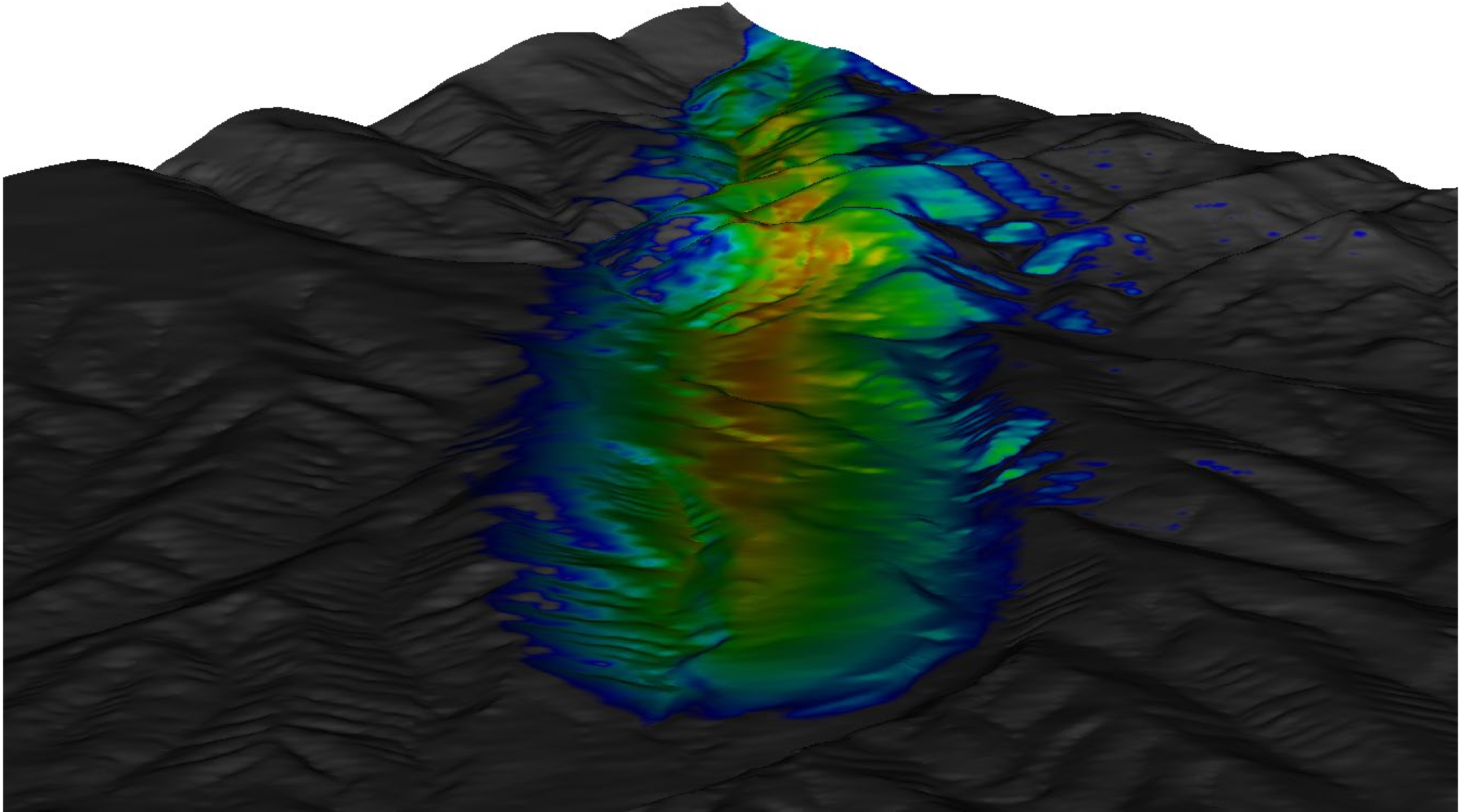

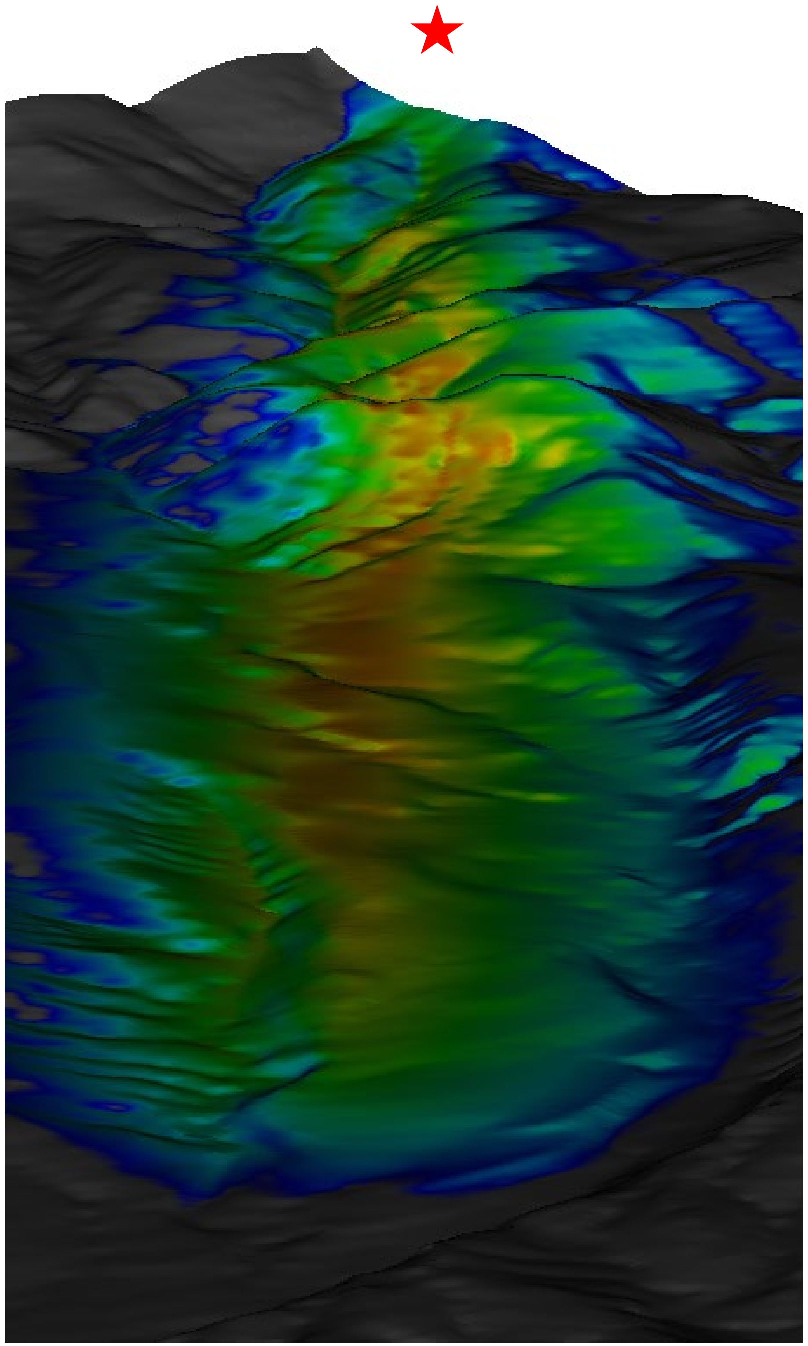

Near Field scattering from 10m x 10m WGF ground elements

Windowed Green function!

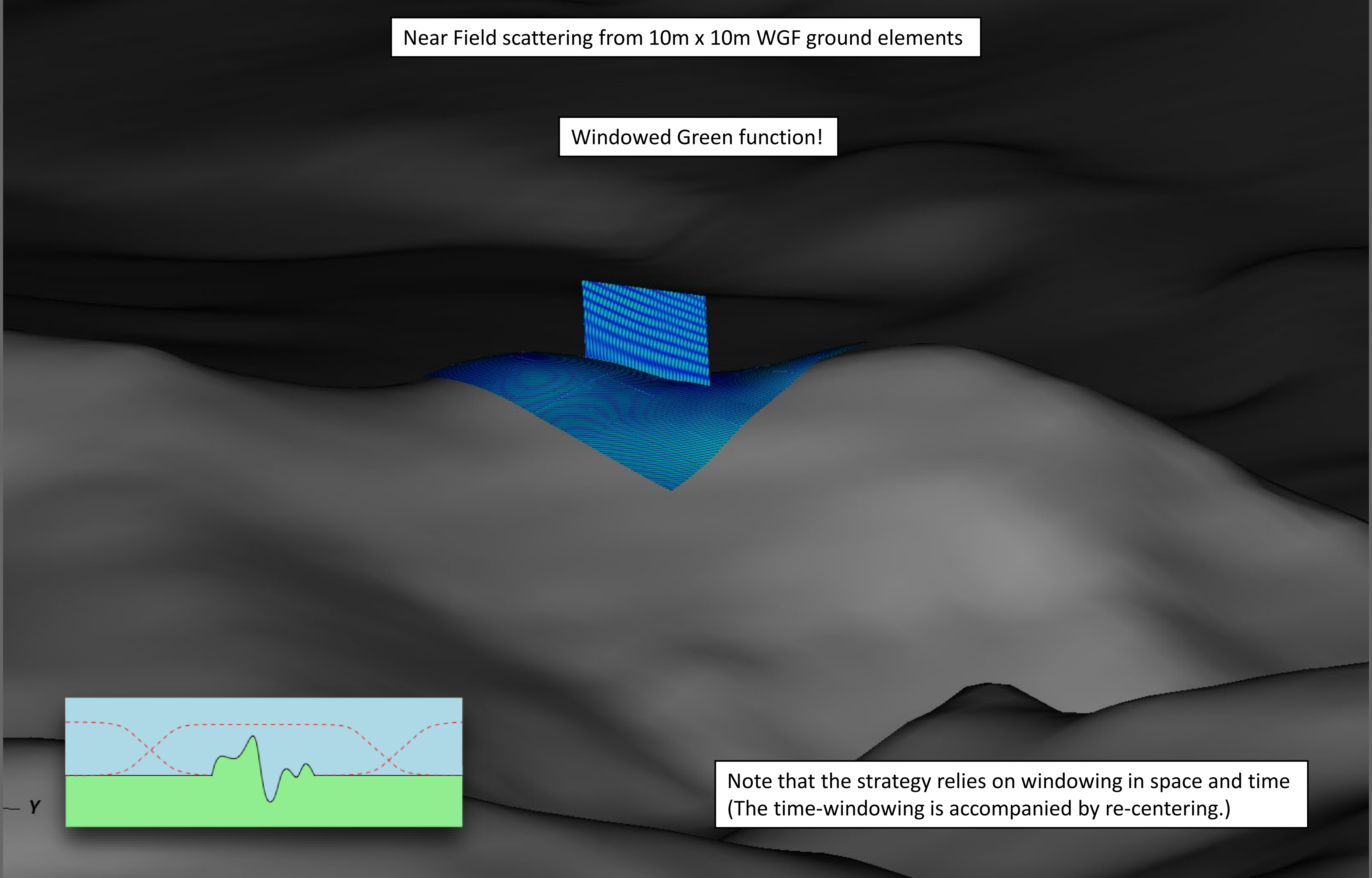

Note that the strategy relies on windowing in space and time
(The time-windowing is accompanied by re-centering.)

Time-domain scattering in presence of *terrain*

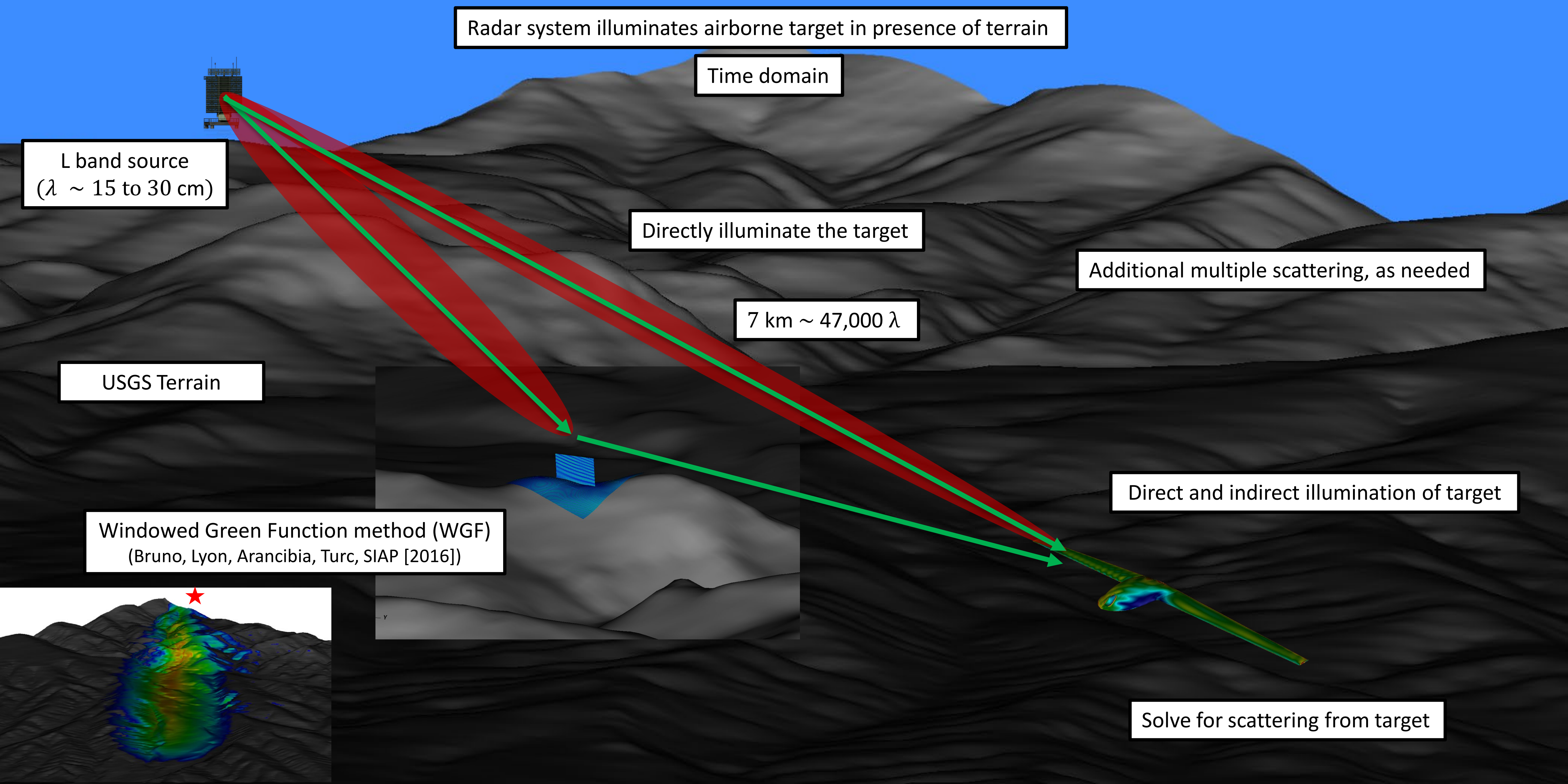

Combine Frequency Domain solutions to recover Time Domain

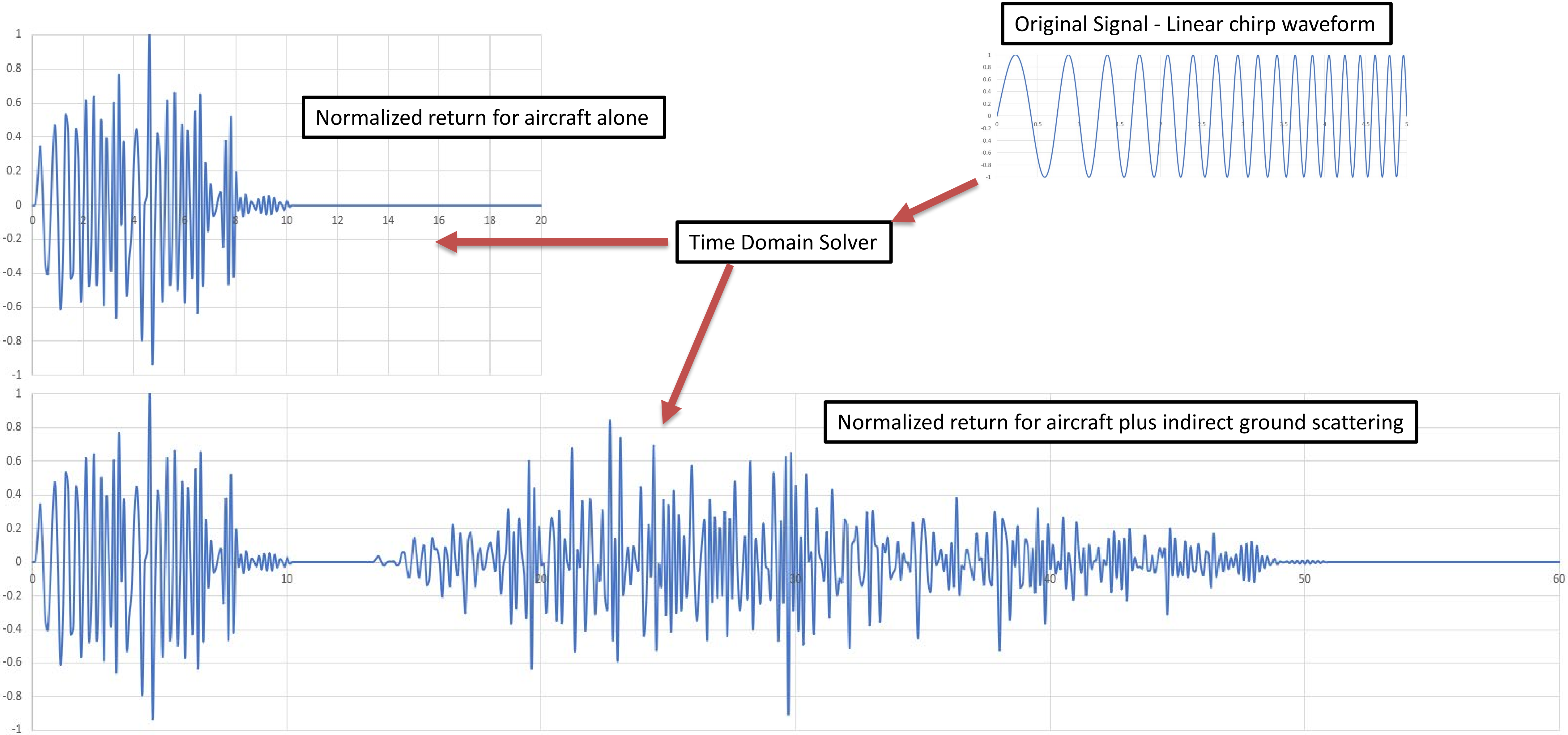

Bruno and Voss, In progress

Comparison to experiment: NIST 5G compatibility study for Aircraft carrier-based AN/SPN-43 ATC radar @ 3.55 GHz

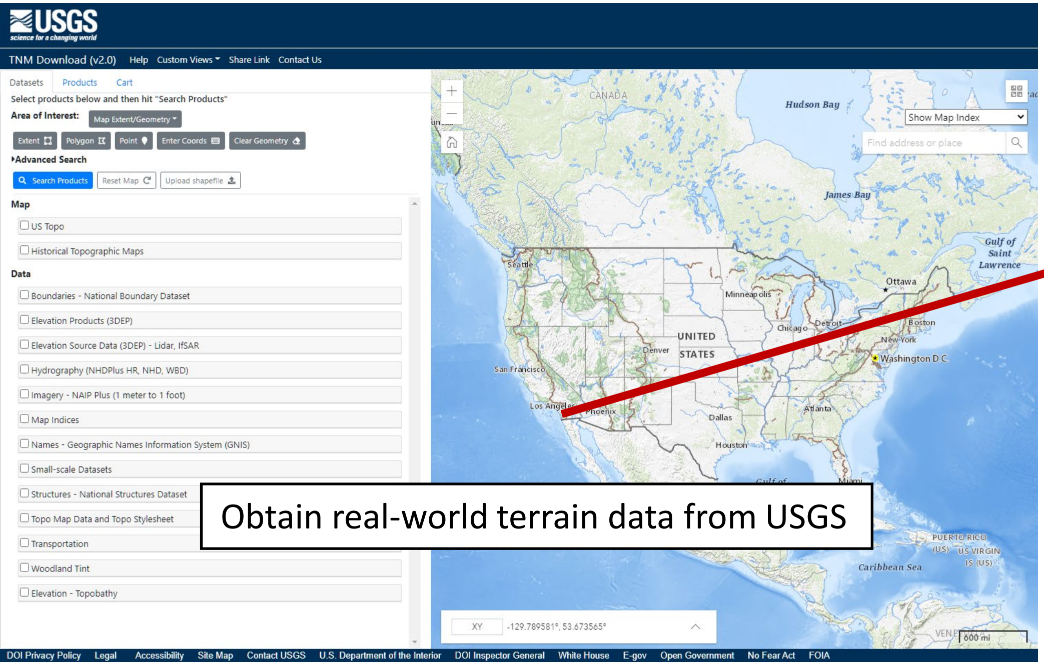

Obtain real-world terrain data from USGS

San Diego

San Diego Coast

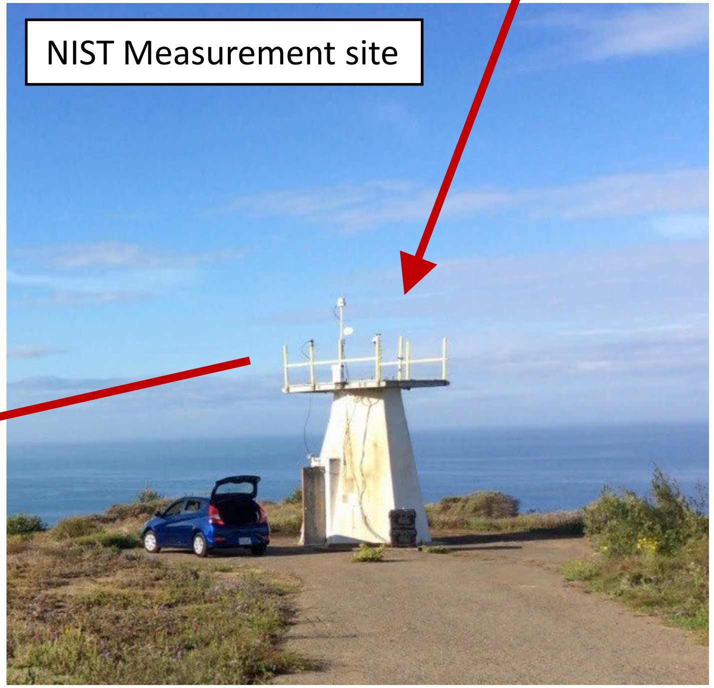

NIST Measurement site

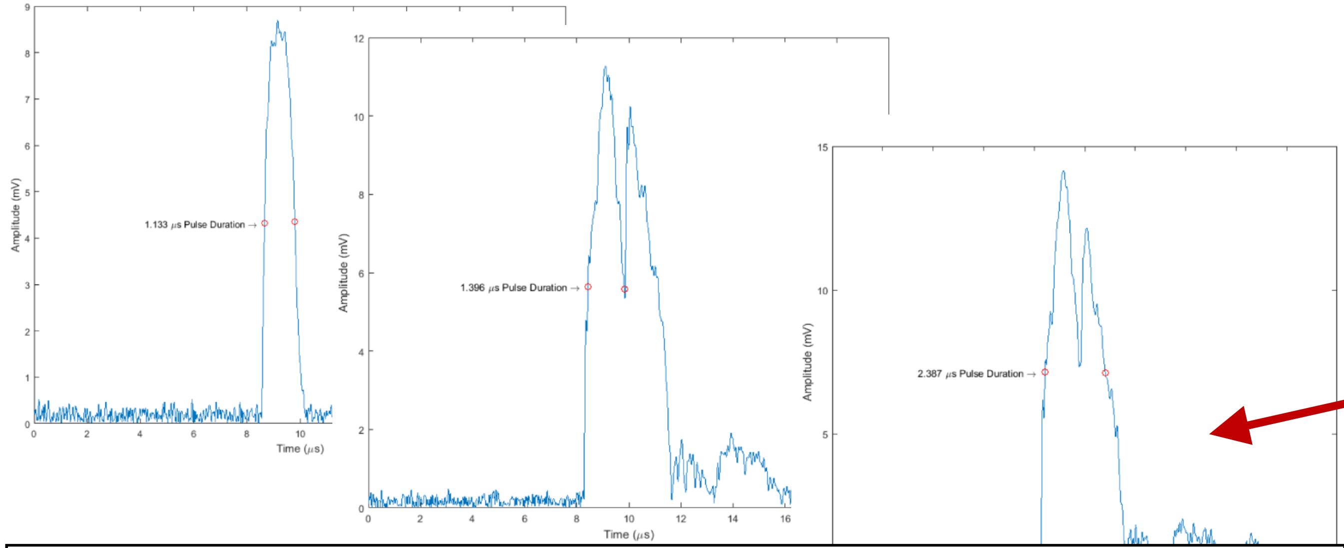

Experimental data: 3.55GHz spectrum observations (NIST Technical Note 1954, [2017])

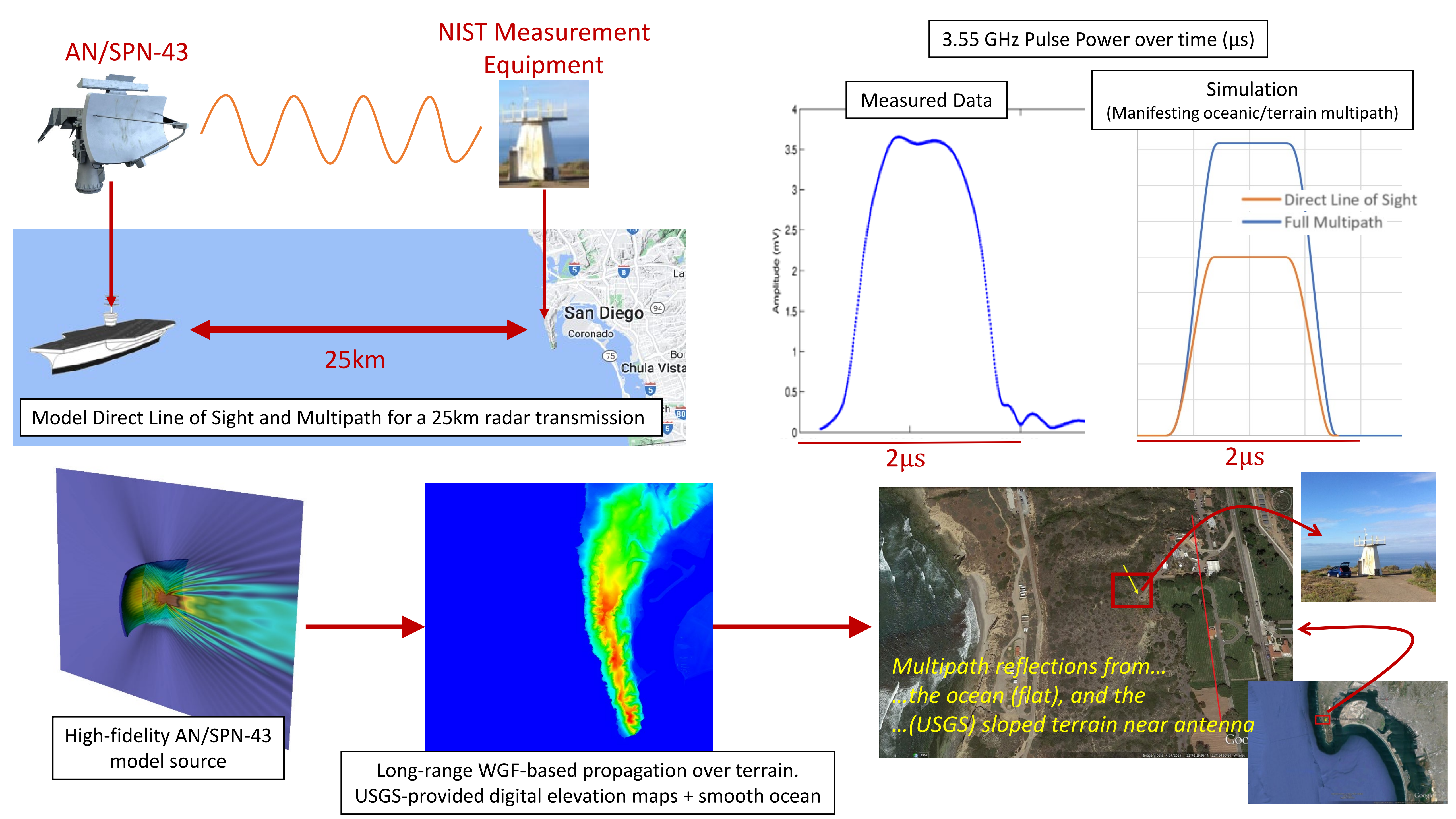
AN/SPN-43
NIST Measurement Equipment
San Diego
Coronado
Chula Vista
25km
Model Direct Line of Sight and Multipath for a 25km radar transmission
3.55 GHz Pulse Power over time (μs)
Measured Data
Simulation
(Manifesting oceanic/terrain multipath)
Amplitude (mV)
4
3.5
3
2.5
2
1.5
1
0.5
0
Direct Line of Sight
Full Multipath
2μs
2μs
High-fidelity AN/SPN-43 model source
Long-range WGF-based propagation over terrain.
USGS-provided digital elevation maps + smooth ocean
Multipath reflections from…
…the ocean (flat), and the
…(USGS) sloped terrain near antenna

Additional secondary scatterer (large ship)

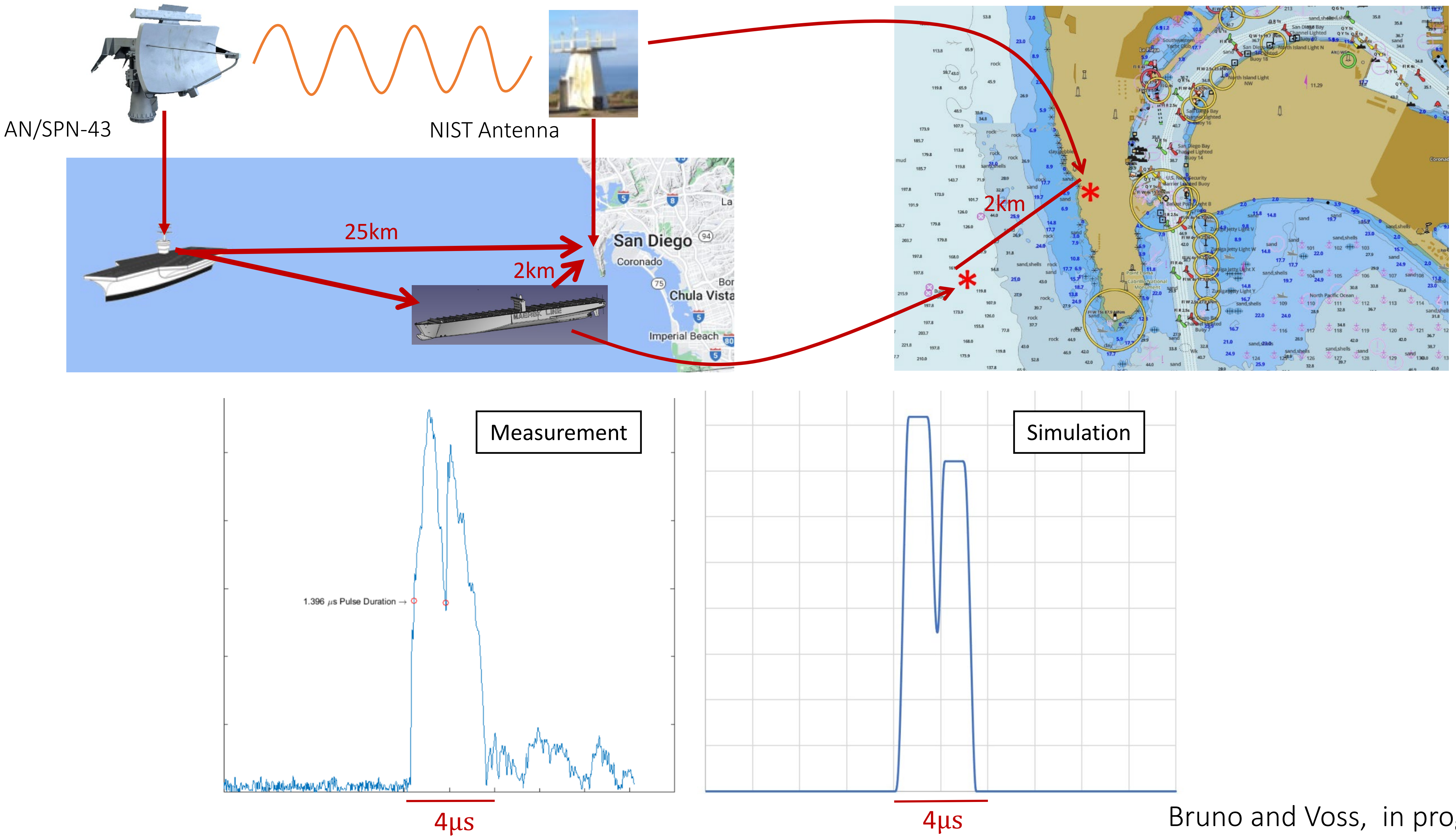

Bruno and Voss, in progress

Topics

- IFGF Parallelization approach: space-filling Z-curves and cone-segment parallelization
- OpenMP on 28-core server and MPI on 1680 cores
- Metamaterials: near cm-scale photonics modeling, optimization and design
- Time-domain frequency-time hybrid solver
- Long-range time-domain propagation over terrain
- ➢ Long-range propagation: Screened WKB (S-WKB).

EM propagation. E.g. $f = 0.3$ GHz—100 GHz → $\lambda \approx (3 \cdot 10^5$ km/s) / f = 100 cm—0.3 cm

[E.g. 40 km at C-band ($\lambda = 5$ cm) → 800,000 λ.]

$10^4\ \lambda — 10^7\ \lambda$

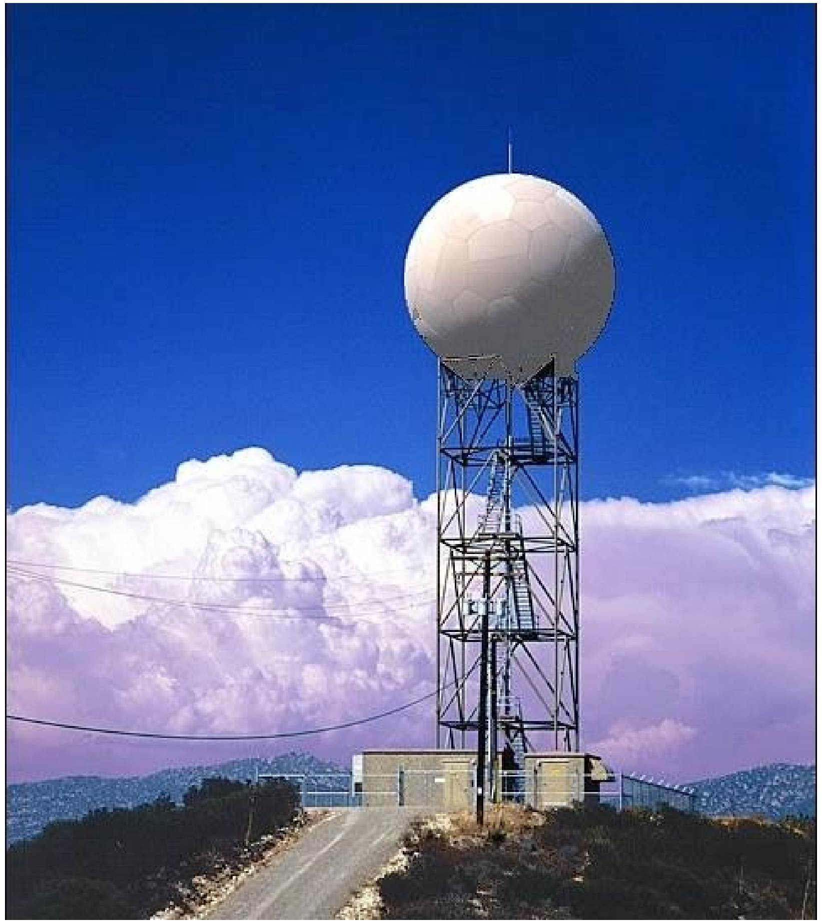

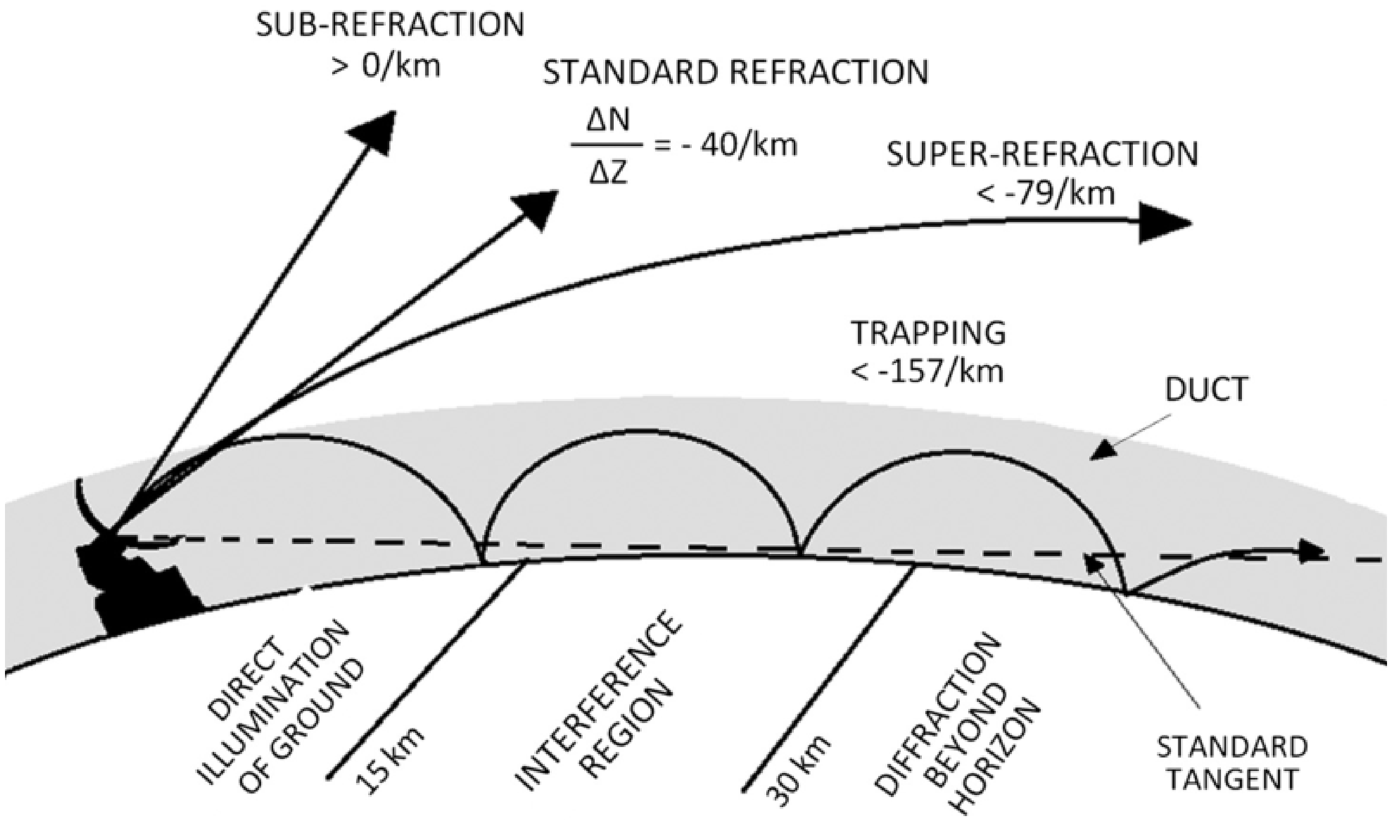

Schematic: Tepecik and Navruz, Int. J. Electron. Commun [2018]

3D ocean acoustics. E.g. 4 Hz—100 Hz $\rightarrow \lambda \approx (1500 \text{ m/s}) / f = 15$ m—400 m

2D sound speed field along a ray

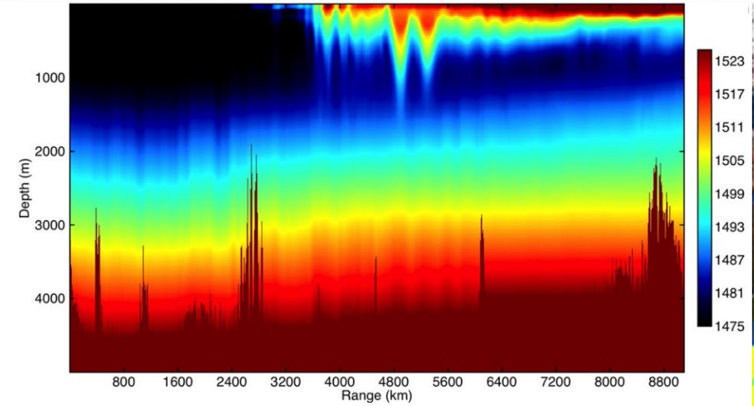

4Hz transmission loss evaluated via a parabolic equation algorithm

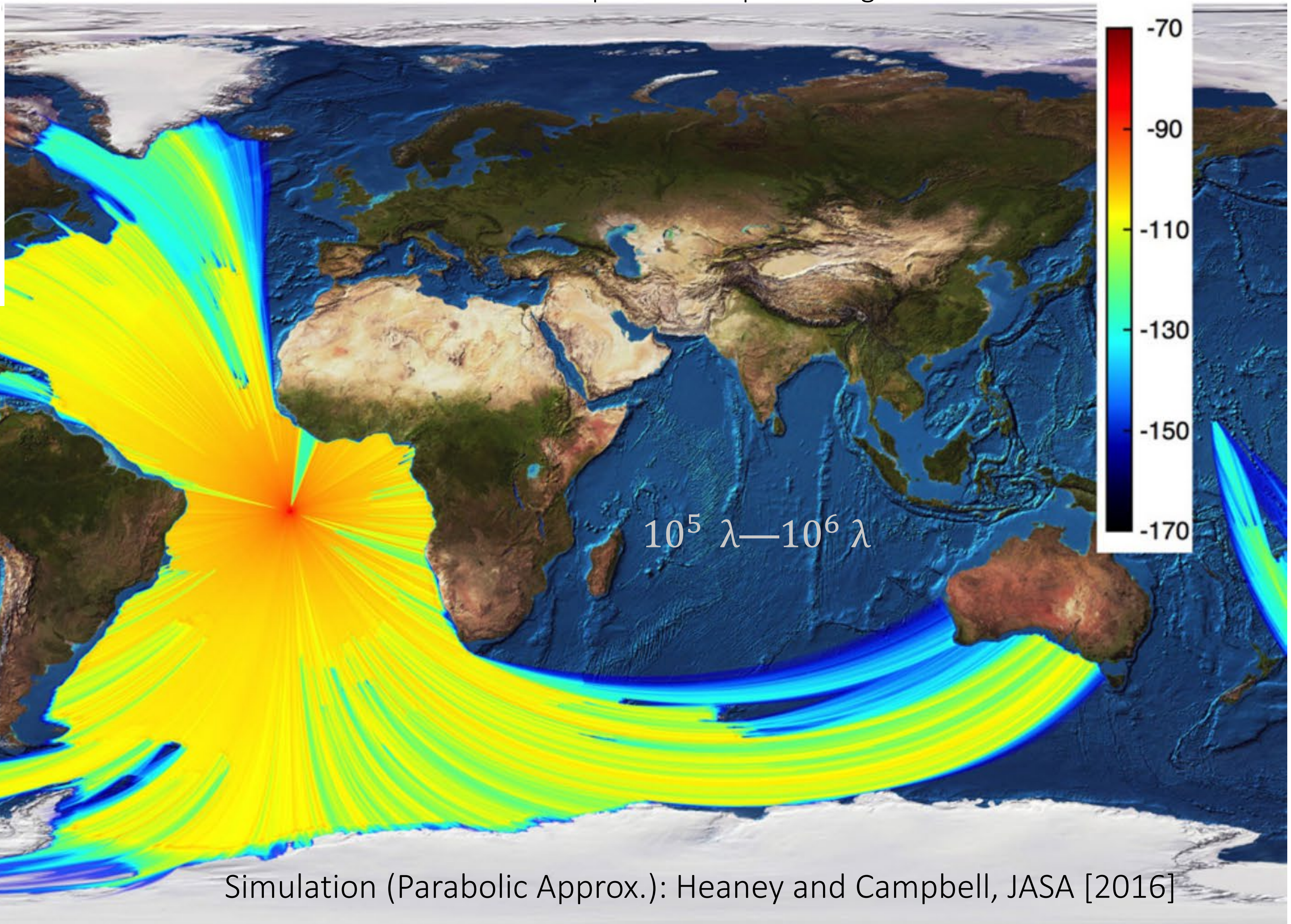

Simulation (Parabolic Approx.): Heaney and Campbell, JASA [2016]

3D seismology. E.g. 20 Hz—50 Hz → λ = 250 m—40 m

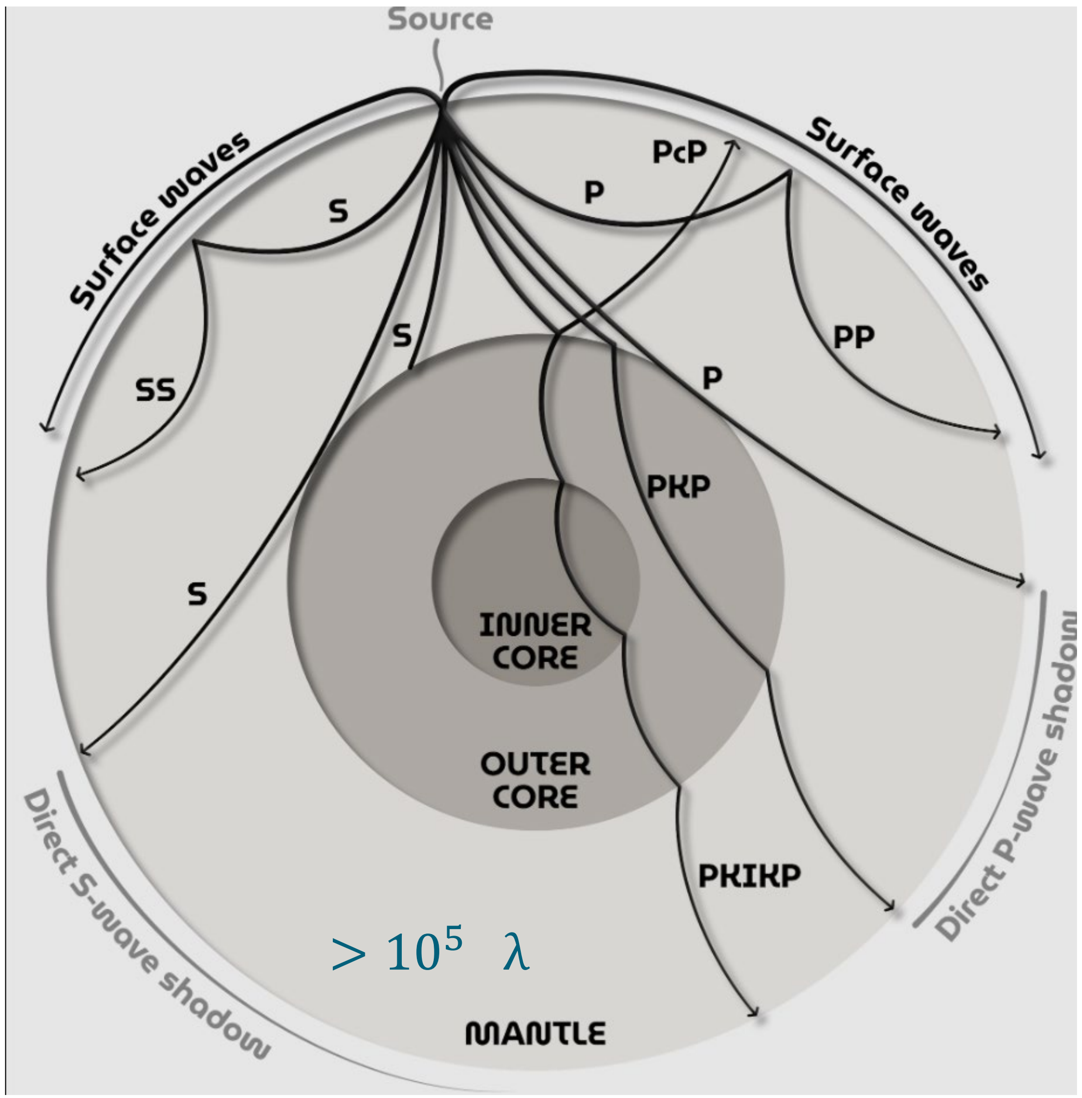

$> 10^5 \ \lambda$

v (m/s)	f (Hz)	λ (m)
2000	50	40
3000	40	75
4000	30	133
5000	20	250

Abgrall and Benamou, "Big ray-tracing and eikonal solver on unstructured grids…" Geophysics [1999]

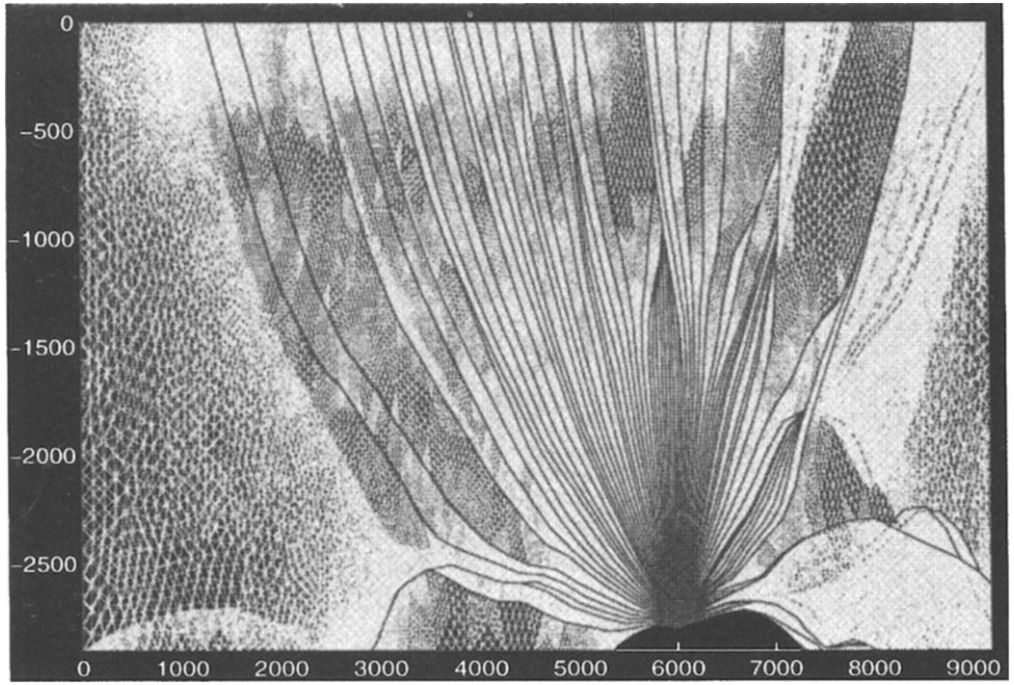

Millions of wavelenths in electrical/acoustic size

Emblematic example: Simple geometry, medium-size electromagnetic atmospheric propagation problem.
Smooth refractivity variations $n = n(x, z)$.

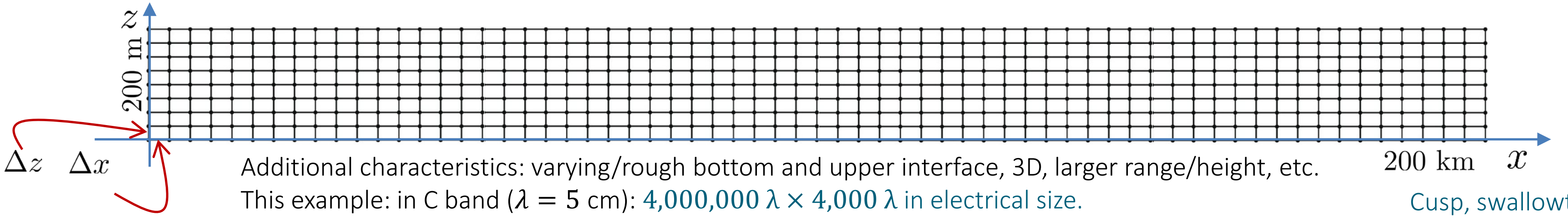

Additional characteristics: varying/rough bottom and upper interface, 3D, larger range/height, etc.
This example: in C band ($\lambda = 5$ cm): $4{,}000{,}000\,\lambda \times 4{,}000\,\lambda$ in electrical size.

Cusp, swallowtail and butterfly catastrophes
(out of the seven Thom's Elementary catastrophes)

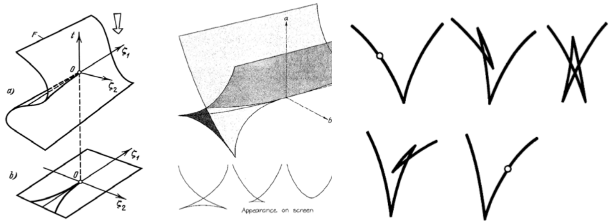

- Direct numerical simulation: unfeasible in 2D, and even more so in 3D
- Physical Optics and WKB (Wentzel, Kramers, Brillouin [1926] and Jeffreys [1923], Keller et al. [1956], Born and Wolf [1959], Babič [1963], Kravtsov (1964), Maslov [1965], Ludwig [1966], Arnold [1967], Hörmander [1971], Leray [1972], Thom [1972], Berry [1975]...): Ray tracing and energy transport. Uniform expansions (in free-space, based on multiple derivatives of the unknown generalized phase). More later. } Caustics.
- Parabolic Equation (Leontovich & Fock [1944], many subsequent versions and improvements, including Wide angle parabolic approximation following Tappert [1973]): Factors out forward incident beam and eliminates back-propagation in finite-difference and Fourier-based contexts. } $\Delta z \leq \lambda/4,\ \Delta x \sim\ (2-50)\cdot\Delta z$ $(\Delta x \lesssim 12.5\lambda)$ Finite differences (dispersion), or Fourier (lowest order, narrow).
- Phase-Screen Method (Wu [1998]): Assumes constant refractivity along each vertical volumetric z-screen.
- Gaussian Beams (Babič and Buldreyev 1960's, Hörmander [1971], Babič and Pankratova [1973], Ralston [1976, 1982], Popov [1982], Tanushev, Engquist, Tsai, [2009]): Some details later. } Second-order phase approximation.
- Kinetic formulation: (P.-L. Lions and Paul [1993], Markowich and Mauser [1993], Ryzhik, Papanicolaou and Keller [1996], Engquist and Runborg [1996]): Some details later. } Particle density.
- Dynamic Surface Extension: (Steinhoff, Fan, and Wang [2000], Ruuth, Merriman, and Osher [2000]): Eulerian-Lagrangian grid-centric algorithm. Some details later. } Grid-centric algorithm.

Classical WKB Approximation

$$\Delta u(\mathbf{r}) + k^2 \varepsilon(\mathbf{r}) u(\mathbf{r}) = 0$$

WKB Ansatz:

$$u(\mathbf{r}) = e^{ik\psi(\mathbf{r})} \left(A_1(\mathbf{r}) + \frac{A_2(\mathbf{r})}{ik} + \frac{A_3(\mathbf{r})}{(ik)^2} + \dots \right)$$

log – log

$$\begin{aligned}
&(ik)^{+2} \left[(\nabla\psi)^2 - \varepsilon(\mathbf{r}) \right] \\
&+(ik)^{+1} \left[2\nabla\psi \cdot \nabla A_1 + A_1 \nabla^2 \psi \right] \\
&+(ik)^{+0} \left[2\nabla\psi \cdot \nabla A_2 + A_2 \nabla^2 \psi + \nabla^2 A_1 \right] \\
&+(ik)^{-1} \left[2\nabla\psi \cdot \nabla A_3 + A_3 \nabla^2 \psi + \nabla^2 A_2 \right] + \dots = 0
\end{aligned}$$

$$(\nabla\psi)^2 = \varepsilon(\mathbf{r})$$ Eikonal Equation (Rays)

$$2\nabla\psi \cdot \nabla A_1 + A_1 \nabla^2 \psi = 0$$ Energy Transport Equation

$$2\nabla\psi \cdot \nabla A_2 + A_2 \nabla^2 \psi + \nabla^2 A_1 = 0$$ Higher-order Transport

$$\dots$$

Curved rays as a broken line limit

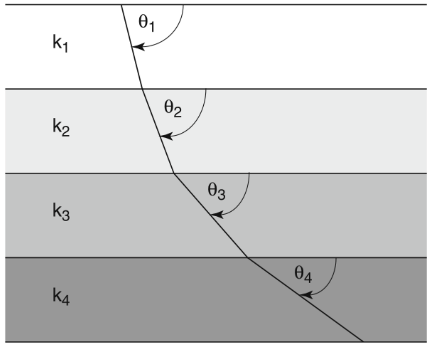

The main cause of breakdown of the geometrical ray approximation is caustics ($A_1 = \infty$), [...] interfaces, critical points and shadows. Higher-order terms in the asymptotic ray series are of little use [...]

C. Chapman, "Fundamentals of Seismic Wave Propagation," [2004].

Point-source test case: $u(\boldsymbol{r}) = H_0^1(k|\boldsymbol{r}|)$

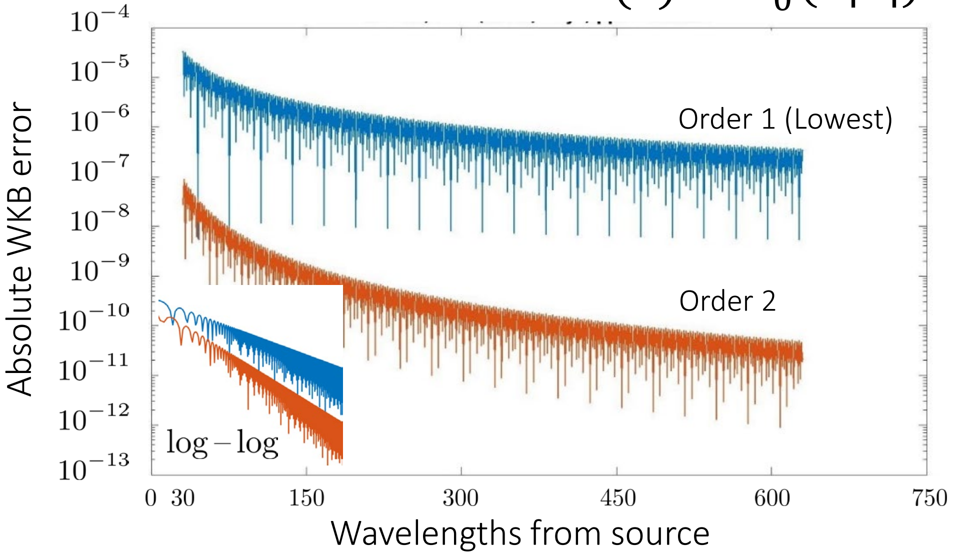

Acuña and Bruno, "Efficient high-order WKB implementation", in progress

Difficulties at Caustics

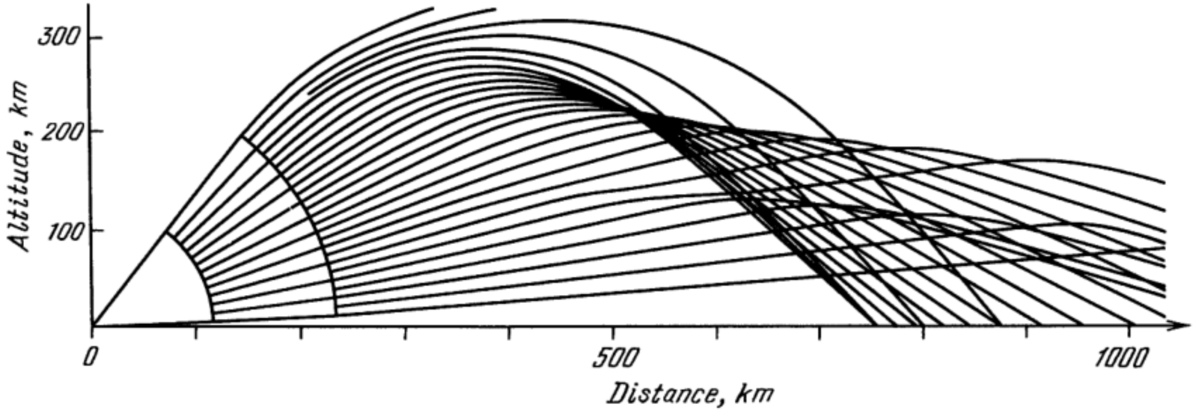

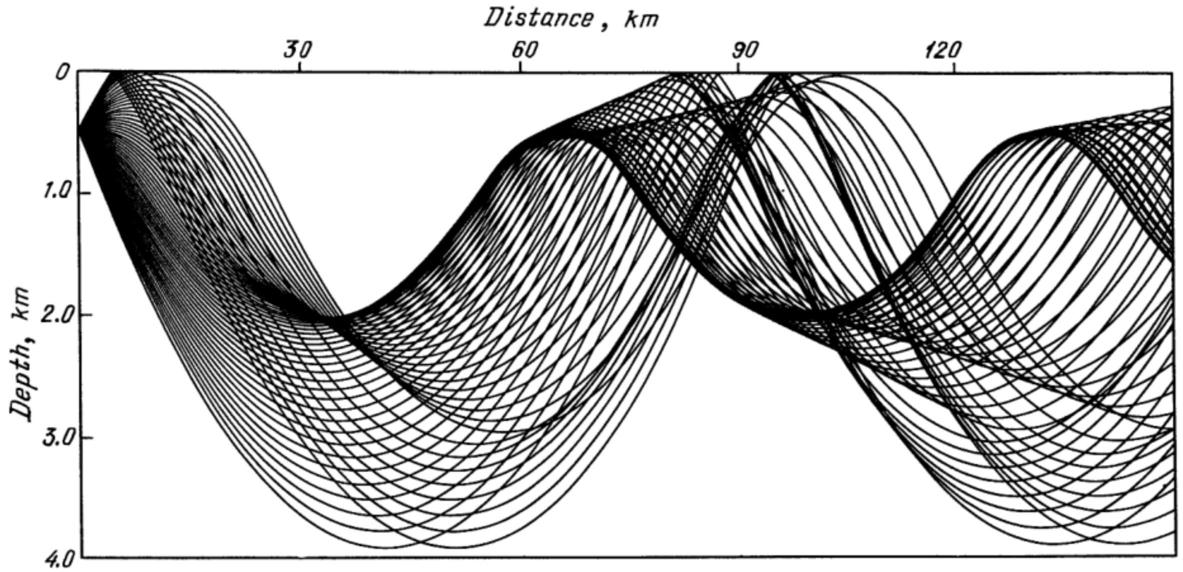

Kravtsov and Orlov, ”Caustics, Catastrophes and Wave Fields,” [1993]

- Cross-section of a ray tube vanishes → infinite intensity predicted. Unphysical!
- Ray field continues to span a region beyond a caustic, and so does the amplitude, which is given in terms of the Jacobian J of the ray mapping.
- After a caustic the field requires a correction: beyond a caustic the amplitude must be corrected by the factor $(-i)^m$.
- The approximation still breaks down at caustics, and is inaccurate near caustics.
- The KMAH index m—after Keller, Maslov, Arnol'd and Hörmander—encodes the number and type of caustics the ray has traversed. Caustic type needs to be determined. Generally not used in practice.
- Extensive literature. Focus on classification. Unclear how implementation of these ideas could be accomplished to simulate realistic configurations.

Difficulties at Caustics: catastrophes

A "catastrophe“ is a qualitative and jumpwise variation of the state of the system.

In geometrical optics, catastrophes occur as a change in the number of rays coming into a given point of space.

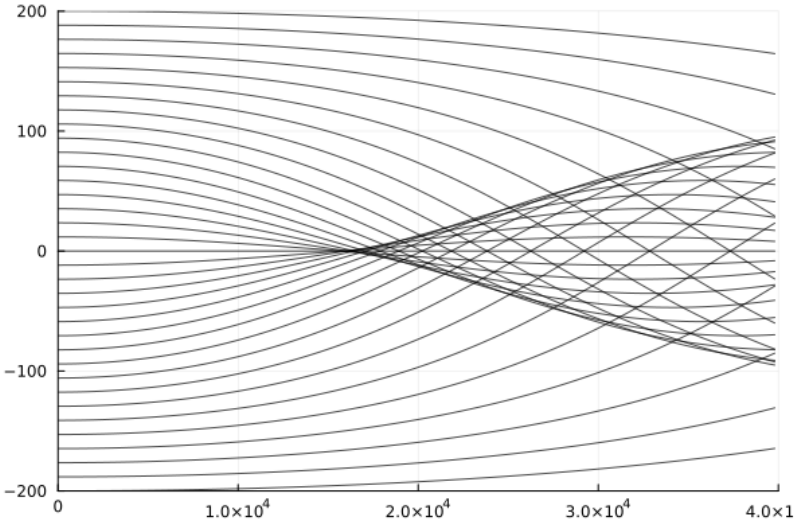

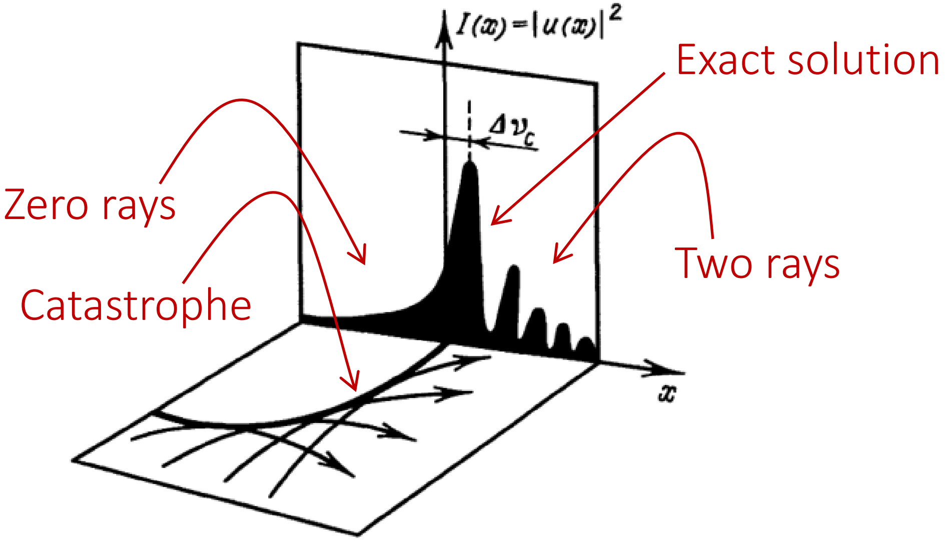

Kravtsov and Orlov, ”Caustics, Catastrophes and Wave Fields,” [1993]

Proposed approach: Screened WKB (S-WKB).

Produce accurate field values, including at and around caustics, by avoiding WKB caustics.

The Screened-WKB Method

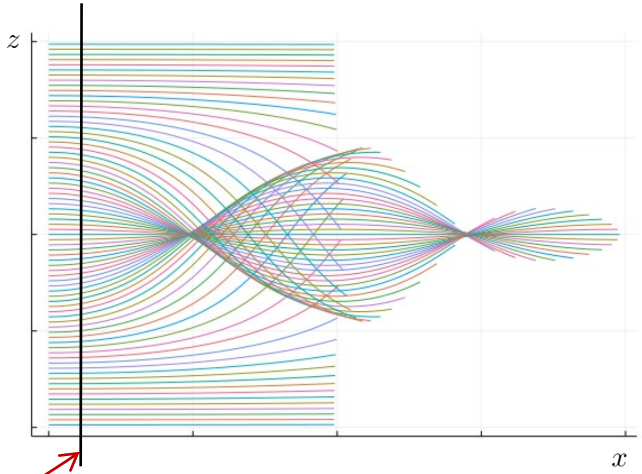

– Obtain FFT along screen

$$u^{inc}\Big|_{x=x_0} = \sum_{m=-M/2+1}^{M/2} a_m e^{imz}$$

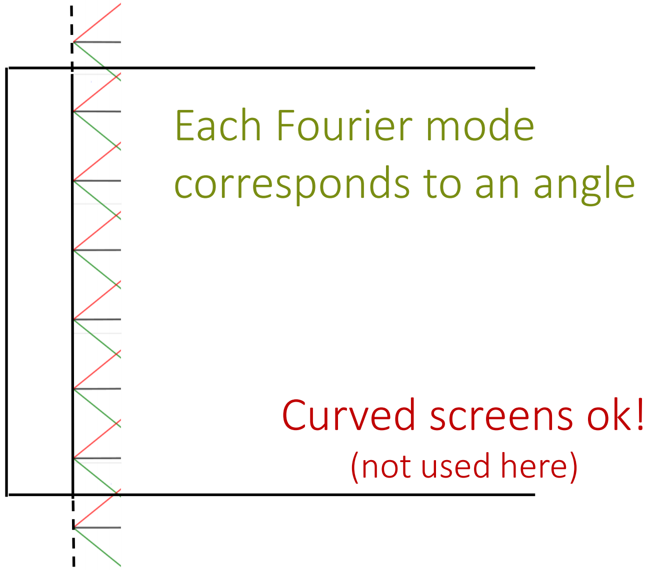

– Compute (z-dependent) incidence angles, one for each mode e^{imz} (using Eikonal equation at $x = x_0$)

$$u^{inc} \approx \sum_{m=-M/2+1}^{M/2} a_m e^{im\cdot z + i(k^2 n^2(z) - m^2)^{1/2}\cdot(x - x_0)}$$

(to first order in $(x - x_0)$)

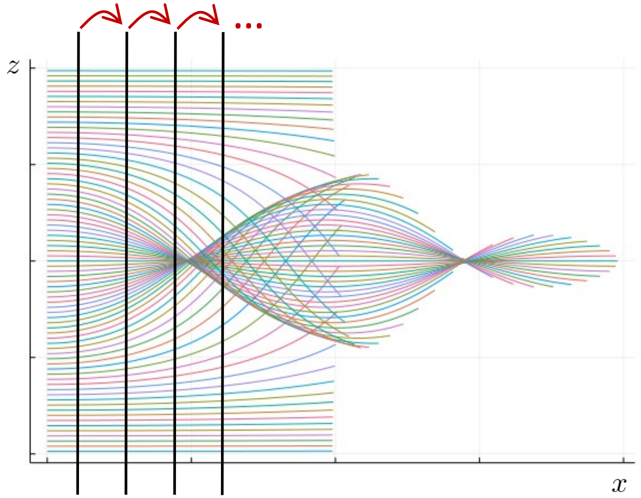

– Propagate each mode separately via WKB

– Use local intensity for each ray

– Sum the series at present screen (requires interpolation)

– Repeat: Obtain FFT along screen...

The modes do not suffer from caustics... in neighborhoods of fixed width around every screen. Irrespective of whether the screen is far, close to, or intersecting a physical caustic.

O. Bruno and M. Maas, [2023] (arxiv.org/abs/2301.03814)

Test case: Exact Solution

Separation of variables, assuming $n(x,z) \ = \ n(z)$

- Propagation across a "smooth dielectric waveguide"

$$n(x,z) = n(z) = \ 1 \ + ae^{bz^2} \text{ with values such as e.g. } a \ = \ b \ = \ 10^{-4}.$$

(Refractivity $N = (n-1) \times 10^6 \sim \mathcal{O}(10^2)$.)

- Exact solution obtained by separation of variables and numerical solution of Sturm-Liouville eigenvalue problem in z with oscillatory exponential variation in x.

- C-band radar ($\lambda = \ 0.05$ m)

- E.g. 400 m in height $(8{,}000\lambda)$ and 200 Km in range $(4{,}000{,}000\lambda)$.

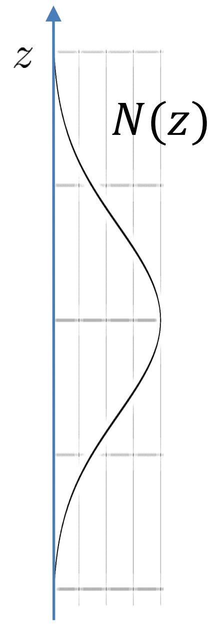

Typical range of atmospheric variation

Solution (Real Part)

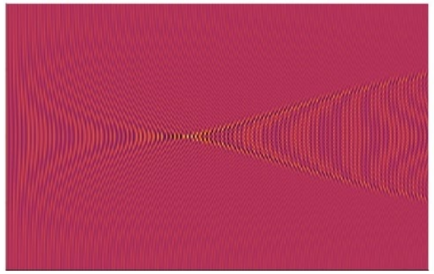

40 km, C-band ($\lambda = 5\ cm$), 800,000 λ

Screens

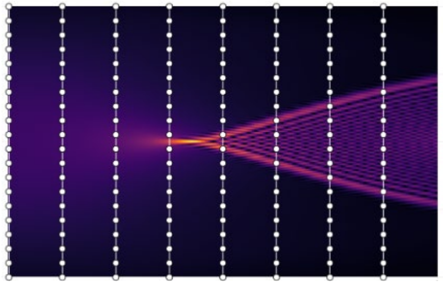

Exact Solution (intensity)

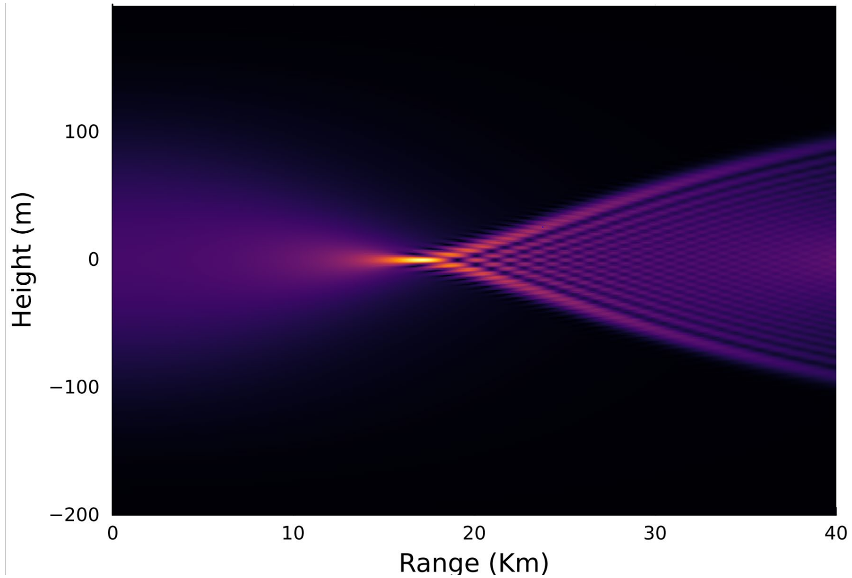

Screened-WKB Solution (intensity)

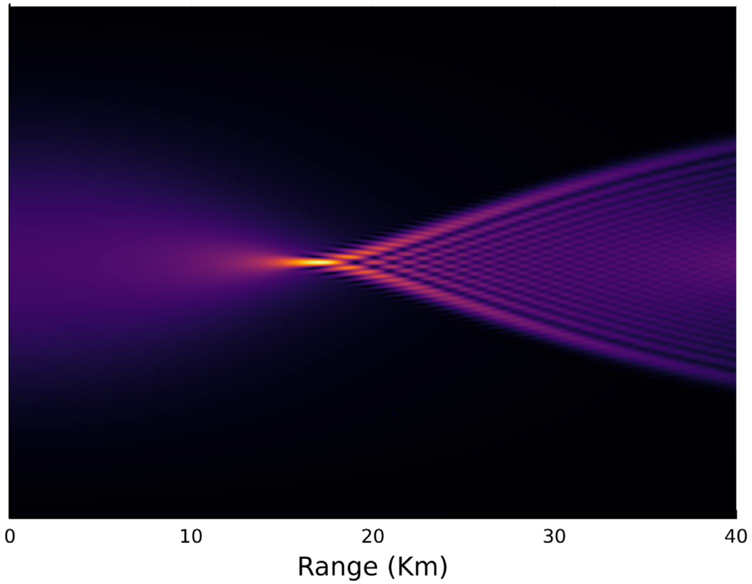

Intensity and Rays

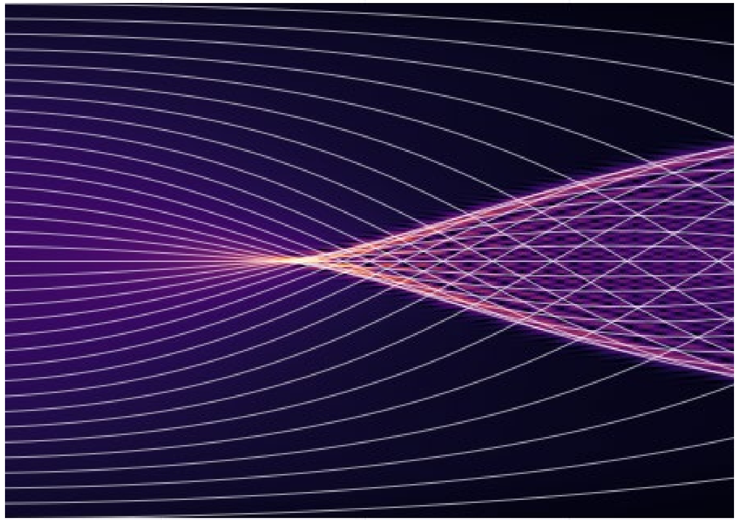

Function $N(z)$

Quantitatively typical atmospheric range

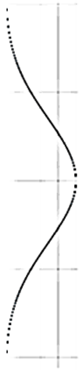

Maximum Rel Error: 10^{-5}

(Comparison with exact solution)

2 min single-core computation

Rays

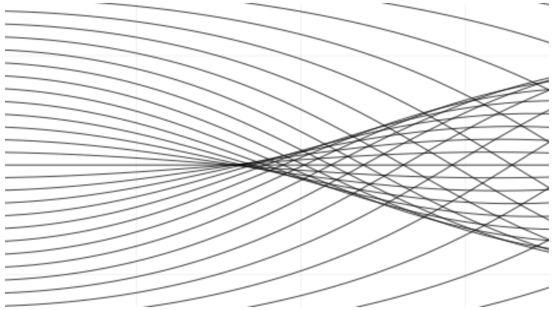

Screened-WKB

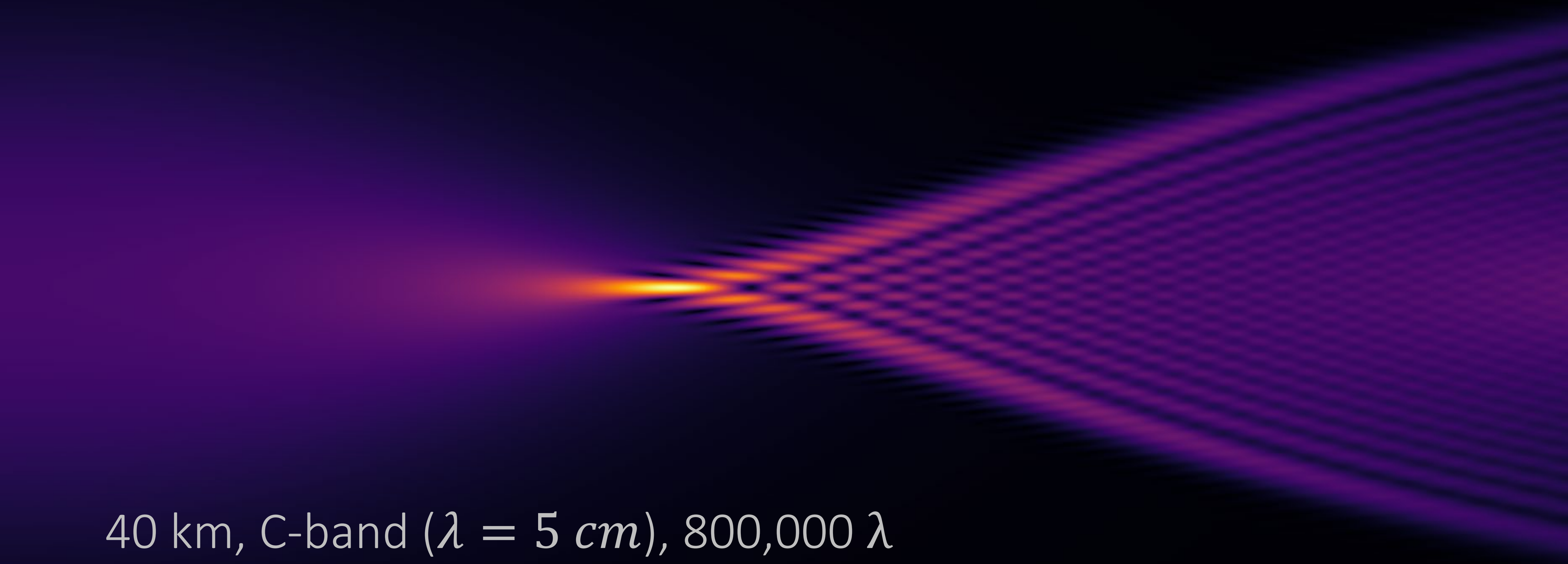

40 km, C-band ($\lambda = 5\ cm$), 800,000 λ

Maximum Rel Error: 10^{-5}

O. Bruno and M. Maas, [2023] (arxiv.org/abs/2301.03814)

Berry, “Waves and Thorn's theorem”
Adv. in Ph. [1965]
Experiment

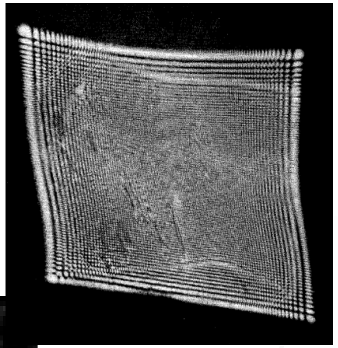

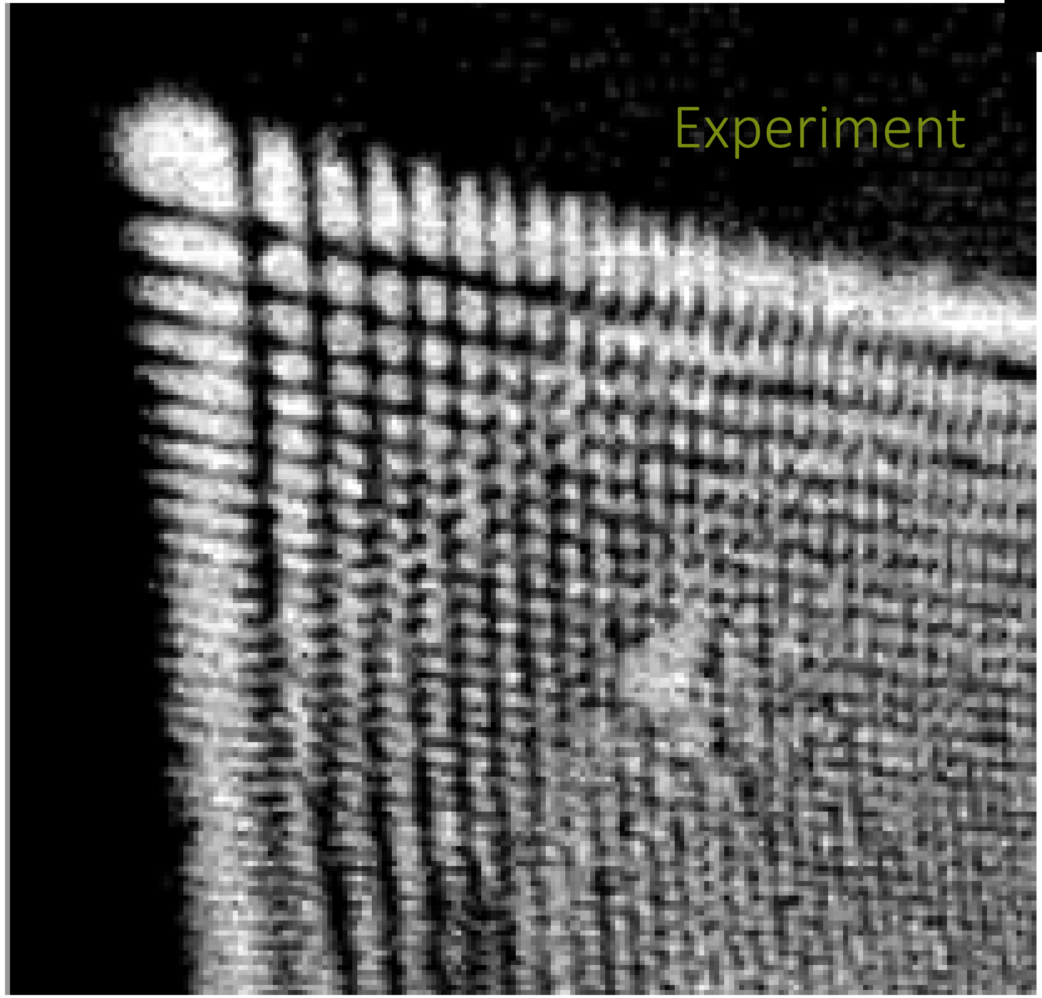

Similar features in the exact and S-WKB solutions

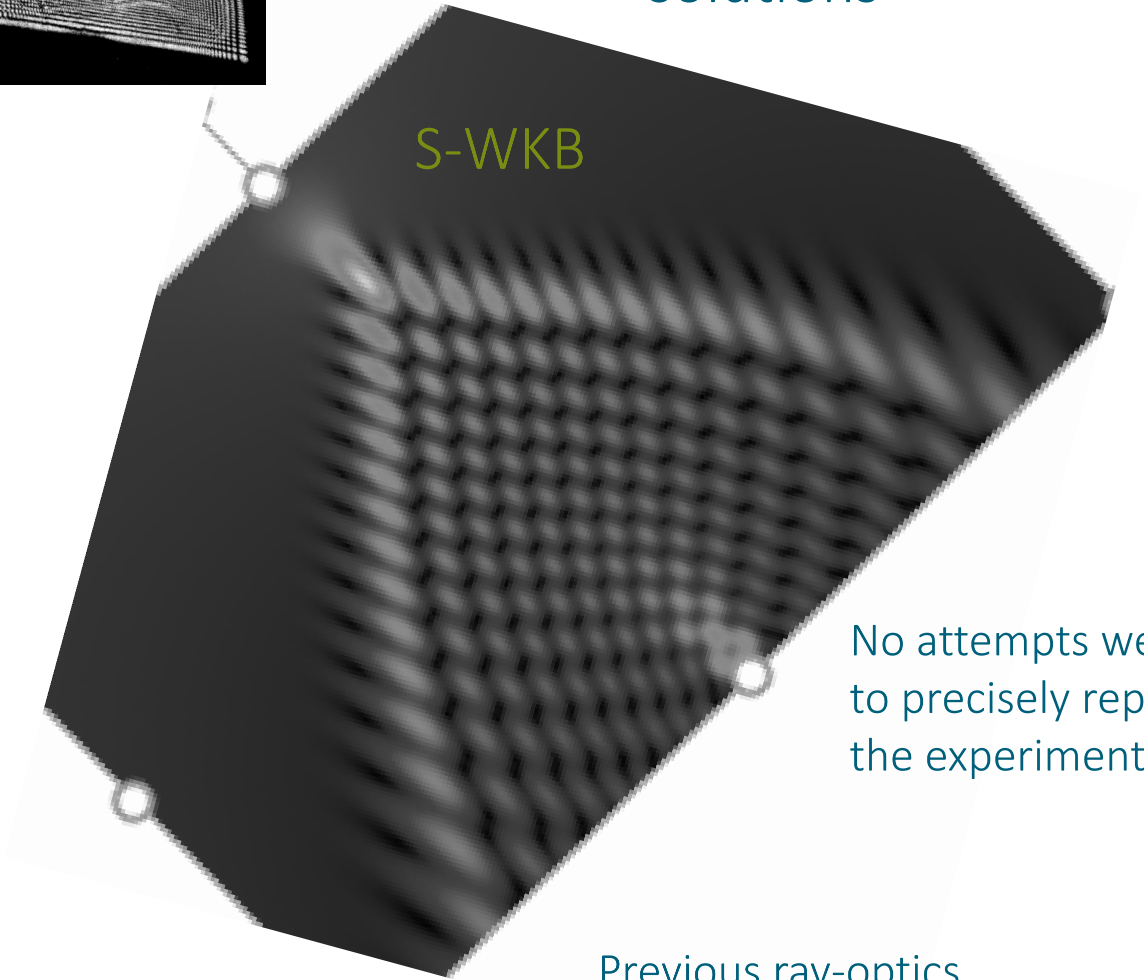

No attempts were made to precisely represent the experimental setup

Previous ray-optics evaluation of such post-caustic features?

Multiple Caustics

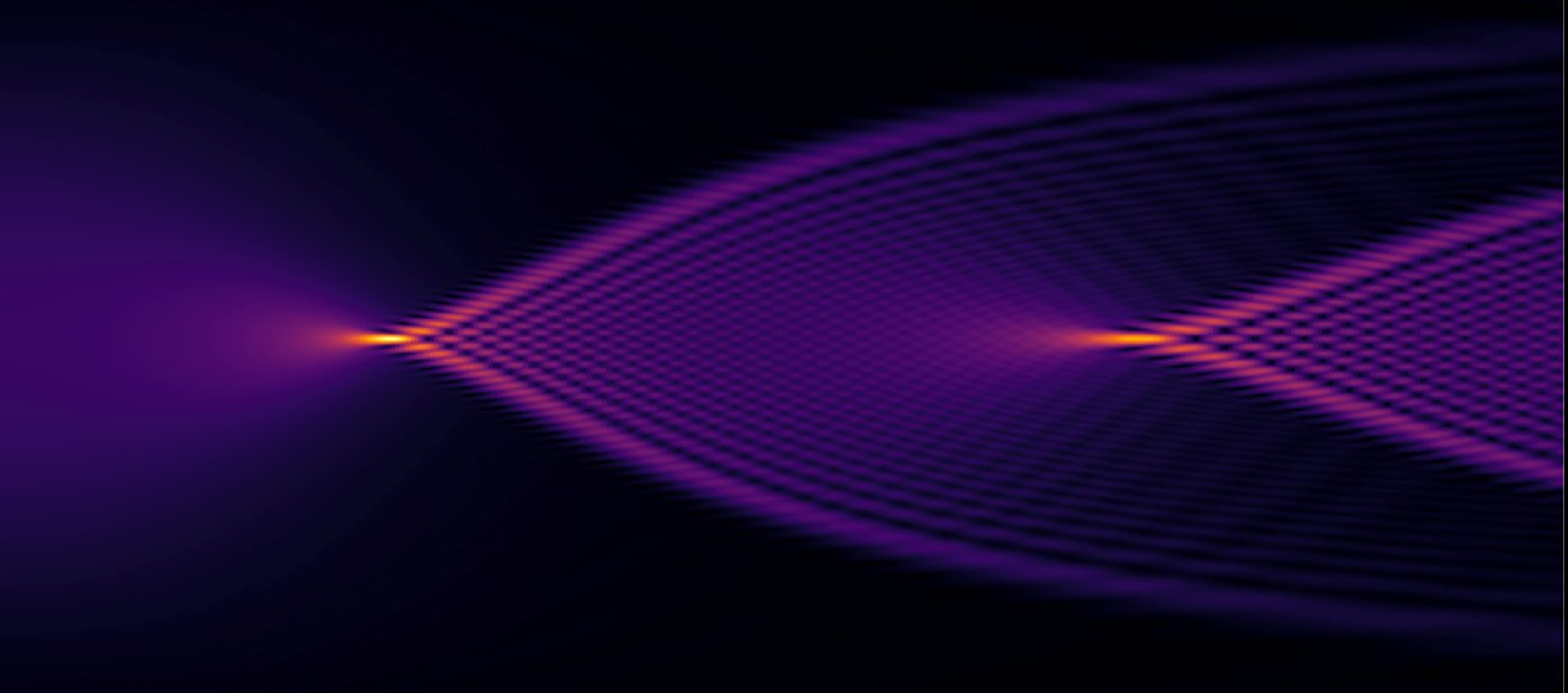

Multiple Caustics

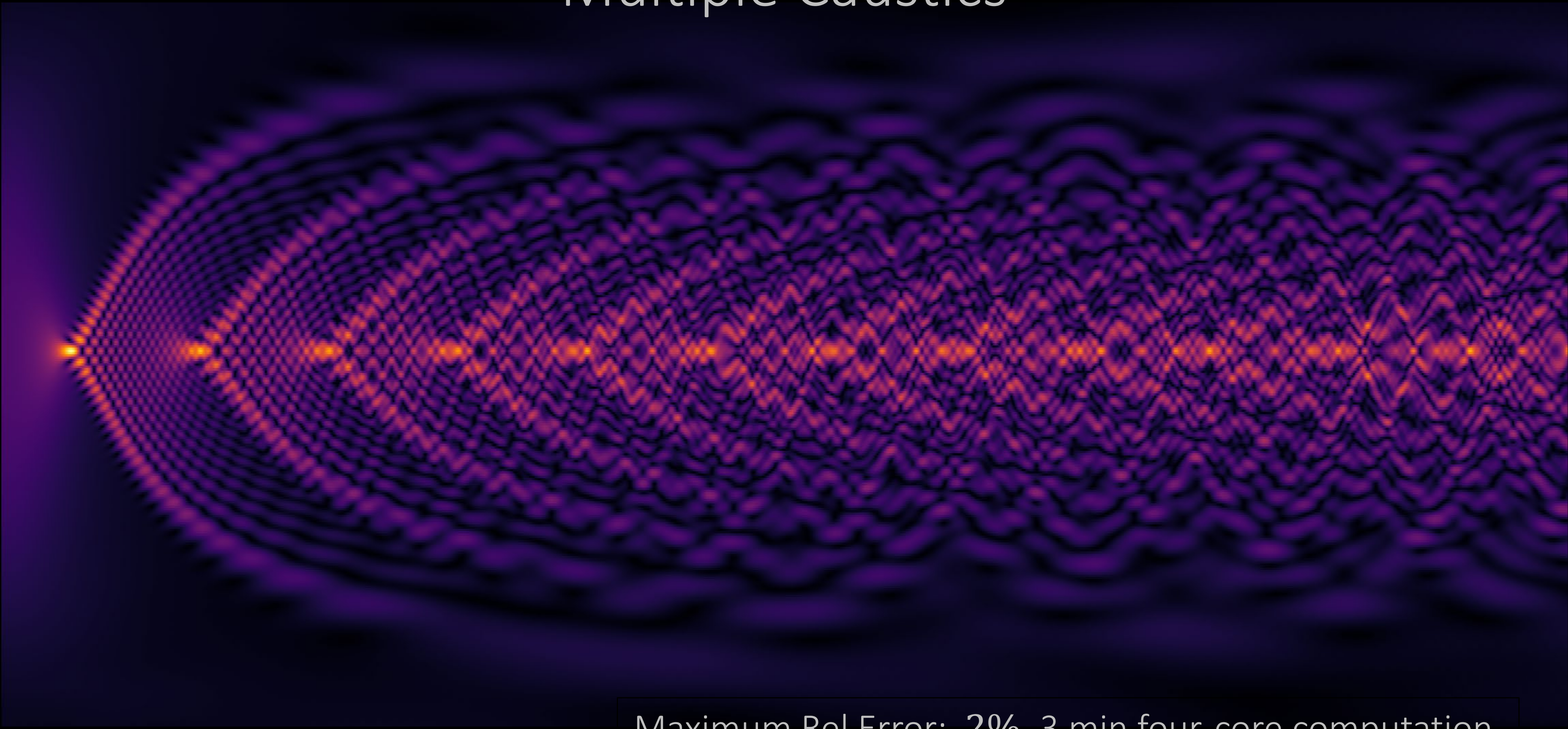

Maximum Rel Error: 2%. 3 min four-core computation.

(Comparison with exact solution)

Bouncing back and forth…

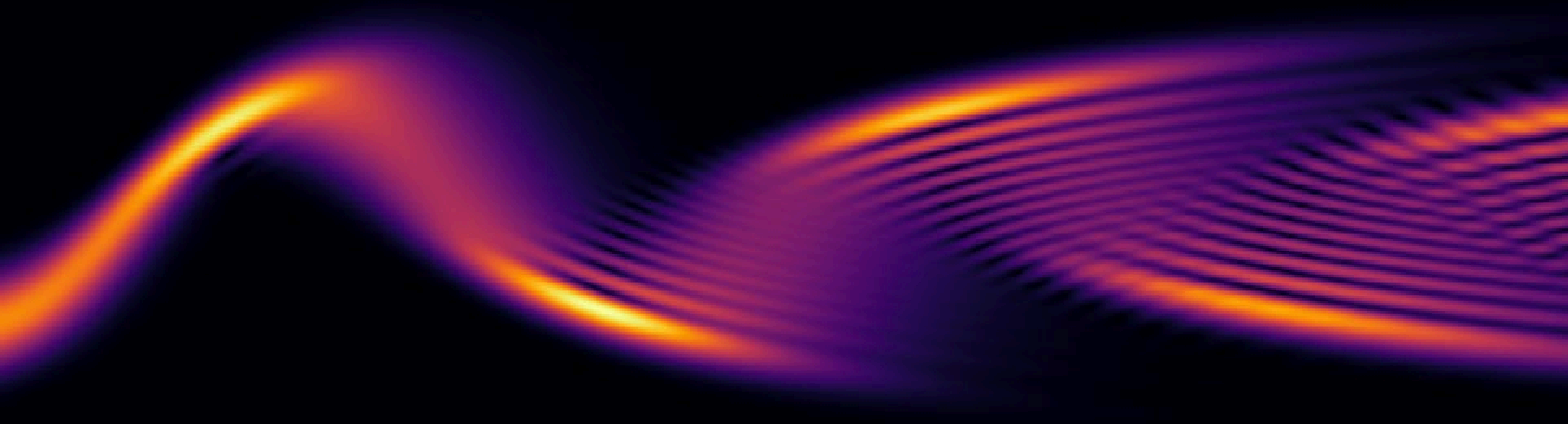

Same setup; C-Band propagation across 200 Km in range

$$a = 10^{-4}$$
$$b = 10^{-3}$$

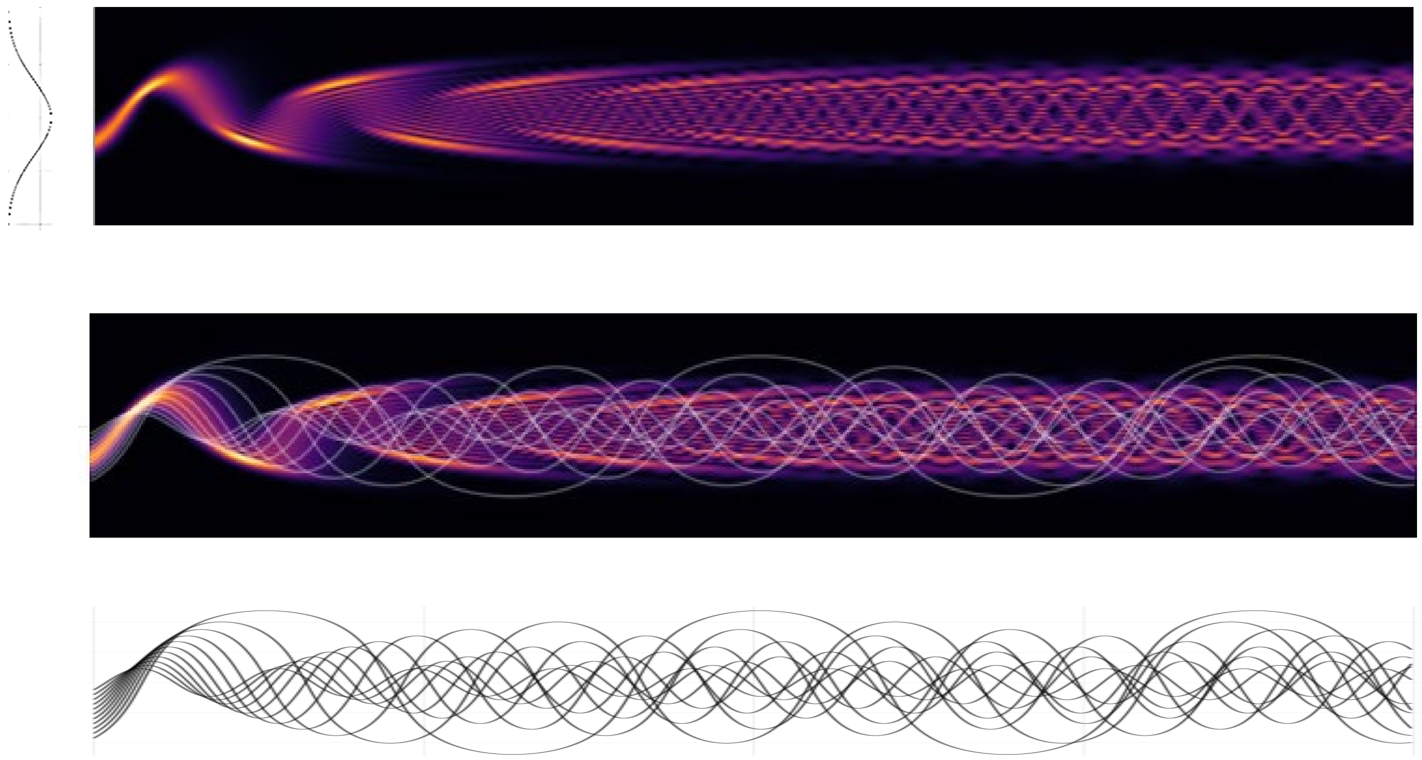

4 million wavelengths,
Maximum Rel
Error: 0.1%
(4 min in single-core)

Essentially constant error

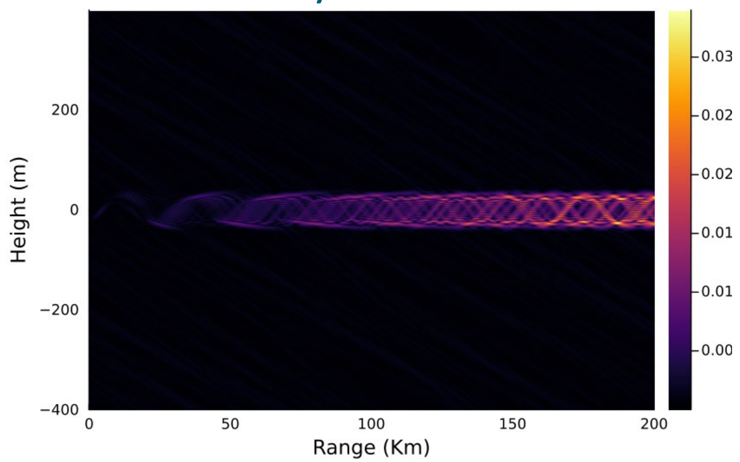

One screen per kilometer (1 km = 20,000 λ)

Lens: Propagation along refractivity gradient

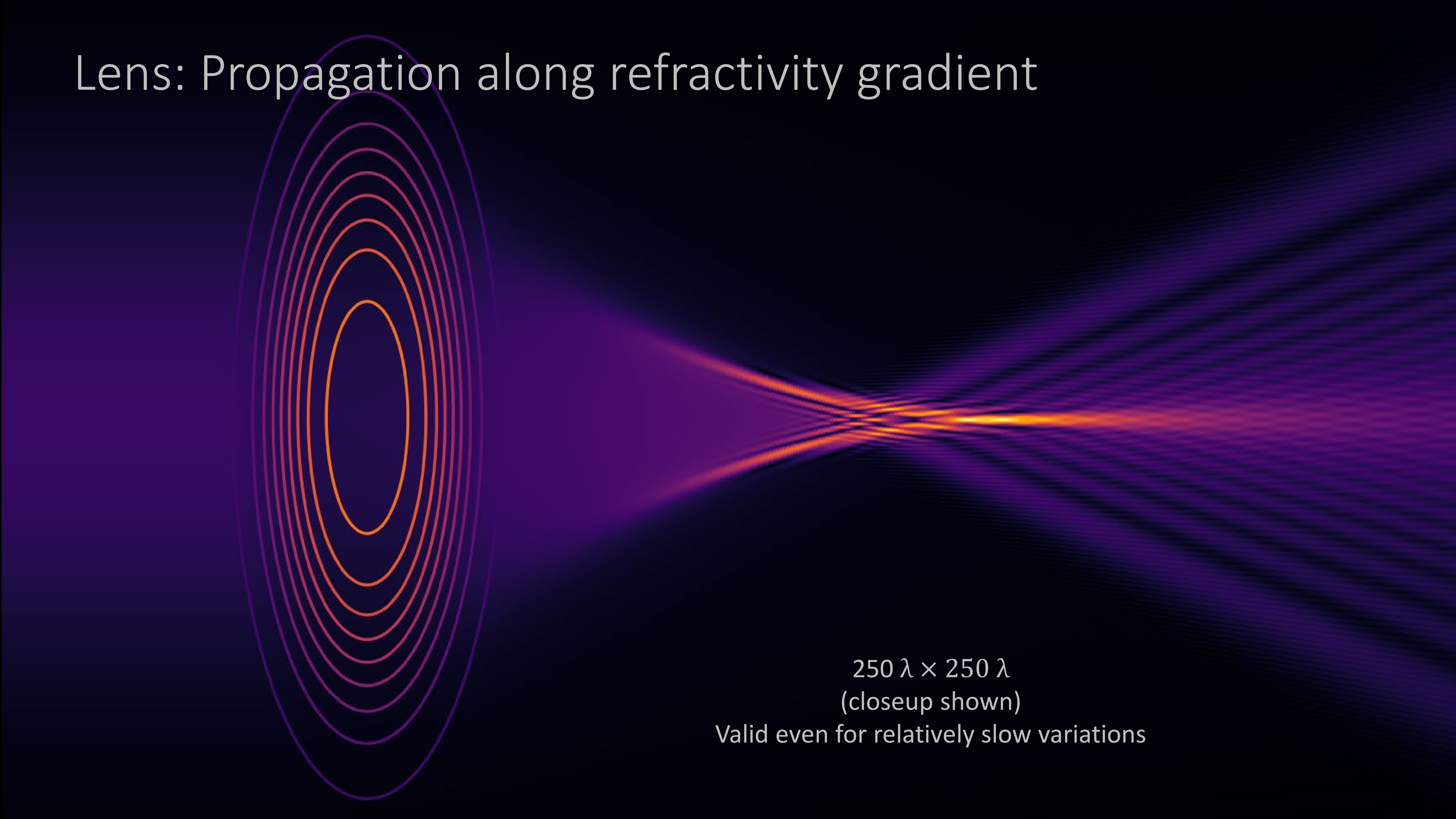

$250\,\lambda \times 250\,\lambda$

(closeup shown)

Valid even for relatively slow variations

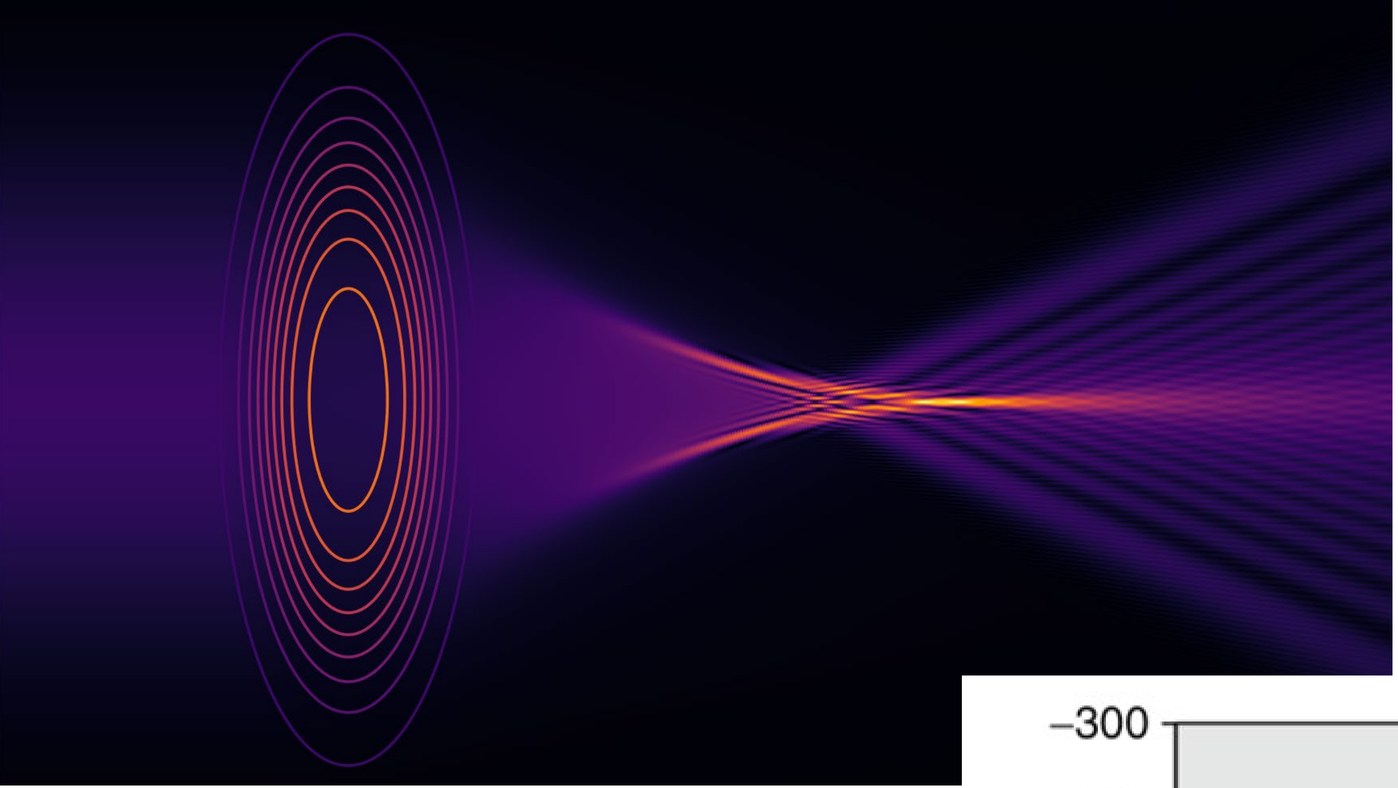

S-WKB

$250\,\lambda \times 250\,\lambda$

Parabolic Equation, SoA

(Example selected to "illustrate the full potential of numerical PE solutions to complex acoustic problems")

Jensen, "Computational Ocean Acoustics" [2011]

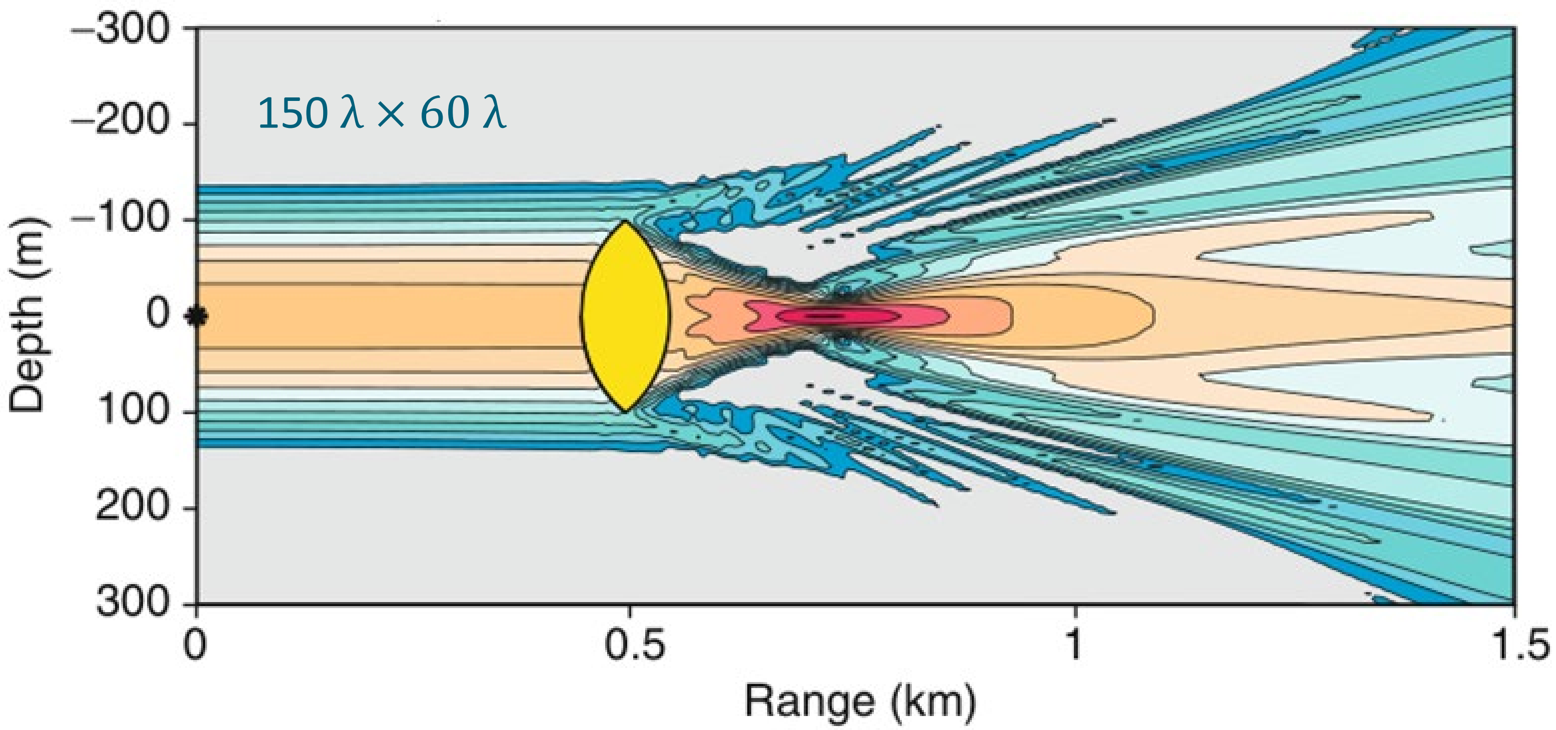

Mentioned earlier: Gaussian beams

$$u(\mathbf{r}) = e^{ik\psi(\mathbf{r})}\left(A_1(\mathbf{r}) + \frac{A_2(\mathbf{r})}{ik} + \frac{A_3(\mathbf{r})}{(ik)^2} + \dots\right)$$

– Gaussian beams: additional approximation, by seeking the phase ψ in the form of a quadratic polynomial, with a Hessian matrix that is evolved along the ray. (Babič and Buldreyev 1960's, Hörmander [1971], Babič and Pankratova [1973], Ralston [1976, 1982], Popov [1982], Tanushev, Engquist, Tsai, [2009].)
  - Eliminates ray-bunching at caustics. Intensity remains bounded at caustics.
  - $k \to \infty$ convergence has not been established theoretically, and is believed to be slow.
  - Initial beam representation is a challenging optimization problem, as illustrated in the graphs below:

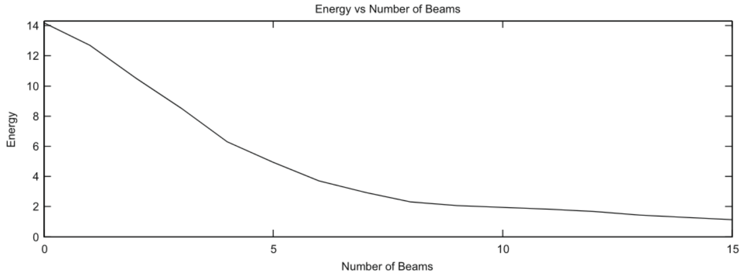

Fig. 7. Energy norm difference between the wave field and the extracted Gaussian beam wave field as a function of the number of extracted beams for the double slit experiment.

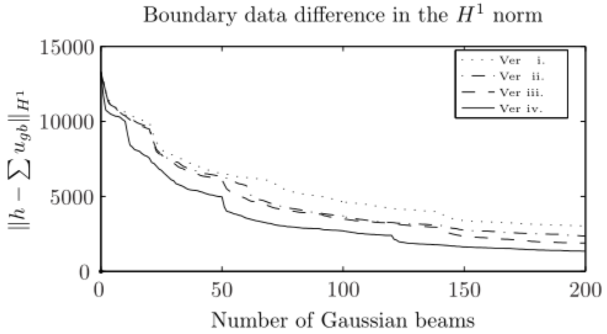

Real part of the wave field
Finite Differences

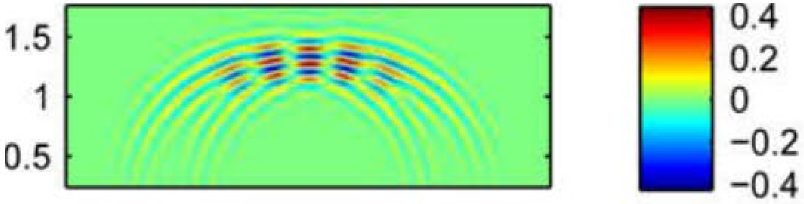

Real part of the wave field
Gaussian Beams

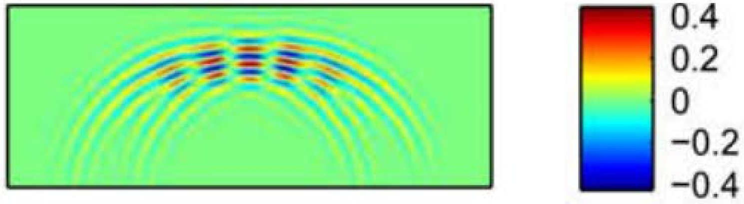

Difference

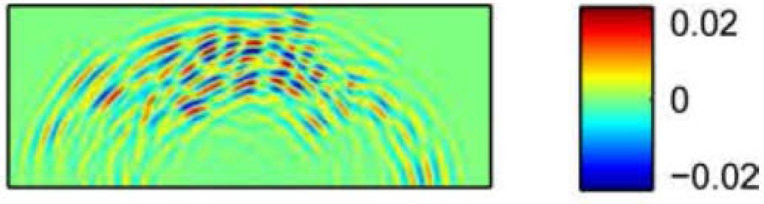

Numerical illustrations from: Tanushev, Engquist, Tsai, JCP [2009]
Tanushev, Tsai, Fomel and Engquist, SEG Meeting [2011]

Mentioned earlier: Dynamic Surface Extension (DSE)

Wave-front surface is propagated on a Cartesian discretization. Introduced in [SFW]

Algorithm elements ([SFW] version)

1. Eulerian-Lagrangian grid-centered algorithm for propagation of variables at each time step.
2. Uniform Cartesian grid.
3. Surface point closest to Cartesian grid point associated to grid point.
4. Evolve per the given velocity distribution.

Algorithm elements ([RMO] version)

1. Use a uniform Cartesian grid.
2. For each x in the grid, initially set an associated tracked point to equal the closest point on the surface.
3. Evolve the tracked point according to the local dynamics.
4. Reset each tracked point to equal to the closest point on the updated surface (defined to be the locus of all tracked points)
5. Update normals.

Fronts

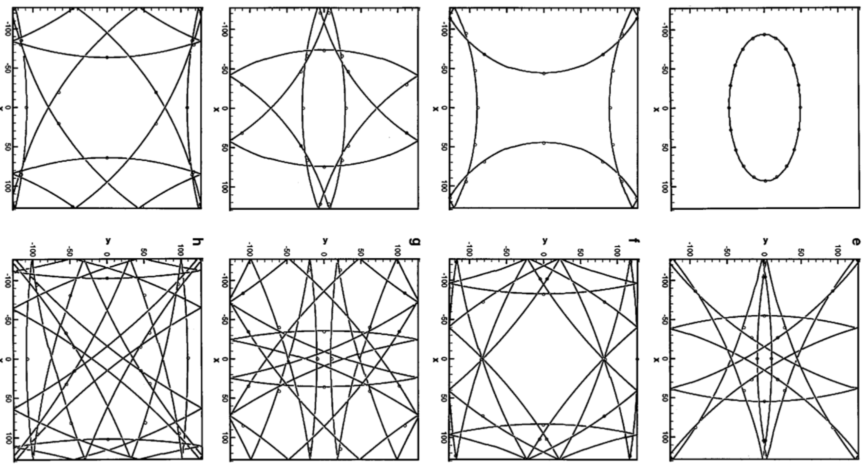

[SFW] Steinhoff, Fan, Wang, JCP [2000]

Fronts

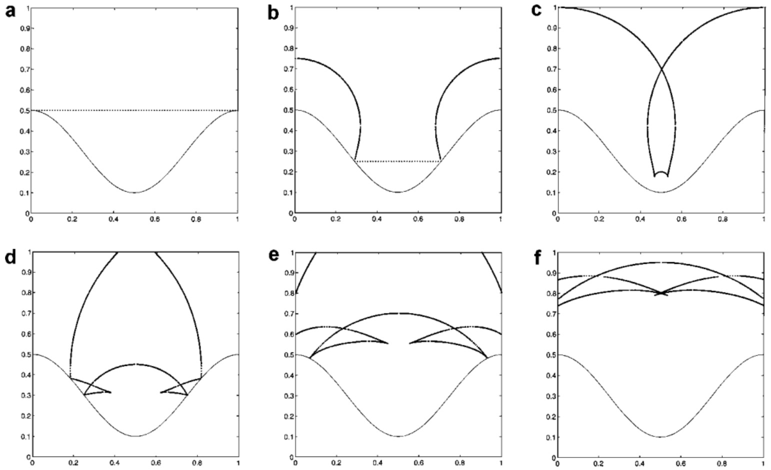

Amplitude

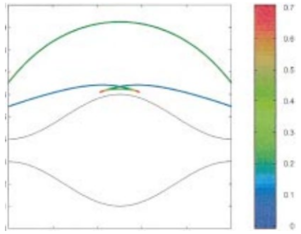

[RMO] Ruuth, Merriman, and Osher, JCP [2000]

DSE does not produce field values or amplitudes

([RMO] evaluates the amplitude as inversely proportional to curve “expansion ratio” (stretching))

Mentioned earlier: Kinetic formulation

View each ray tracing equation as describing the motion of a "particle" (e.g. photon, phonon)

- Density of particles $f(t, x, p)$ propagated along rays. (p = direction of propagation of particle at x.)
- Liouville equation
- Difficulty: the correct initial condition (and solution) is the "Wigner measure": a δ-function that vanishes for "incorrect" directions p.
- Physical field intensities: use of integral moments.

(Smooth) Point-source test. No caustics.

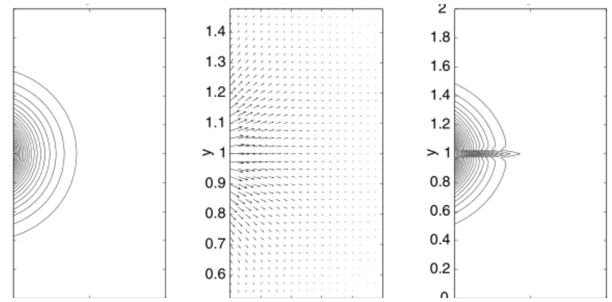

Lax-Friedrichs

Godunov (not correct)

Errors $\gtrsim \mathcal{O}(10^{-3})$

L^∞	Lax–Friedrichs unsplit		Lax–Friedrichs split		Godunov split		Nessyahu–Tadmor unsplit		Nessyahu–Tadmor split	
n	error	order	error	order	error	order	error	order	error	order
10	9.49e-2		1.78e-1		3.04e-1		6.64e-2		8.99e-2	
		1.26		0.85		0.06		1.26		0.91
20	3.97e-2		9.87e-2		2.91e-1		2.76e-2		4.78e-2	
		1.21		0.55		0.02		1.71		1.07
40	1.71e-2		6.73e-2		2.87e-1		8.46e-3		2.28e-2	
		1.15		0.73		0.02		1.70		0.80
80	7.71e-3		4.06e-2		2.83e-1		2.61e-3		1.31e-2	
		1.09		0.85		0.01		1.57		0.91
160	3.63e-3		2.26e-2		2.82e-1		8.75e-4		6.98e-3	

$[n \times (4n)$ spatial discretization used$]$

Lens. Error estimates not provided for configs. w/ caustics.

$$n(x,y) = \begin{cases} 1 & d^2 > 1, \\ \left(\frac{4}{3-\cos(\pi d^2)}\right)^2 & d^2 \le 1, \end{cases}$$

$$d^2 = \left(\frac{x-0.5}{0.2}\right)^2 + \left(\frac{y-1}{0.8}\right)^2$$

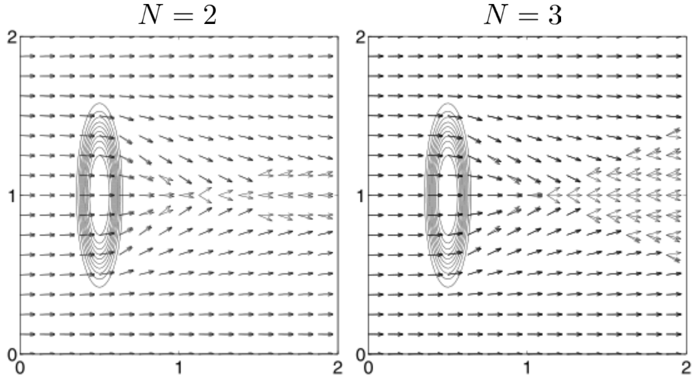

N phases, with angles $\theta_k = \theta_k(t, \boldsymbol{x})$ $(k = 1, \ldots, N)$.

Lens: amplitude rendering ($N = 3$) not provided

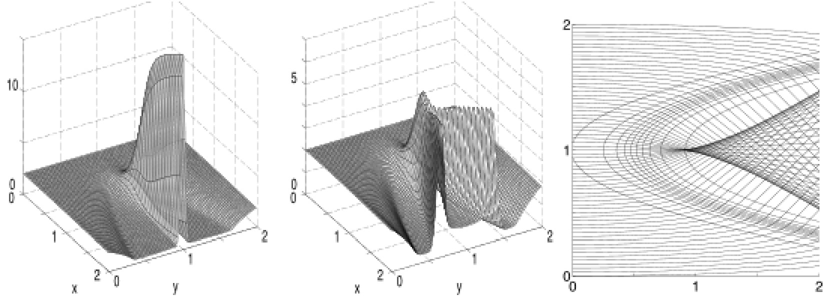

(a) $N = 1$ (b) $N = 2$ (c) Ray-traced solution

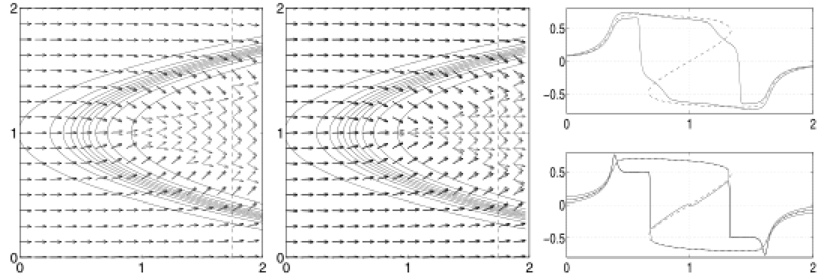

Engquist, Runborg, Acta Numerica [2003]

Screened WKB

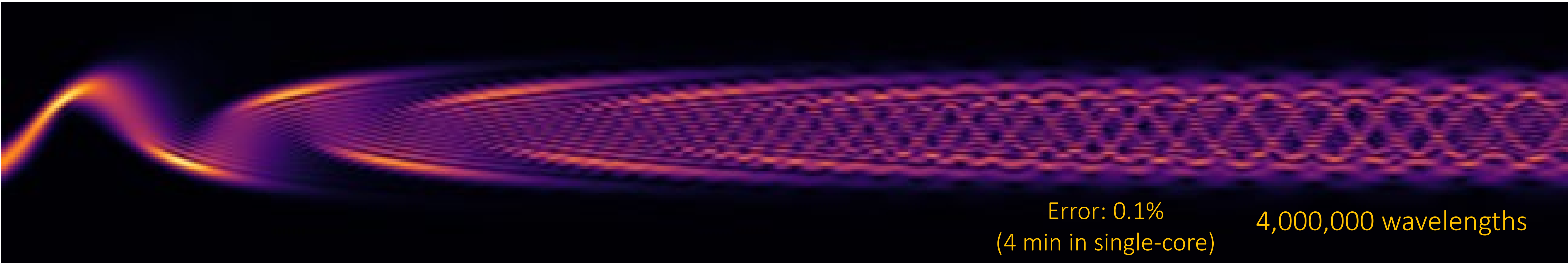

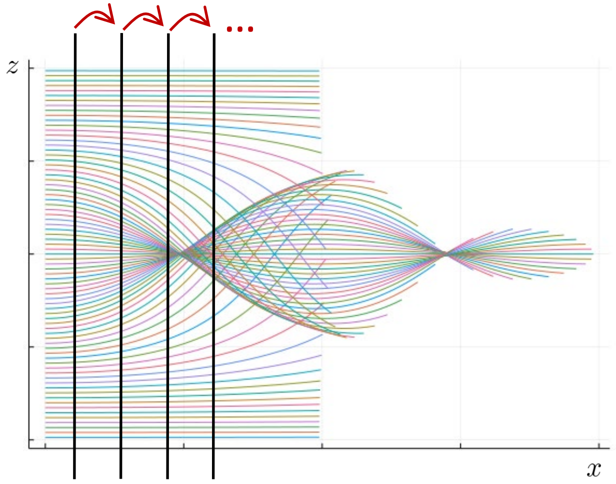

Forthcoming work

Time domain.
Interior domains.
Sparse screen resolution.
Multiple cross-ray screens.
Bottom- and top-surfaces / refractivity discontinuities.
Parallelization, Atmospheric/Oceanic/Seismological/Quantum applications.

O. Bruno and M. Maas, (arxiv.org/abs/2301.03814)

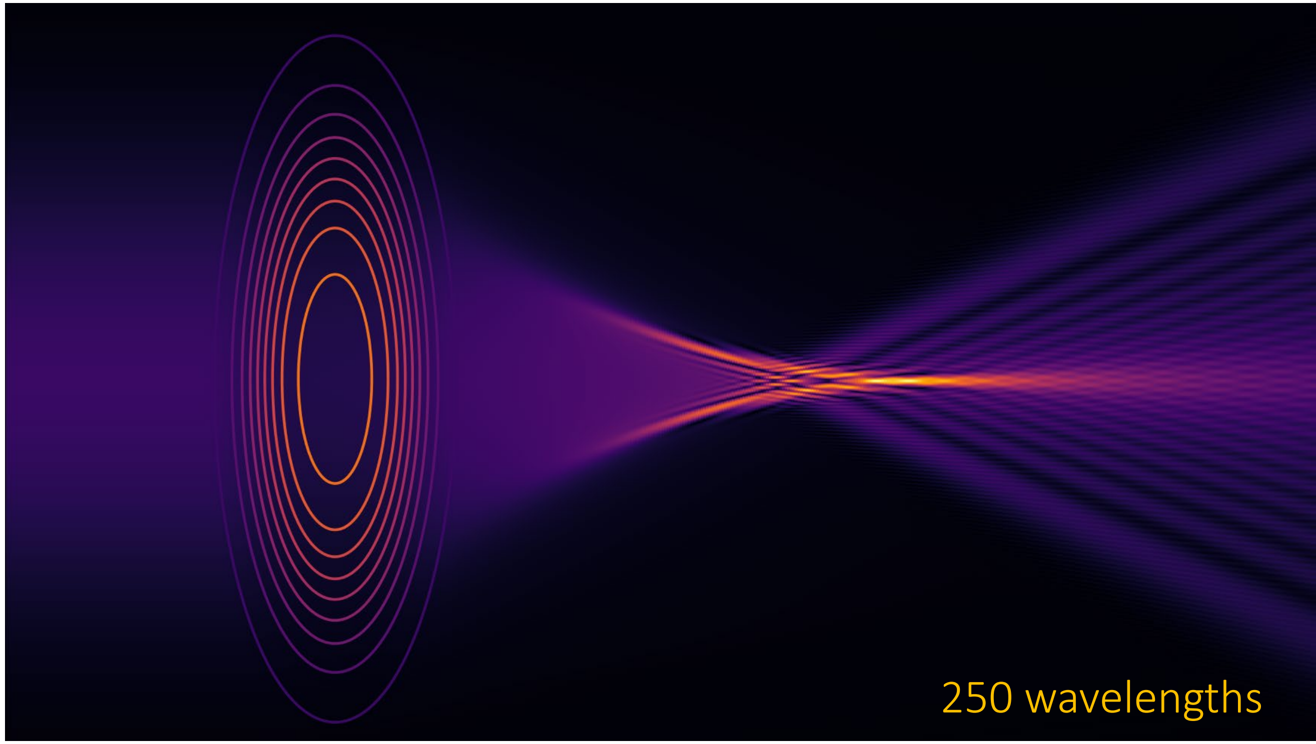

Topics

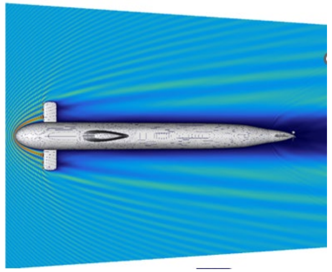

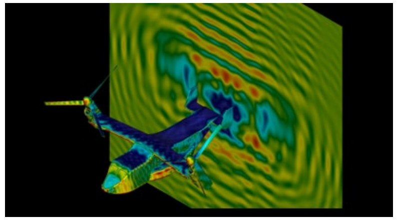

– Interpolated Factored Green Function (IFGF): FFT-free acceleration algorithm

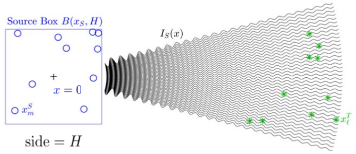

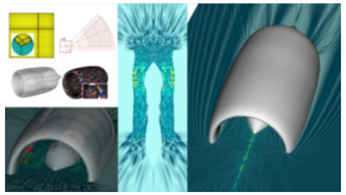

– OpenMP on 28-core server and MPI on 1680 cores

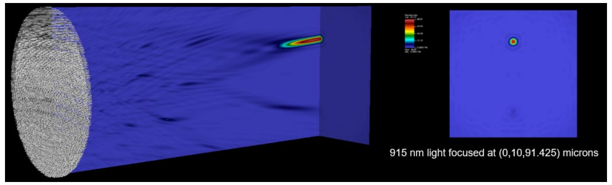

– Metamaterials: large computer cluster, photonics modeling

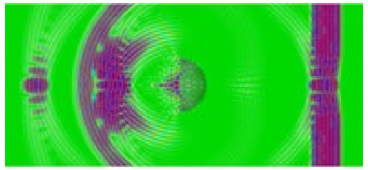

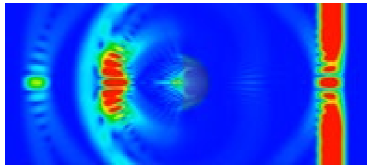

– Time-domain frequency-time hybrid solver

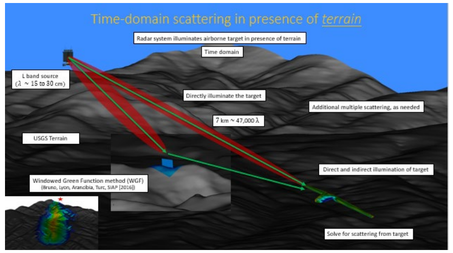

– Long-range time-domain propagation over terrain

– Long-range propagation: Screened WKB